Structural Reliability of Non-Slender Loadbearing Concrete Masonry Members under Concentric and Eccentric Loads

by

Seyed Abdol Hadi MOOSAVI NANEHKARAN

A thesis submitted in partial fulfillment of the requirements for the degree of

Doctor of Philosophy

in
Structural Engineering

Department of Civil & Environmental Engineering
University of Alberta

Abstract

Although the reliability levels of structural steel and reinforced concrete structures designed to the Canadian codes and standards have been investigated substantially in the past four decades, studies on the reliability of masonry structures are limited. Based on some preliminary studies in 1980s, the design of masonry structures using the limit states method was introduced in the 1994 edition of the Canadian standard S304 in order to provide more uniform and economical design guidelines. However, the limit states design criteria were not supported by a rigorous reliability-based analysis. The investigation reported herein was carried out to contribute to filling the gap in our knowledge on the reliability of structural masonry members designed using the limit states method, to establish reliability levels for masonry comparable to other structural materials and to help remove any unnecessary conservatism in the masonry design process. The first order reliability method was used to assess the reliability of unreinforced and reinforced non-slender concrete masonry walls under combined axial load and out-of-plane bending. In this research, only non-slender walls having a slender ratio (kh/t) not requiring consideration of second order effects are considered. Nevertheless, the procedure for performing the reliability analysis for walls with larger kh/t is proposed and explained.

Acknowledgement

I would like to express my special appreciation and thanks to my advisors, Dr. Yasser Korany and Dr. Samer Adeeb. They have been tremendous mentors for me on being a professional research scientist. Their advices on research work have been invaluable.

I would also like to thank my committee members, Dr. Shelley Lissel, Dr. Carlos Cruz Noguez, Douglas Tomlinson, Dr. Marwan El-Rich for serving as my committee members.

Table of Contents

List of Tables

List of Figures

Notation

d	reinforcement depth
d_n	nominal reinforcement depth
D/D_n	bias factor for dead load
e	eccentricity of axial load
f_m	compressive strength for masonry
f'_m	nominal compressive strength for masonry
f_y	yield stress for reinforcement
f_{yn}	nominal yield stress for steel reinforcement
$G(\boldsymbol{x})$	limit state function
kh/t	slender ratio
M	out-of-plane bending moment
M_D	random variable for bending moment due to dead load
$M_{D,n}$	bending moment due to nominal dead load
M_L	random variable for bending moment due to live load
$M_{L,n}$	bending moment due to nominal live load
M_r	random variable for bending moment component of resistance
$M_{r,n}$	nominal bending moment component of resistance
M_W	random variable for bending moment due to wind load
$M_{W,n}$	bending moment due to nominal wind load
P	axial load on the wall
P_D	random variable for axial load due to dead load
$P_{D,n}$	axial load due to nominal dead load
P_L	random variable for axial load due to live load
$P_{L,n}$	axial load due to nominal live load
P_r	random variable for axial load component of resistance
$P_{r,n}$	nominal axial load component of resistance
P_W	random variable for axial load due to wind load
$P_{W,n}$	axial load due to nominal wind load
t	wall thickness
t_n	nominal wall thickness
V_{model}	coefficient of variation of the strength prediction model

V_P coefficient of variation of the professional factor

V_{spec} coefficient of variation related to the differences between the measured and actual parameters of the test specimens.

V_{test} coefficient of variation of the measured masonry capacity due to inaccuracies in the test measurements and/or the definition of failure

$\boldsymbol{x}$ vector of random variables

β reliability index

β_T target reliability index

ρ_w workmanship factor

$\rho_{r(D+L)}$ rate of loading for live load

$\rho_{r(D+S)}$ rate of loading for snow load

$\rho_{r(D+W)}$ rate of loading for wind load

ρ_s steel reinforcement ratio

ρ_b balanced reinforcement ratio

ϕ_m resistance factors for masonry

ϕ_s resistance factors for steel reinforcement

Chapter 1

Introduction

1.1 STRUCTURAL RELIABILITY OF MASONRY STRUCTURES

The term *structural masonry* represents that type of construction in which a large number of small modular units are mortared together to produce structural elements in a building (Hatzinikolas and Korany 2005). Typically, these modular units are clay bricks, concrete blocks or cut stone. The most common masonry structural element is the wall; however, when properly reinforced, masonry may be used to build columns and beams.

There have been many studies to improve building codes and standards so that the most influential sources of uncertainties are accounted for in the design procedures. These efforts have led to a design criteria called *reliability-based design*. In Canada, although the reliability (safety) levels of structural steel and reinforced concrete structures have been investigated substantially in the past four decades, studies on the reliability of masonry structures are limited. The Canadian standard for the design of masonry structures (CSA S304) has been in the limit states format since 1994 based

on some preliminary studies to provide more uniform and economical design guidelines. However, these design criteria are not supported by rigorous reliability-based analysis. For example, the recent change in the material resistance factor for masonry from 0.55 to 0.60 in the current edition of the standard CSA S304-2014 was justified by simple calculations (Laird et al. 2005) in which the values for the statistical parameters were chosen based on judgement.

Some research was performed on the structural reliability of masonry walls during 1980s based on the design expressions in the standard of the time (Turkstra and Daly 1978; Turkstra and Ojinaga 1980; Turkstra et al. 1982; Turkstra et al. 1982; Turkstra 1983; Turkstra et al. 1983; Turkstra 1984; Turkstra 1989). In these studies, workmanship effects, which have a significant influence on reliability levels, were applied based on judgement and very limited experimental data (Brick Institute of America 1969; Turkstra 1983). Therefore, there is a strong need for a comprehensive assessment of the design expressions of the current standard in order to establish reliability levels for masonry comparable to other structural materials and to help remove any unnecessary conservatism in the masonry design process.

The research described herein focuses on the reliability analysis of a main category of masonry walls, namely, flexural masonry walls under axial compression and transverse loading. Masonry walls (unreinforced or reinforced) are the most common structural members in masonry construction.

Masonry walls are often built to transfer concentric and eccentric gravity loads as well as lateral loads due to wind or earthquake. These vertical members experience beam-column action to transfer combined axial and

bending loads and their behaviour is governed by the interaction of material strength and member stability. These structural members have a complicated behaviour due to reasons like the composite nature of masonry, pre-failure cracking, and slenderness effects.

After the adoption of limit states design for masonry, sections may be designed to be more slender and economical. Therefore, members undergo larger deflections compared to those designed using the working stress method. The limited research performed on the structural reliability of masonry walls during 1980s (Turkstra and Daly 1978; Turkstra and Ojinaga 1980; Turkstra et al. 1982; Turkstra et al. 1982; Turkstra 1983; Turkstra et al. 1983; Turkstra 1984; Turkstra 1989), was based on the design expressions of the standard of the time and the analytical models to consider slenderness effects were all approximate. Consequently, a comprehensive assessment of the design expressions of the current standard is required.

1.2 MOTIVATION

The research herein is motivated by the following concerns regarding reliability levels of masonry structures.

The design of masonry structures using the ultimate limit states method needs to be supported by rigorous reliability analyses to achieve two main goals: calculate the current reliability levels for various masonry structural members and ensure that reliability levels for masonry structures are consistent with other structural materials.

Masonry material properties, construction methods, and inspection levels have improved over the past two decades. However, these improvements have not been reflected in the design standard based on a comprehensive

reliability analysis. For example, the increase of the material resistance factor for masonry, ϕ_m, from 0.55 to 0.60 in the current edition of CSA S304-2014 was justified by a two-page calculation based on statistical values selected mostly by judgment (Laird et al. 2005).

Also, the quality of workmanship has a substantial effect on masonry strength (Turkstra 1989) and therefore the workmanship factor needs to be probabilistically quantified and applied. This will also affect the structural reliability levels.

1.3 OBJECTIVES & SCOPE

It is clear that the reliability of all types of masonry members under all loading conditions cannot be investigated in one study. The most common structural members in masonry construction are loadbearing masonry walls and they have a complex behaviour due to reasons such as the composite nature of masonry, pre-failure cracking, and slenderness effects. Therefore, the scope of this study is limited to the reliability analysis of load-bearing masonry walls under axial compression and out-of-plane bending. In particular, the ultimate limit state of masonry walls under axial compression and out-of-plane bending will be studied. However, the shear mode of failure is not considered in this work. The scope of this study does not include masonry shear walls and masonry infill shear walls. This study performs a complete reliability analysis on non-slender walls where slenderness effects are negligible and proposes an algorithm for expanding the analysis to walls where slenderness effects should be taken into account. This is further elaborated in Chapter 2.

Both reinforced and unreinforced load-bearing masonry walls constructed from hollow concrete blocks and type S mortar were investigated.

The main objectives of this study are:

Objective 1: To select a proper behavioural model for masonry walls under axial & out-of-plane bending to be used in the reliability analysis;

specific aim 1: To perform a comprehensive literature review on behavioural models (Chapter 2),

specific aim 2: To compare different models & select a model which is proper for iterative calculations (Chapter 2),

specific aim 3: To verify the selected model with experimental results (Chapter 3),

specific aim 4: To examine the sensitivity of the selected behavioural model to various material and geometrical parameters (Chapter 4).

Objective 2: To propose a limit state function for non-slender walls under axial compression only and under axial compression combined with out-of-plane bending moment (Chapter 5).

Objective 3: To collect statistical data for the parameters involved in the proposed limit state function (Chapter 5);

specific aim 1: To collect statistical data for different load types,

specific aim 2: To collect statistical data for resistance parameters (geometrical & mechanical properties).

Objective 4: To assess the reliability levels provided by the design expressions & material resistance factors in the Canadian masonry design standard for non-slender flexural masonry walls (Chapter 5);

Objective 5: To examine the effect of changing masonry resistance factor on current reliability levels (Chapter 5);

Objective 6: To propose an algorithm and the framework for performing reliability analysis on masonry walls with slenderness effects to assess the reliability levels provided by the design expressions and material resistance factors in the 2014 edition of CSA S304 for this category of walls (Chapter 6).

1.4 LAYOUT OF THE DISSERTATION

In Chapter 1 of this dissertation, current chapter, an introduction to the background information about structural reliability of masonry structures is given. The motivation, objectives and scope of the research study and organization of the dissertation are also presented.

Chapter 2 contains a summary about previous research relevant to structural reliability of masonry structures, analytical models for load-bearing masonry walls and their mechanical behaviour, the effect of workmanship.

Chapter 3 illustrates the basics for development of a behavioural model for the analysis of non-slender load-bearing masonry walls; reinforced or unreinforced. The outcome of this model is the interaction diagram between axial compression and out-of-plane bending moment resisted by a given masonry wall.

This model is capable of capturing material nonlinearities, i.e. post-cracking and crushing of masonry and yielding of steel reinforcement. The masonry is presumed to be a homogeneous material with some tension strength. This model is then verified with experimental results in the literature.

Chapter 3 also explains the moment-magnifier method that can be used as an alternative to finite element method to extend the reliability analysis for masonry walls with slenderness effects.

Chapter 4 contains results of an analysis to assess the sensitivity of the behaviour of non-slender masonry walls under axial load and out-of-plane bending to various material and geometrical parameters.

In Chapter 5, a limit state function for non-slender masonry walls under axial load and out-of-plane bending is proposed. Then, first order reliability method (FORM) is used to assess the reliability levels according to the statistical properties for the contributing parameters. The statistical properties for loading is adopted from the most recent study for loading information in Canada. The statistical properties for masonry compressive strength is derived in this study by establishing an experimental database from numerous recent prism tests. Results for this comprehensive analysis are presented and discussed.

In Chapter 6, an algorithm for extending the study for masonry walls with slenderness effects is proposed along with a framework and scope of the future study.

Lastly, Chapter 7 concludes the text with summary of results and conclusion.

Chapter 2

Summary of Prior Related Research

GENERAL

This chapter summarizes previous research and studies relevant to structural reliability concept, categorization of load-bearing walls based on slenderness, structural reliability of masonry structures, behavioural models for load-bearing masonry walls, mechanical properties of materials in masonry construction, effect of workmanship, statistical properties for loading and masonry construction and experimental studies on load bearing masonry walls and prism compression tests.

2.1 STRUCTURAL RELIABILITY APPROACH

Similar to any engineered design, there are many sources of uncertainty in structural design. The parameters of the load-carrying capacities and the loading of structural members can be considered as random variables rather than deterministic quantities. In the context of structural reliability, structures should be designed to serve their function within a finite probability of failure. In other words, it is expected that the structures are

designed with a reasonable safety level. In general, the reliability of a structure is its ability to fulfill its design purpose for some specified design lifetime within an acceptable probability of failure. In practice, these acceptable or expected safety levels are achieved by specifying design values for minimum design loads, maximum allowable deflection as well as load/resistance factors in design guidelines. Codes and standards have evolved so that design criteria take into account some of the sources of uncertainty in design. Such criteria are often referred to as reliability-based design criteria. Therefore, code requirements such as minimum design loads, maximum allowable deflections and load/resistance factors should be the results of extensive reliability analyses where sources of uncertainty in design are taken into account. Concisely, five essential steps for the development of practical probability-based resistance criteria can be considered: (1) to define limit states that needs to be considered (2) To establish mathematical models using principles of mechanics and experimental data to predict the behaviour of masonry walls subjected to various load conditions; (3) to establish procedures, based on probability theory, for measuring quantitatively the structural performance (limit state probability or reliability index); (4) to specify target reliability measures by assessing reliabilities inherent to existing designs that have performed satisfactorily and other considerations; and (5) to determine resistance factors to ensure that the performance objectives of the specification, expressed in reliability terms, are met.

As mentioned above, the first step in any reliability analysis is to define a criterion for deciding whether the performance of the engineered product is satisfactory. Such criterion is called a limit state. In terms of structural reliability analysis, there are two main categories for limit state; namely, ultimate limit state and serviceability limit state. Ultimate limit state involves collapse of all or part of structure such as tipping or sliding, rupture,

progressive collapse, plastic mechanism instability, corrosion, fatigue and deterioration. Serviceability limit state, on the other hand, involves disruption of normal use of the structure. Examples for serviceability limit state are excessive deflections, vibrations and local damage.

To perform reliability analysis for a given limit state, the limit state needs to be defined mathematically as a limit state function. General form of a limit state function is $G(\boldsymbol{X}) = 0$ where $\boldsymbol{X}$ is a vector including random variables involved in the limit state function. A very simple case for an ultimate limit state function would be $G(\boldsymbol{X}) = R - S = 0$ where R is the resistance and S is the load on the structure. R and S are both random variables and one of the main steps in any reliability analysis is to determine the statistical properties of the important parameters involved such as, values for mean and coefficient of variation (COV) and distribution type. Useful explanations of random variables and functions of random variables are given elsewhere, e.g. Nowak (2000).

The structure is described as safe when $G(\boldsymbol{X}) > 0$ and the problem of reliability analysis is to calculate the probability of failure which is defined by $G(\boldsymbol{X}) < 0$. With a given limit state function such as $G(\boldsymbol{X}) = 0$, where vector $\boldsymbol{X}$ includes the random variables involved, a generalized reliability problem can be formulated as follows (Melchers(1999)):

$$p_f = P[G(\boldsymbol{X}) \leq 0] = \int \dots \int_{G(\boldsymbol{X}) \leq 0} f_{\boldsymbol{X}}(\boldsymbol{X})\, d\boldsymbol{X} \qquad \text{(Eq. 2.1)}$$

p_f is the probability failure of a structural member and $f_{\boldsymbol{X}}(\boldsymbol{X})$ is the joint probability density function for the n-dimensional vector $\boldsymbol{X}$ of basic variables. Even for the simple case of $G(\boldsymbol{X}) = R - S$, Eq. 2.1 changes to a convolution integral and analytic solution is possible only for very special cases of limited practical interests. Therefore, several techniques have been introduced to address this problem which are briefly discussed in the following.

2.1.1 TECHNIQUES FOR STRUCTURAL RELIABILITY ANALYSIS

Integration & Simulation Methods

Simulation is one possible way to approach reliability problems. Simulation, as the name implies, is to numerically simulate some phenomenon and then to investigate the number of times some event of interest (e.g. failure to function) occurs. Results of previous tests (or other information) can be used to establish the probability distributions of the important parameters in the problem. Then this distribution information is used to generate samples of numerical data and the limit state criteria are investigated in the end. The basic concept behind simulation is relatively straightforward but the technique can be computationally exhaustive. Some of the simulation techniques are named in the following. The details for these methods can be found in reliability analysis references such as Melchers (1999) and Nowak (2000).

- Direct or Numerical Integration
- Monte Carlo Methods
- Importance Sampling
- Latin Hypercube Sampling
- Rosenblueth's 2K+1 Point Estimate Method
- Directional Simulation

Second-Moment & Transformation Methods

The basic concept behind these methods is to simplify the probability density function $f_X()$ in the integrand. The simplest case is when each variable is represented only by its first two moments i.e. by its mean and standard deviation. This is also known as the "second-moment" level of representation of variables. Higher moments, which are usually referred to as distribution types, describe skew and flatness of the distributions.

"Second-moment" methods became popular because of their simplicity and gained a measure of acceptance among researchers after a study by Cornell (1969). The second-moment concept led to several extensions and improvements. The most important improvement is that with iteration it is now possible to approximate the actual probability distributions in $f_X( )$ with normal probability distributions and still good estimates of failure probability is obtainable. Some of these extended methods are

- First-Order Second-Moment (FOSM)
- First-Order Reliability Method (FORM)
- Second Order Reliability Method (SORM)

The final result from all these methods are reliability indices. Reliability index or safety index is denoted as β. For a very simple case where the limit state function is defined as $G(\boldsymbol{x}) = R - S$ with R and S representing the resistance and load respectively and both following a normal distribution, β is related to the probability of failure as $p_f = \Phi(-\beta)$ where $\Phi()$ is the standard normal cumulative distribution function. For other more complex cases, β can only be related to a "nominal" probability failure. A modified definition of reliability index was introduced by Hasofer and Lind in 1974 (Nowak (2000)). The modification was to calculate the limit state function at a point called the "design point" on the failure surface $G(\boldsymbol{x}) = 0$. The design

point is characterized by yielding the least β over the failure surface which corresponds to the real probability of failure. Since, the design point is not known beforehand, an iteration technique is required to solve for the reliability index. Additional information on the reliability index can be found in reliability analysis references such as Nowak (2000) and Melchers (1999).

Calculated reliability indices are then compared with target reliability indices proposed by code and standard organizations (β_T) which are functions of a range of factors including the type of failure, estimated cost of failure and existing levels of safety (Lawrence and Stewart 2009) and serve as approximate measures of the acceptable probability of failure (CSA S408 2011). CSA S408 (2011), Guidelines for the Development of Limit States Design, suggests various target reliability indices depending on the type of failure (gradual vs. sudden) and the consequence of failure or safety class (Table 2-1).

Table 2–1 Target reliability indices from CSA S408 (2011) for 30-years (50-years) building lifetime

	Type of Failure	
Safety Class	**Gradual**	**Sudden**
Not serious	2.5 (2.3)	3.0 (2.8)
Serious (normal buildings)	3.5 (3.4)	4.0 (3.9)
Very serious*	4.0 (3.9)	4.5 (4.4)

It is assumed that for very serious consequences there is better quality control

Joint Committee on Structural Safety (JCSS 2001a) adds considerations for the risk of investment by relating the target reliability to the relative cost of enhancing the structural reliability in addition to the risk to human life. (Table 2–2) shows target reliability indices from JCSS (2001a). Numbers in brackets correspond to 50-years reference period and were calculated and added to this table so they are comparable with numbers in Table 2-1.

Table 2–2 Target reliability indices from JCSS (2001a) for 1-year (50-years) reference period and ultimate limit states

Relative cost for enhancing the structural reliability	Failure consequences		
	Minor[a]	Average[b]	Major[c]
Large	3.1 (1.7)	3.3 (2.0)	3.7 (2.6)
Medium	3.7 (2.6)	4.2 (3.2)[d]	4.4 (3.5)
Small	4.2 (3.2)	4.4 (3.5)	4.7 (3.8)

[a]e.g. agricultural buildings
[b]e.g. office buildings, residential buildings or industrial buildings
[c]e.g. bridges, stadiums or high-rise buildings
[d]recommendation for regular cases

While FOSM takes into account only the mean and COV values for random variables involved, FORM also can reflect the type of distribution for each of the random variables. Therefore, FORM gives more accurate results. SORM yields even more closer results to exact solutions at a cost of more computational time. However, the difference between results from FORM and SORM are noteworthy when the failure surface has very sharp curves and FORM always yields practical approximations Melchers (1999). FORM is supported by CSA 408, Guidelines for the development of limit states design standards, and is adopted in this research study. When using FORM/SORM, attention should be given to the ordering of dependent random variables and the selection of initial points for the iterative algorithm. Moreover, the results for the design point should be assessed to ensure that they do not contradict physical reasoning (JCSS 2001b). Further fundamentals for reliability analysis can be found in literature such as Melchers (1999), Nowak (2000) and JCSS (2001b).

A brief iterative algorithm for FORM procedure, proposed by Rackwitz-Fiessler in 1978 and adopted in this study is shown in Figure 2-1. Reliability index derived from this method is the Hasofer-Lind reliability index introduced before. Details for Rackwitz-Fiessler procedure can be found in Nowak (2000). Step 4 in the iterative algorithm shown in Figure 2-1 involves

calculating reduced variates of design point parameters, $X^* = \{x_i^*\}$ which are shown as $\{z_i^*\}$. For normally distributed random variables $z_i^* = (x_i^* - \mu_{xi})/\sigma_{xi}$. For random variables with other distribution types, first equivalent mean and distribution needs to be found as μ_{xi}^e and σ_{xi}^e and then $z_i^* = (x_i^* - \mu_{xi}^e)/\sigma_{xi}^e$. Procedures for calculating these equivalent values are illustrated in Nowak (2000). Figure 2-2 illustrates how different part of this research study contribute to the reliability analysis. An important step is to define a failure criteria and define it in a mathematical form i.e. limit state function. Then all the involved random variable should be introduced to reliability algorithm with their statistical information i.e. mean, coefficient of variation and distribution type.

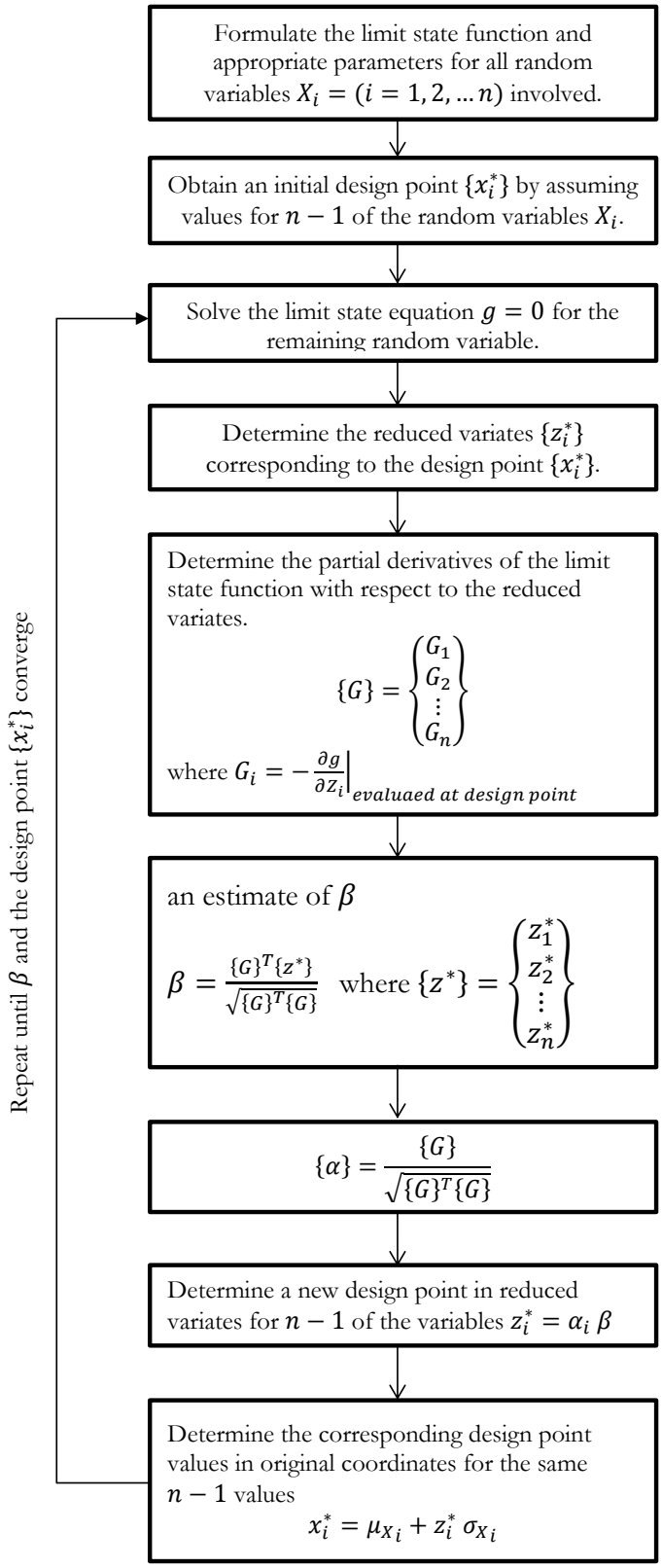

Figure 2-1: Algorithm for Rackwitz-Fiessler procedure (Nowak 2000)

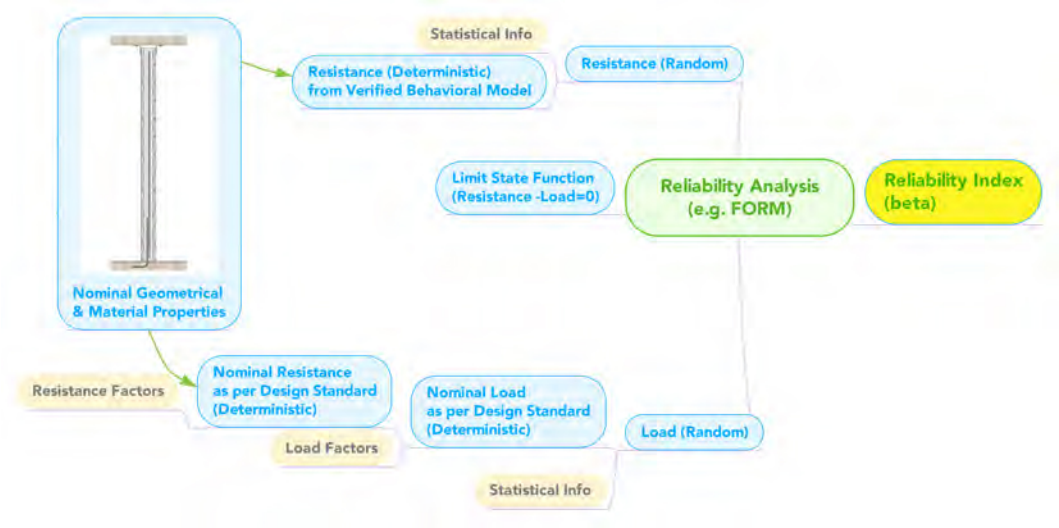

Figure 2-2: Inter-relation of different parts of the study for reliability analysis

2.2 CATEGORIZATION OF LOAD-BEARING WALLS IN CSA S304-2014 BASED ON REINFORCEMENT & SLENDERNESS

With the development of rational analysis and design methods, confident construction of masonry walls with larger slenderness ratios has been possible. Before introduction of limit states design methods in CSA S304-94, slenderness effects of walls were considered by applying reduction coefficients on wall capacity (Drysdale and Hamid 2005). Limit states requirements for design of unreinforced masonry walls and reinforced masonry walls are given in section 7 and section 10 of CSA S304, respectively. The following are the clauses from CSA S304 classifying load bearing masonry walls based on their slenderness ratio. These clauses are reproduced here to explain how non-slender walls in this study compare with standard definitions.

7 Design of unreinforced walls and columns

⋮

§ 7.7.5.1 Slenderness ignored

The effects of slenderness can be neglected when the ratio of effective height-to-thickness (slenderness ratio), kh/t, is less than

$(10 - 3.5(e_1 / e_2))$.

Note: See Clause 7.5.1 for information on the factor k.

§7.7.5.2 Maximum slenderness

The slenderness ratio, kh/t, shall not exceed 30.

⋮

10 Design of reinforced walls and columns

⋮

§10.7.3.3 Slenderness limits

§10.7.3.3.1 Slenderness ignored

The effects of slenderness can be neglected when the ratio of effective height-to-thickness (slenderness ratio), kh/t, is less than

$(10 - 3.5(e_1 / e_2))$.

Note: See Clause 10.5.1 for information on the factor k.

§10.7.3.3.2 Effect of slenderness with kh/t less than or equal to 30

Except as provided in Clause 10.7.3.3.1, if the slenderness ratio, kh/t, does not exceed 30, the procedures 10.7.4.2 or 10.7.4.3 shall be applied.

§10.7.3.3.3 Slender walls with kh/t greater than 30

If the slenderness ratio, kh/t, of a wall is greater than 30, the design procedures and requirements of clause 10.7.3.3.2 and 10.7.4.6 shall be applied.

Note: The maximum slenderness for column is kh/t.

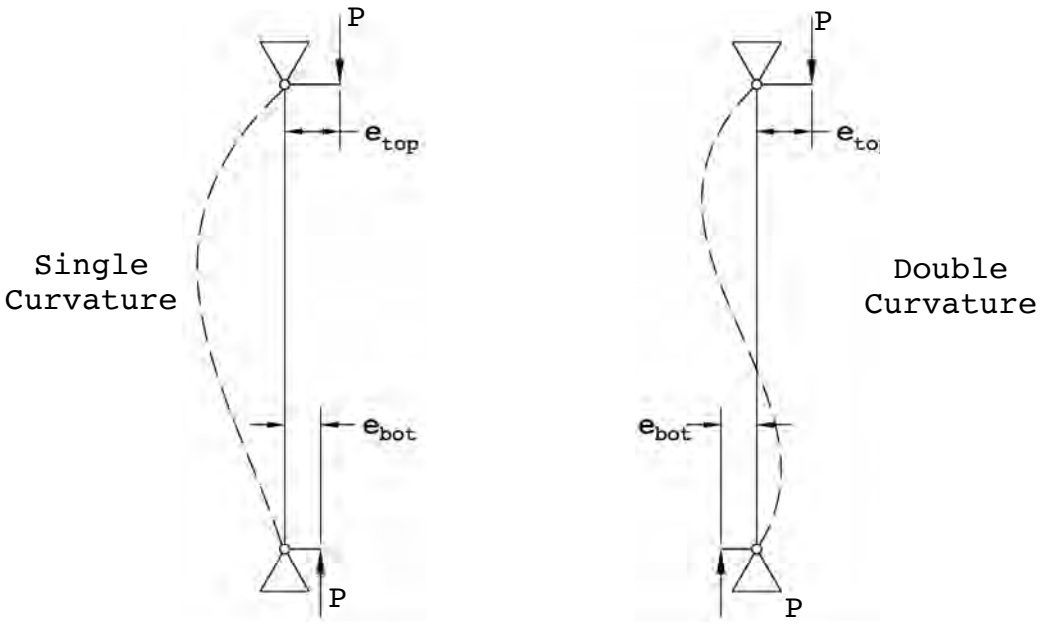

Figure 2-3: Eccentricities at top and bottom of a compression member

Where k is the effective length factor for compression members and e_1 and e_2 are the smaller and larger virtual eccentricity of axial load acting on top and bottom of the wall, respectively (Figure 2-3). So according to CSA S304, slenderness effects should be considered for walls where, kh/t, is between $(10 - 3.5(e_1/e_2))$ and 30; and for unreinforced masonry walls, kh/t cannot be greater than 30 and for reinforced masonry walls with kh/t greater than 30 specific provision are prescribed. It can be shown that the limit of 30 for kh/t is an approximate equivalent to the limit of 100 for kh/r for solid rectangular sections used in reinforced concrete structures where r is the radius of gyration (§10.13.2, CSA A23.3). It should also be noted that the approximated limit of 30 for kh/t is slightly conservative for fully grouted walls but is rather restrictive for partially grouted sections where for the same wall thickness, the radius of gyration is larger. For steel, maximum limit for kh/r is 200 (§25.7.3.1, CSA S16). Beyond these slenderness limits, the

behaviour of compression members is expected to be dominated by elastic buckling and for slenderness ratios less than these limits, behaviour is dominated by strength of the material. Therefore, compression capacities of members with slenderness ratios greater than these values are very low and the mode of failure in such cases is dominated by buckling.

Theoretically, all walls experience slenderness effects and design standards define where neglecting slenderness effects is allowed. According to previous research, it is reported that for all kh/t less than $(10 - 3.5(e_1/e_2))$, effects from slenderness is less than 10% at failure and therefore ignored in CSA S304 (Drysdale and Hamid 2005). However, as it will be shown in the next paragraph, this limit is according to single curvature loading and is conservative for double curvature cases (Figure 2-3). In the case of double curvature bending, the balancing shear force at the supports, tends to reduce the slenderness effects in early stages before failure. Therefore, there are cases of kh/t greater than $(10 - 3.5(e_1/e_2))$ that the slenderness effects are less than 10% at failure. Therefore, the term "non-slender" within this text, is not specifically limited into the first category of CSA S304 where $kh/t < 10 - 3.5(e_1/e_2)$. This category of the standard covers very short walls which normally are not present in masonry construction. The term "non-slender" in this text, is used to refer to walls where slenderness effects are less than 10% and negligible even if the slenderness ratio is bigger than $10 - 3.5(e_1/e_2)$. Therefore, the results of reliability analysis in this study relate to many of loadbearing walls in practice.

For instance, considering a wall with $f_m = 5$ MPa, $t = 190$ mm, $\rho_s = 0.0013$, the P-M interaction diagram according to CSA S304 is shown in Figure 2-4. P-M interaction diagram for a wall (or column) is constructed based on a failure criteria and presents the largest combination of axial load (P) and bending moment (M) that a section can resist for any given eccentricity. The

failure criteria according to CSA S304 is when the extreme compression fibre in masonry reaches a strain of 0.003. This compression strain corresponds to masonry crushing. The straight line represents $e/t = 10\%$ without slenderness effects and intersects with the interaction diagram at about $P = 390$ kN and $M = 7.4$ kN. m. The other two curves represent two scenarios with slenderness effects using the moment magnifier method. One curve is associated with a short simply supported wall, with $k = 1$, $h = 1240$ mm and with $e_1 = e_2 = t/10 = 19$ mm (single curvature) and therefore, $kh/t = 10 - 3.5(e_1/e_2)$. The other curve is associated with a wall, with $k = 1$, $h = 2800$ mm (normally seen in construction) and with $e_1 = -e_2 = t/10 = 19$ mm (double curvature) and therefore, $kh/t > 10 - 3.5(e_1/e_2)$. It is observed that both curves intersect with the interaction diagram at about $P = 376$ kN and $M = 8.0$ kN. m exhibiting about 13% magnification in bending moment at failure if compared to $M = 376 \text{ kN} \times 0.019 \text{ m} = 7.14$ kN. m and this is very close to 10% mentioned earlier. The intention of this example is to show that depending on the curvature patterns and eccentricity values, several cases can be found for $kh/t > 10 - 3.5(e_1/e_2)$ where secondary effects are about 10% or less. Thus, as mentioned earlier, the results of reliability analysis in this study can relate to many of scenarios of loadbearing walls in practice. Nevertheless, this investigation should be extended to walls where slenderness effects are more significant by direct reliability analysis.

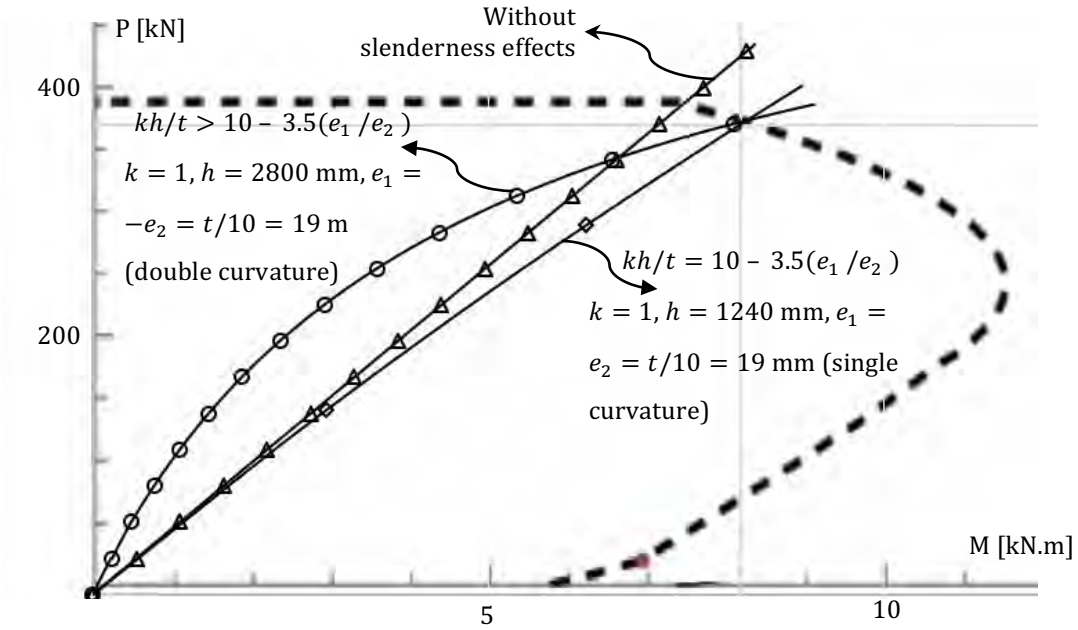

Figure 2-4: An example scenario where slenderness effects is less than 10% for a wall where $kh/t > 10 - 3.5(e_1/e_2)$

But the more important reason of studying "non-slender" walls separately and expanding the analysis to walls for which slenderness effects are considerable is that the Canadian building standards uses partial factor format to isolate different sources of uncertainty. Other than the fact that each load type has its own load factor, on the resistance side, there are three resistance reduction factors, namely, ϕ_m, ϕ_s, and ϕ_e (or ϕ_{er}). ϕ_m and ϕ_s are material resistance factors for masonry and steel reinforcement, respectively, and ϕ_e (or ϕ_{er} for the case of reinforced walls) is the resistance factor for member stiffness used in the determination of slenderness effects on the capacity of the masonry. A reasonable way of calibration of ϕ_m and ϕ_e, assuming that ϕ_s is the same for both reinforced masonry and reinforced concrete standards, is to deal with them separately. Therefore, this study presents a complete analysis on non-slender walls to provide a tool for

calibrating ϕ_m and in the next step proposes steps for the analysis of slenderness-sensitive walls for calibration of ϕ_e (or ϕ_{er}).

It is noteworthy that CSA S304 suggests two methods for considering slenderness effects when kh/t is less than 30 but higher than 10 – $3.5(e_1/e_2)$. These two methods are the moment magnifier method and the $P-\delta$ (load-displacement) method. Details for these methods are given in CSA S304 and are elaborated elsewhere such as Drysdale and Hamid (2005). The moment magnifier method is the more convenient alternative since the secondary moment is calculated directly as the product of factored moment and a magnifier coefficient. On the other hand, $P-\delta$ is an iterative procedure to work out the secondary moment resulting from deflection.

2.3 RELIABILITY OF MASONRY STRUCTURES

Reliability analysis of structural members is fully connected with standard requirements and those requirements are regional and local. The following sections explains how limit state design criteria was adopted over time in different regions. It is worth mentioning that each standard from each region has its own approach of adopting limit state criteria in terms of definition of limit state, design expressions, load/resistance factors designation and target reliability index. Moreover, structural reliability analysis needs to be done with local statistical information for each standard. Therefore, direct comparison of standard expressions and factors won't yield reliable conclusions. The sought goal in the following sections, other than observing major reliability studies which led to adoption of limit states criteria in CSA S304, is to point out and discuss some specific differences between approaches in CSA S304 and standards in other regions. Current Canadian guideline for designing reinforced and unreinforced masonry walls is CSA

S304-2014 This standard is referenced through this research for calculating specified resistance to the factored loads specified in NBCC.

2.3.1 CANADA

Preliminary safety analysis for masonry walls started in 1980. As a first step, walls under axial compression and out-of-plane bending moment and columns were considered. The purpose was to recognize the main parameters of a new masonry code based on limit states approach and the problems involved in development of such design procedures. The main problems were named to be the selection of a basic code format, specification of basic material strengths, treatment of the very significant uncertainties due to workmanship and inspection, and uncertainties in structural analysis. The reliability analysis results indicated that the design equations of the time did not provide consistent safety levels for different structural elements or for walls under different loading conditions. The results also suggested that the safety levels for masonry walls are relatively higher than those for other structural materials (Turkstra and Ojinaga 1980).

Afterwards, limit states design approach for load bearing masonry walls with minor axis bending was reviewed. The theoretical model involved the concept of an average value of flexural stiffness EI_{eff} dependent on the cracking pattern of the wall at a load level near failure. Since the proposed theoretical model did not account for buckling problems, a limiting slenderness, h/r, of 80 to 85 was assumed. For a solid wall this represents a h/t ratio of approximately 25. Moreover, because the theoretical results showed bias with respect to end eccentricity, a set of correction factors was applied to theoretical values. These correction factors were not based on any reasonable explanation (Turkstra et al. 1982).

In the same year (1982) the same researchers outlined the principles of development of a new limit states design code for unreinforced load bearing masonry structures in Canada and proposed a new code formulation for the design of eccentrically loaded walls. The reliability analysis performed, accounted for uncertainties due to material variability, workmanship, dead and live load magnitudes, load analysis, modelling errors, etc. The introduction of a modelling error variable was due to the fact that the analytical model for estimating wall capacity was unable to produce unbiased results. Uncertainties in net area and thickness were considered to be embedded in workmanship parameter. The results suggested that the code of the time was more conservative for single curvature than for double curvature with safety generally increasing with wall slenderness ratios. Also, there was a significant decrease in safety level for large eccentricities which was attributed to the fact that wall cracking is very sensitive to eccentricity and involves a great deal of uncertainty. It was concluded that ϕ factors of approximately 0.60 and 0.2 for inspected and uninspected masonry would yield average β values of around 4.5 (Turkstra et al. 1982).

Turkstra, based on a similar analysis approach, suggested to use 0.7 for masonry material strength reduction factor for specially inspected masonry to provide a safety index in the order of 4.0. And for masonry with routine inspection, material reduction factor was reduced to 0.4 for both clay and concrete units (Turkstra 1983). Also, in this research, for reinforced masonry, two cases were studied, i.e. heavily-reinforced and lightly-reinforced walls. It was shown that safety indices tended to decline with increasing eccentricity, to be nearly independent of live to dead load ratios and increase slightly with slenderness ratios. Finally, based on examination of a variety of results, the same values for masonry material strength reduction factor were suggested, namely, 0.7 for specially inspected workmanship and 0.4 for normally inspected workmanship. However, these

factors were suggested with $\gamma_s = 0.5$ for reinforcement steel where γ_s is strength reduction factor for reinforcement steel.

(Turkstra 1984) presented an overview of the development of a limit states design code for masonry without adding any new analysis. However, he suggested that with limiting design eccentricities to around 25% of the wall thickness $\phi = 0.6$ seems appropriate to achieve $\beta = 4.0$. This analysis was also reported in Turkstra (1989) with more discussions.

Following the above-mentioned studies, the limit states design method was included in the 1994 edition of S304 standard as an alternative to the traditional allowable stress design method (ASD). In the original draft of CSA S304.1-94, it was decided to use a single class of inspection and $\phi_m = 0.40$ was proposed according to the above-mentioned analyses which also included slenderness effects (Turkstra 1983; Turkstra et al. 1983). However, this was superseded and slenderness effects were considered separately and a resistance factor was applied directly to the effective flexural stiffness (EI_{eff}). So, in the 1994 edition of CSA S304.1, $\phi_m = 0.55$ was used based on a limited analysis that was later presented in (Laird et al. 2005) and then in 2004, following the increase in the resistance factor for concrete ϕ_c, the same analysis was used to justify increasing ϕ_m from 0.55 to 0.60 in the current edition of the masonry design standard, CSA S304-2014.

Changes in CSA S304-2004 from the previous CSA S304.1-94 were reported by (Laird et al. 2005). Mandatory limit state design and new resistance factors for masonry strength and stiffness and new load factors were a few of those changes. As mentioned earlier, the resistance factor for masonry, ϕ_m, was increased from 0.55 to 0.60. However, that did not affect the flexural tensile strength because the tabulated values for flexural tensile strength were reduced to compensate the increase in ϕ_m. As stated earlier, a short

statistical derivation by Drysdale (1992) was referenced to justify the rationale for the increase in ϕ_m.

Another change in CSA S304-2014 was the increase in the resistance factor for member stiffness, ϕ_{er}, from 0.65 to 0.75. This change was matched with the change in CSA A23.3 1994 (Laird et al. 2005) and was not based on any reliability analysis. ϕ_{er} is used in determination of slenderness effects for reinforced walls and columns.

Therefore, there is a need for a comprehensive structural reliability analysis to support parts of CSA S304 and the objective of this study is to investigate non-slender walls under combined axial load and out-of-plane bending.

2.3.2 U.S.

Structural reliability assessment for reinforced concrete has always led that for structural masonry. Calibration of resistance factors for ACI 318, Building Code Requirements for Structural Concrete, was done by determining these factors based on load and load combination factors specified by the ASCE Standard 7 (1998), Minimum Design Loads for Buildings and other Structures. The study included the development of calibration procedure, development of statistical models for load and resistance, reliability analysis for selected representative structural components and materials designed according to the ACI 318 1999 edition, selection of the target reliability indices, and finally determination of the recommended resistance factors for new editions of ACI 318 (Nowak et al. 2005). The considered load components were dead load, office live load, wind, snow, and earthquake. Statistical models of the loads are based on the data in (Nowak 2000). Monte Carlo simulation was used to assess the statistical parameters of resistance

for beams (in bending and shear), slabs (in bending and shear), and columns (Nowak et al. 2005).

By 1980s, the design criteria in the United States for engineered masonry construction was based on linear analysis and working stress design principles; however, efforts were underway to adopt the limit states design criteria following European countries. In one of these initial studies (Ellingwood 1981), first order reliability analysis was used to assess reliability indices for masonry walls under axial compression with and without eccentricity. It was concluded that there was sufficient amount of data on the strength and behaviour of masonry walls to start considering probabilistic limit states design as a basis for the standards; however, additional data was necessary in certain areas. For instance, there were not sufficient test replicates to establish confidently the probability distribution of strength. Moreover, there were limited data with which to establish the effect of workmanship or differences between laboratory and in situ walls in a statistical sense.

In a subsequent study, a comparison was made between using partial resistance factors and using overall resistance factor for the safety checking format of design expressions (Ellingwood and Tallin 1984). It was concluded that by isolating uncertainties in material properties (masonry and reinforcement steel) and applying different material strength reduction factors to each material, the reliability levels can be maintained more consistent over different cases of loading patterns.

The same authors investigated both non-slender and slender walls. They explored the effect of parameters such as eccentricity, e/t, slenderness, h/t, statistical correlation between different variables, reinforcement ratio. In all of the analyses, inspected workmanship was assumed and it was

acknowledged that additional work is needed to determine how to take workmanship into account (Ellingwood and Tallin 1985).

Reliability levels for other aspects of masonry construction are also studied. For example, Zorapapel (1991) studied the effects of system ductility and redundancy on the reliability of buildings whose lateral force resisting system is series of concrete masonry walls. The research was limited to walls with lateral force on top accompanying the axial load on the wall. Some other recent reliability analyses also include masonry walls subjected to explosive loads (Eamon 2007).

(ACI 530 2011) still permits for both allowable stress and strength design of structural masonry members. Unlike CSA S304-2014 which prescribes using partial strength-reduction factor for material strength, (ACI 530 2011) applies a global reduction factor,ϕ, on the nominal strength of the structural members. As mentioned earlier, partial reduction factors tend to yield more consistent reliability levels over different loading cases. Reduction factors in ACI 530 (2011) are different for various loading cases. For example, for combinations of flexure and axial load in reinforced masonry, ϕ shall be taken as 0.90, and in unreinforced masonry, ϕ shall be taken as 0.60. Also for masonry subjected to shear, the value for ϕ shall be taken as 0.80. There are also different ϕs for anchor bolts and bearing in masonry construction. Using global strength reduction factors versus partial strength reduction factors, is one of the important differences between the ACI 530-11 and CSA S304-2014.

2.3.3 EUROPE

Eurocode 6 (EC6) draft was first published in 1988 and is one of the standards that are issued by the European Committee for Standardization

(CEN). After a period of discussions on the draft form, the first part was issued in 1995 as a "pre-standard" or ENV under the title "*Part 1-1: General rules for buildings; Rules for reinforced and unreinforced masonry"* (Fyfe 2000). The code was used on a voluntary basis in a trial period. After making necessary amendments, the document was reissued as Eurocode 6 (EC6). Moreover, Eurocode 6 superseded, BS 5628: Part 1 (the British code of practice for structural use of unreinforced masonry). EC6 is based on limit state principles and the values for the partial factors of safety for material properties, γ_m, have been chosen by the Drafting Panel based on the best experience available to them (Fyfe 2000). γ_m is material strength reduction factor for masonry in EC6 similar to $1/\phi_m$ in CSA S304. These values are set out in Table 2–3. Since the final γ_m values may need to be modified to fit the conditions and the target level of reliability in the Member States, the values shown in Table 2–3 are boxed.

Table 2–3 Partial factors of safety, γ_m, ENV 1996-1-1 (1995)

γ_m		Category of execution		
		A	*B*	*C*
Category of manufacturing control of masonry units	*I*	1.7	2.2	2.7
	II	2.0	2.5	3.0

From Table 2–3, it can be seen that there are two different situations for the category of manufacturing control, and three different situations for the category of constructions control. While by satisfying the requirement of category '*I*', there is about 10% of benefit compared to category '*II*', there is a benefit of about 35% for meeting category '*A*' of construction control compared to category '*C*'. This shows the intrinsically high variability associated with the construction phase. Combining the effect of both measures, there would be a 45% reduction in γ_m, i.e. from 3.0 to 1.7. In

addition to the fact that CSA S304-2014 uses different design expressions from Eurocode 6, CSA S304-2014 does not recognize different levels of inspection and construction.

Reliability studies on masonry construction are more extensive in Europe than other regions. For example, Brehm and Lissel (2012) reported a comprehensive study on the reliability of unreinforced masonry bracing walls where the reliability was determined by SORM. Some other studies also performed preliminary reliability analysis on different types of structural members such as Schueremans and Van Gemert(1998) on masonry shear walls for historical masonry buildings and Casas (2011) on reliability assessment of masonry arch bridges.

2.3.4 AUSTRALIA

There have been notable studies on structural reliability of masonry members in Australia. In an earlier investigation, unreinforced brick masonry walls in flexure were studied (Stewart and Lawrence 2002). Many sources of uncertainty were considered such as discretizing of masonry unit thickness, unit bond strength, hypothesis of failure mechanism, and load intensity. The results showed that reliability levels are most affected by wall width, workmanship, discretizing of masonry unit thickness. It was indicated that reliability levels for masonry walls are comparable to, and in some cases higher than, for other structural materials.

Subsequent studies showed that the Australian standard for masonry structures, AS3700-2011, is unnecessarily conservative for walls loaded concentrically in compression. Therefore, recommendation was made that ϕ for walls loaded concentrically in compression be increased from 0.45 to 0.75 in AS3700-2011. These result was based on a reliability-based code

calibration (FORM) using experimental data from several research works. Both slender and non-slender masonry walls were studied in this analysis (Stewart and Lawrence 2006).

In another research, the reliability of unreinforced masonry in vertical bending was assessed in order to calibrate the capacity reduction factor, ϕ, in the Australian Masonry Structures Code AS 3700. Different factors influencing the reliability of masonry in vertical bending were studied, including model error, wall height and discretization of wall thickness. It was concluded that the $\phi = 0.6$ in code of the time should be decreased to 0.47 if a target reliability of $\beta_T = 4.3$ is required.(Lawrence and Stewart 2009)

Similar to ACI 530-11, AS 3700-2011 uses a global reduction factor for the structural member; while in CSA-S304-2014, uncertainties are isolated and different reduction factors are applied to each, namely, ϕ_m for masonry strength, ϕ_s for reinforcement steel and ϕ_{er} (ϕ_e) for effective flexural stiffness.

2.4 BEHAVIOURAL MODELS FOR LOAD BEARING WALLS

As noted earlier, in order to perform a comprehensive reliability analysis leading to development of practical probability-based resistance criteria, there is a need for a behavioural model that predicts the strength of the wall based on mechanical and geometrical properties given. This section covers different types of behavioural models in the literature including both analytical and numerical models.

Bending behaviour of load bearing masonry walls is considerably affected by out of plane lateral loads. This behaviour is highly nonlinear due to two

aspects; (1) nonlinear material characteristics involving nonlinear stress-strain relationship in compression and tensile cracking in masonry and yielding in steel reinforcement, (2) second order effects as a result of out-of-plane deflection of the member which is also known as slenderness effects.

2.4.1 ANALYTICAL MODELS

To obtain an estimate of the safety level implied in any design procedure, an unbiased theoretical formulation is of great advantage. There have been several studies on the analysis of masonry members subjected to eccentric compressive loads. The major goal of these studies has been developing a technique for analysis of the stability of masonry members under simultaneous axial compression and out-of-plane moment. The challenges in coming up with an accurate model that predicts the strength of a masonry wall include nonlinearities such as tensile cracking of masonry joints, compressive crushing of masonry, nonlinear stress-strain relationship of masonry under compression, and geometric nonlinearities in large deflections (slenderness effects).

In most of the leading studies, significant simplifying assumptions were adopted which prevented accurate enough results (Yokel and Dikkers 1971; Sahlin 1971; Tesfaye and Broome 1977; Schultz and Mueffelman 2003; Drysdale and Hamid 2005). These assumptions include linear behaviour of masonry material under compression, adopting stress-strain behaviour similar to concrete for masonry material, and selecting a constant reduced flexural stiffness (EI) over the height of cracked masonry walls.

In some other studies, differential equations were derived according to partially cracked members (Chen and Atsuta 1973; Frisch-Fay 1977; Frisch-Fay 1980; Romano et al. 1993; Ganduscio and Romano 1997; De Falco and

Lucchesi 2002). In other words, the presence of uncracked regions was also considered in those studies.

In all the aforementioned cases, the equations were derived for particular combinations of loading or boundary conditions. For example, one of the widely studied cases is a cantilever member subjected only to an eccentric point load at the top (Yokel et al. 1971; Chen and Atsuta 1973; Frisch-Fay 1975; Frisch-Fay 1977; De Falco and Lucchesi 2002). Other cases include cantilever members under eccentric gravity loads (Sahlin 1971) or its own weight (Tesfaye and Broome 1977; Frisch-Fay 1980), cantilever members under simultaneously vertical and lateral loads (Romano et al. 1993; Ganduscio and Romano 1997).

(Turkstra et al. 1982) used an "equivalent" linear analysis and acknowledged that it was approximate. Ultimate prism compression strength, f'_m, was used as a basic mechanical property representative of several factors such as shape of masonry units, mortar type and mortar bedding arrangements. The main assumption was that the flexural rigidity EI is given by the initial tangent modulus of elasticity and an effective moment of inertia. The effective moment of inertia was given by expressions for different end eccentricity ratios. It was stated that this model was not able to produce unbiased estimate of experimental results. Therefore, a modelling variable was introduced to alleviate this problem. This approach was also utilized in a few other publications e.g. (Turkstra 1983; Turkstra 1989).

As another approach, moment magnifier method was used to account for slenderness effects by (Ellingwood and Tallin 1985). It was stated that statistical data for Euler load, P_E, depends on the rigidity EI of the cracked section and on the fixity of the ends of the walls. It was acknowledged that statistical information for EI for masonry is unavailable. Moment magnifier

method is a fast approach and more accurate expressions for *EI* revealed from recent studies make this method more reliable. However, numerical simulations, such as finite element method, are always the most comprehensive yet accurate approach.

2.4.2 NUMERICAL SIMULATIONS

The most practical yet comprehensive approach to account for material nonlinearity, uncracked regions, different load and restraint conditions, different cross sections (grouted or partially grouted) or even non-prismatic members is to select an appropriate numerical simulation. Therefore, for a comprehensive reliability analysis, choice of numerical simulations is more sensible.

(Rots 1991) identified three basic approaches for modeling the mortar bed joints: macro-modeling where bed joints are smeared out, simplified micro-modeling where bed joints are represented by masonry unit-mortar interface, or detailed micro-modeling where mortar bed joints are modeled by continuous elements. (Payne et al. 1990) carried out a mixed finite element and finite difference analysis considering the masonry unit and the bed mortar joint separately. The unit-interface approach, where the mortar properties are neglected and the joints are modelled as potential lines of cracking failure, is better suited for two-way dynamic analysis where load reversals may occur and is mostly used to study the in-plane behaviour of unreinforced masonry (Lotfi and Shing 1994). However, the application of this approach is extended to out-of-plane analysis recently (Martini 1997). In smeared joint approach, masonry composite is treated as a homogeneous material with mechanical properties representing the effect of both masonry unit and mortar bed joint. Therefore, the whole member is represented by the same kind of element. This approach is desirable because of its simplicity

and efficiency and is suitable for modeling the overall behaviour of masonry members (Romano et al. 1993). This method has been widely used for simulating the out-of-plane behaviour of unreinforced masonry members under compression.

A finite element model was developed by (Suwalski and Drysdale 1986) that used 2-dimensional triangular elements for the masonry and Goodman Joint elements for bond between reinforcement and grout, and between the mortar and the blocks. The analysis was incremental and included large deformations with provisions made at each step for cracking, crushing and debonding to be identified and incorporated into the model. The smeared crack approach was used to model cracking and the stiffness of a cracked element was modified by reducing the stiffness of the element in the direction of the largest principal tensile stress.

Masonry load-bearing walls are generally long enough to be analyzed or tested ideally as wide columns with free side edges that are under uniform axial load and lateral loading. (Ganduscio and Romano 1997) stated that if the effects of lateral edge restraints are negligible, the analysis of masonry wall can be advantageously carried out by idealizing the member as a beam-column. This fact has been used in many numerical studies afterwards.

A simplified finite element analytical technique was developed to predict the capacity of reinforced load-bearing masonry walls under different loading conditions (Liu 2002). This analytical technique accounted for non-linearity of the masonry stress-strain relationship, different eccentric axial loadings, point applied or distributed lateral loads, single and double curvature effects, fixed or simple end supports, various patterns of reinforcement, and nonlinear loading and unloading. This model was used to calculate effective flexural stiffness (EI) of cracked masonry walls more accurately in order to

assess slenderness effects. Bernoulli beam element was used and the behaviour of the wall was captured by gradually applying the load/displacement by performing step-by-step finite element model. Element stiffness matrices at each step were constructed based on the flexural stiffness, EI, read from the slope of the moment-curvature curve for the corresponding axial load. Therefore, at each single step the moment-curvature curve for the corresponding axial load had to be constructed.

(Vassilev et al. 2002) presented a numerical model for the analysis of structural members under eccentric compression. The equilibrium was formulated in the deformed state and took account of the effect of deflections on the bearing capacity. For a realistic modelling of the composite material behaviour in compression and bending a parabolic stress-strain function was assumed. The solution of the system was obtained within an iterative numeric procedure, based on the discretization of the structure into finite segments, the piecewise linearization of its parameters. The piecewise integration of the equilibrium differential equation led to a formulation in terms of the transfer matrix method. The ultimate state is recognized either by equilibrium bifurcation and loss of stability or collapse due to material failure. Similar to the work by (Liu 2002), at each step, the transfer matrix was established based on the slope of the moment-curvature curve for the corresponding axial load.

(Lu 2003) developed a comprehensive two-dimensional finite element model for axially-compressed and transversely-loaded unreinforced masonry walls assuming one-way bending. The model is capable of capturing post-cracking and post-buckling behaviour of slender URM members and it considers both material and geometric nonlinear analysis of the walls. Similar to the model by (Liu 2002) for reinforced masonry walls, the wall was idealized as a beam–column and assuming that cross sections remain plane after

deformation, the finite element model simulated the entire load–deflection behaviour by using planar beam-column elements. The model is applicable to a large variety of load combinations and restraint conditions, as well as solid or hollow cross-sections. Finite tensile strength of masonry was assumed, and a realistic stress–strain relationship for masonry in compression was employed. Masonry was treated as a homogeneous material with some tensile strength. The displacement-control method and the arc-length control method were implemented and used to trace the entire equilibrium path. The major difference between this model and the work done by (Liu 2002) was in the construction of the stiffness matrix. Instead of constructing the moment-curvature curve for each axial load level and reading the flexural stiffness, EI, from the graph to establish the stiffness matrix, the stiffness matrix is worked out directly from the constitutive stress-strain relationship of the materials and the corresponding strain state for each element. This eliminates solving involved equations which include integrations over the cross section.

The method used by (Lu 2003) for unreinforced masonry walls was extended for investigating the mechanics and behaviour of slender post-tensioned masonry walls (Popehn 2007). Nevertheless, in both studies, there were a few assumptions in formulation of the stiffness matrix for sake of simplification. These assumptions lead to a stiffness matrix corresponding to Timoshenko beam element which does not perform as well as the Bernoulli beam element when the beam is thin. Timoshenko beam model takes into account shear deformation, making it suitable for describing the behaviour of shorter beams. It does not perform as well as Bernoulli beam formulation when the beam is typically dimensioned or thin because too much strain energy is taken by shear (Felippa 2012). (Lu 2003; Popehn 2007) used these simplifications so that they can explicitly describe the stiffness matrix and the vector of element nodal forces of the beam element in terms of nodal

displacements of the element and of course the material stress-strain characteristics.

The model used in this study is similar to the model by Lu (2003) except that the material behaviour is updated according to recent literature. The selected material behaviour is explained in the next section. This model is capable of capturing material nonlinearities, i.e. post-cracking and crushing of masonry and yielding of steel reinforcement. The masonry is presumed to be a homogeneous material with some tension strength. This model is 2D and relatively simple to implement and yet, the prediction capability of this model has been verified to be adequate and consistent with experimental results. The behavioural model is explained and verified in chapter 3. These features make this model an appropriate option for a thorough reliability analysis. For non-slender walls where secondary effects are negligible, the behavioural model is used to construct the P-M interaction diagram point by point for different eccentricities starting from pure bending to the case of axial load only. The failure criterion which is used is crushing of the masonry at the extreme compression fibre. This criterion is applied by assuring that the compression strain at the extreme compression fibre is 0.003 (Drysdale, Hamid et al. 1994). Mathematica® is used as the coding language. A sample code for generating P-M interaction diagram is presented in the Appendix.

Although the results of this study are limited to non-slender walls, the algorithm and framework for the case of walls with slenderness effects is proposed at the end. The behavioural model is proposed to be implemented to analyze the walls as beam-column members. As explained before, the formulation of the stiffness matrix is worked out directly from the constitutive stress-strain relationship of the materials and the corresponding strain state for each element. Bernoulli beam element formulation of the stiffness matrix is recommended which gives a better representation of the

behaviour of load-bearing masonry walls under out-of-plane loading. Another approach suggested is to use the moment magnifier method to account for secondary effects. The algorithm and framework for walls with slenderness effects are illustrated in Chapter 6.

2.4.3 MATERIAL BEHAVIOUR

The composite nature of masonry makes it practical to relate the strength of structural masonry members to prism strength rather than to unit and mortar strengths. Nevertheless, it should be noted that full-size structural members usually behave more uniformly than prisms and are less affected by variations in workmanship and materials (Ellingwood 1981). There has been a common assumption that masonry material behaviour is adequately similar to concrete material behaviour. However, recent experimental data from researchers who also investigated the post-peak region of masonry material behaviour, i.e. beyond the strain at maximum strength, suggest that this assumption is not valid and different equations for masonry are needed Liu (2002). Experimental results have shown that the stress-strain relationship for masonry under compression is a nonlinear relationship. This nonlinearity is principally attributed to mechanical characteristics of the mortar joints between the masonry units (McNary and Abrams 1985; Ahmad et al. 1987) and this nonlinearity increases with the decrease in mortar strength (Ahmad et al. 1987).

Equivalent rectangular stress block is used by many standards to represent the ultimate strength and its coefficients are calibrated for the case when the section is under dominant bending. Using the equivalent rectangular stress block for masonry (or concrete) in compression does not adequately represent the effect of stress distribution in the section when compression is dominant over the section (Ellingwood and Tallin 1985).

Although it is possible to take into account different nonlinear stress-strain relationship for bricks/concrete blocks and mortar (Payne et al. 1990), it has been verified by comparison with experimental results that acceptable accuracy can be achieved by considering the masonry material as a continuum with one nonlinear stress-strain relationship that should be based on numerous prism test data (Romano et al. 1993).

In most prior studies, especially in the case of unreinforced members, masonry was assumed to have no tensile strength and a relatively simple stress-strain relationship in compression was used. Examples for those relationships are linear elastic (Yokel and Dikkers 1971; Yokel et al. 1971; Tesfaye and Broome 1977; Schultz and Mueffelman 2003), nonlinear monomial elastic (Romano et al. 1993; Ganduscio and Romano 1997), or linear elastic with bounded compressive strength and deformability (De Falco and Lucchesi 2002). Very few studies accounted for masonry tensile strength along with linear elastic relationship in the compression zone (Chen and Atsuta 1973; Frisch-Fay 1975; Frisch-Fay 1977; Frisch-Fay 1980).

Stress-strain curves of masonry vary from nearly linear for bricks with certain mortars to more nearly parabolic for concrete blocks with other mortars. The assumption of a linear stress block leads to increasingly conservative predictions as load eccentricity increases (Turkstra 1989).

Another fact about masonry stress-strain behaviour is that depending on strain gradient, the flexural compression strength is remarkably more than the axial compressive strength from prism tests. Therefore, a factor equal to or greater than 1.0 was applied to compressive strength of masonry, f_m, depending on the load eccentricity. This factor was equal to unity at $e/t = 0$ to about 1.4 at $e/t = 1/3$ (Ellingwood 1981).

Important parameters in stress-strain relationship for masonry are the masonry compression strength, strain at maximum stress, slope of the falling branch of the stress-strain curve after maximum stress is reached and the ultimate compression strain. These parameters are important because they are needed for calculating the strains in reinforcement using the compatibility approach and finally working out the ultimate flexural strength.

Monomial nonlinear expressions which are normally obtained by least-square fitting, e.g. (Romano et al. 1993) are expressed as

$$\sigma = S\,\epsilon^{\mu} \qquad \text{(Eq. 2.2)}$$

where S and μ are constant parameters. Two weak points for this stress-strain relationship are exhibiting infinite rigidity at $\epsilon = 0$ and not including any softening branch.

(Naraine and Sinha 1989) obtained an exponential stress-strain relationship capable of predicting both hardening and softening behaviour in compression without any singular points.

$$\sigma = E\,\epsilon\,\exp\left(-\frac{\epsilon}{\epsilon_0}\right) \qquad \text{(Eq. 2.3)}$$

This expression was also used by (Lu 2003) and (Popehn 2007) for stability analysis of unreinforced masonry members under simultaneous vertical and out-of-plane lateral loads.

In this study, having masonry compressive strength, the stress-strain relationship is constructed using a model similar to the model proposed by (Priestley and Elder 1983). This model has been shown to have good agreement with experimental data for unconfined masonry and for masonry confined by 3.1 mm thick steel plates in the bed joints. However, for the study herein, it is assumed that the maximum stress occurs at a strain equal to 0.002 compared to 0.0015 assumed by (Priestley and Elder 1983). This was done because it has been shown more recently that the strain at maximum stress is around 0.002 for the currently used materials in the masonry industry (Drysdale and Hamid 2005). The curve consists of three portions: a parabolic rising curve, a linear falling branch, and a final horizontal plateau (constant stress) and is expressed in Equation 2.4. Essentially, compression stress increases with strain (parabolic rising curve) and arrives at a maximum right after initiation of a failure mode which is a combination of vertical splitting and shear/compression failure depending on the relative confinement of masonry prism (Priestley and Elder 1983). The stress-strain curve takes zero slope around maximum stress and falls rapidly as the failure mode dominates and the curve flattens afterwards.

$$\sigma = \begin{cases} f'_m \left[\frac{2\epsilon}{0.002} - \left(\frac{\epsilon}{0.002}\right)^2\right], & \epsilon < 0.002 \\ f'_m \left[1 - Z(\epsilon - 0.002)\right], & 0.002 < \epsilon < \epsilon_{0.2u} \\ 0.2\, f'_m \quad , & \epsilon_{2ou} < \epsilon \end{cases} \qquad \text{(Eq. 2.4)}$$

where

$$Z = \frac{0.5}{\left(\frac{3 + 0.29\, f'_m}{145\, f'_m - 1000}\right) - 0.002} \qquad \text{(Eq. 2.5)}$$

ϵ_{2ou} is also shown in Figure 2-5.

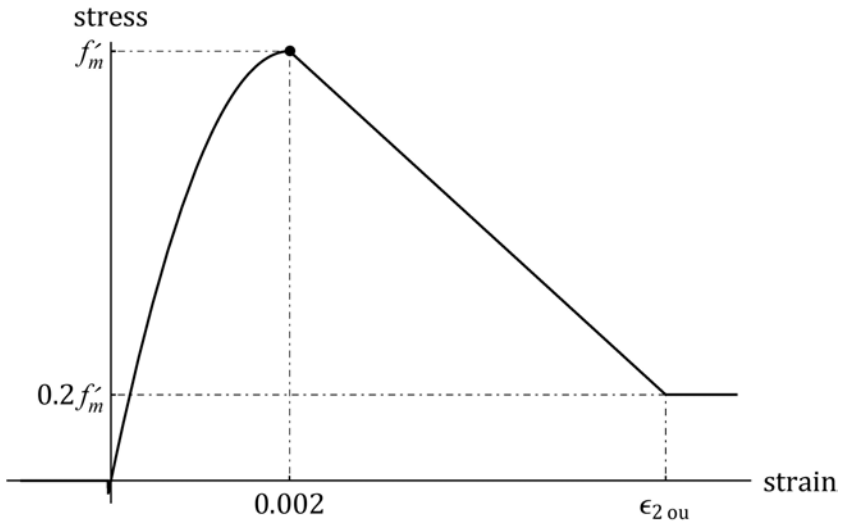

Figure 2-5: stress-strain relationship for masonry

The flexural tensile strength normal to bed joints for solid and hollow masonry depends on the tensile bond between unit and mortar and varies from 0.2 to 1.75 MPa (Drysdale and Hamid 2005). In the research presented here, the stress-strain relationship is assumed linear up to the flexural tensile strength. The flexural tensile strength is considered 0.4 MPa for concrete

brick and block and 0.65 MPa for grouted hollow block and brick according Table 5 in CSA S304-2014. For enhanced numerical convergence, a post-cracking tensile softening branch is included in masonry material behaviour.

The stress-strain relationship for reinforcement steel is assumed to be elastic-perfectly plastic as illustrated below. Statistical properties of reinforcement steel are presented in Chapter 5.

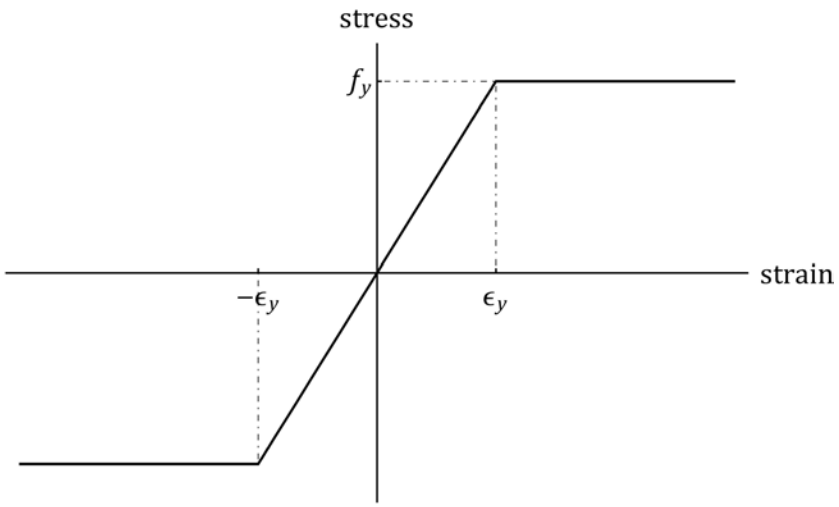

Figure 2-6: stress-strain relationship for reinforcement steel

2.5 EFFECT OF WORKMANSHIP

Workmanship quality has a substantial effect on masonry strength and cannot be neglected. Workmanship relates to construction practices, mason qualifications, and inspection. When the quality control procedures set forth in the standards are followed, the member strength is close to what is observed in laboratory tests; however, it has been shown when the masonry work is uninspected, the ultimate strength of walls is much less. For example,

research has shown that the strength of uninspected unreinforced brick walls tends to be on the order of two third of the strength of the inspected ones (Brick Institute of America 1969; Hendry 1976). Some sources of workmanship and inspection uncertainty are: (a) the thickness and furrowing of mortar joints, (b) grouting procedures, (c) wall or column verticality (wall plumbness), (d) geometrical compliance of structural members with design values (fabrication tolerances), and (e) the level of quality control during construction (Brick Institute of America 1969; Hendry 1976; Turkstra and Ojinaga 1980).

Also, (Hendry 1990) discussed the effect of different site factors on masonry performance and concluded that the following factors are the more important ones (in order of relative importance)

- Incorrect adjustment of suction rate of masonry units
- Failure to fill bed joints
- Bed joints of excessive thickness
- Deviation from vertical plane alignment
- Unfavourable curing conditions
- Incorrect proportioning and mixing of mortar
- Disturbance of units after laying

The combined effect of all factors could result in a wall which is perhaps half of its intended strength (Hendry 1990). However, site provision and control procedures will result in strengths close to those built in the laboratory and therefore, use of excessively large safety factors is unnecessary.

(Fyfe et al. 2000) examined and quantified the effects of various causes of the reduction in the strength of masonry due to workmanship quality through the application of a finite element model. They considered three workmanship defects: 1) misalignment of wall panels. 2) Excessive thickness

of mortar joints. 3) Excessive variations in mortar thickness. It was concluded that that the most effective defect is excessive thickness of mortar joints which produces a safety factor of 1.69 and if all three effects were to occur together, the overall value of the specific partial factor of safety will be 2.08.

(Francis et al. 1971) developed a quantitative mechanism for the compressive failure of brickwork and showed its capability to explain the influence of certain variables on compressive strength. It was shown experimentally and theoretically that the strength of four-brick prism declines as the joint thickness increases and as the lateral tensile strength of the bricks diminishes in relation to their compression strength. The effect of some other well-known parameters like brick and mortar properties, bond strength, and joint reinforcement was also explained in quantitative terms.

As mentioned earlier, bed joint thickness affects the strength of masonry remarkably and directly reflects the level of workmanship. A study was performed at the University Texas, Austin (Grimm 1988) to determine the distribution of the coefficient of variation of bed joint thickness and head joint thickness, and also the deviation of masonry head joint from vertical plumb for 24 arbitrarily selected buildings. The ages of the buildings ranged from 1 to 92 years. 13 of these buildings were less than 17 years old. The buildings were of different occupancy types, i.e. civic, residential, recreational, commercial, educational and religious. For each of the 24 buildings the thickness of 30 bed joints and 30 head joints was measured. It was observed that the bed joint thickness variation is better controlled than head joint thickness variation. As shown in Figure 2-7, the 33 percentiles fell between 11.9% and 15.5 % for coefficient of variation of bed joint thickness. Thus, it was concluded that if the coefficient of variation in bed joint thickness was less than 12%, that aspect of masonry workmanship could be

characterized as good, above 16% as poor, and in between as fair. A similar conclusion was made about head joint thickness according to Figure 2-8, i.e. if coefficient of variation was less than 17%, that aspect of masonry workmanship is good, greater than 21% as poor, and between 17% and 21% as fair.

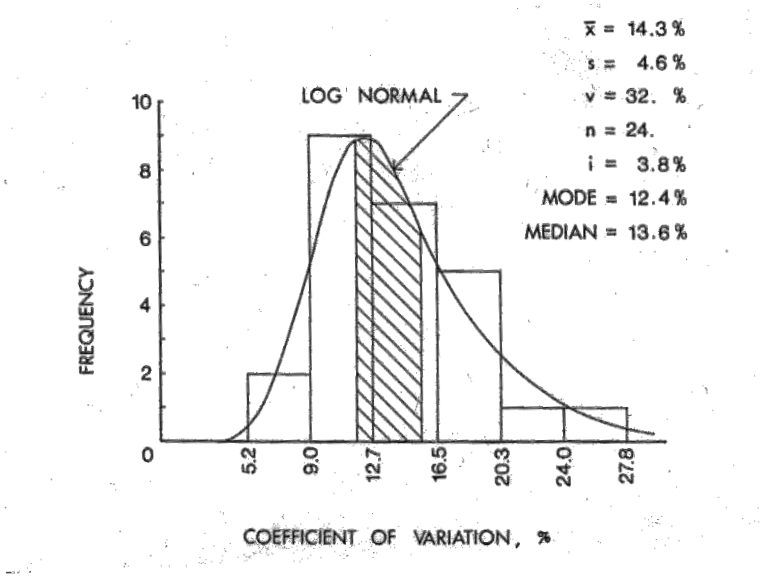

Figure 2-7: coefficient of variation in bed joint thickness in brick masonry (Grimm 1988, with permission from ASCE)

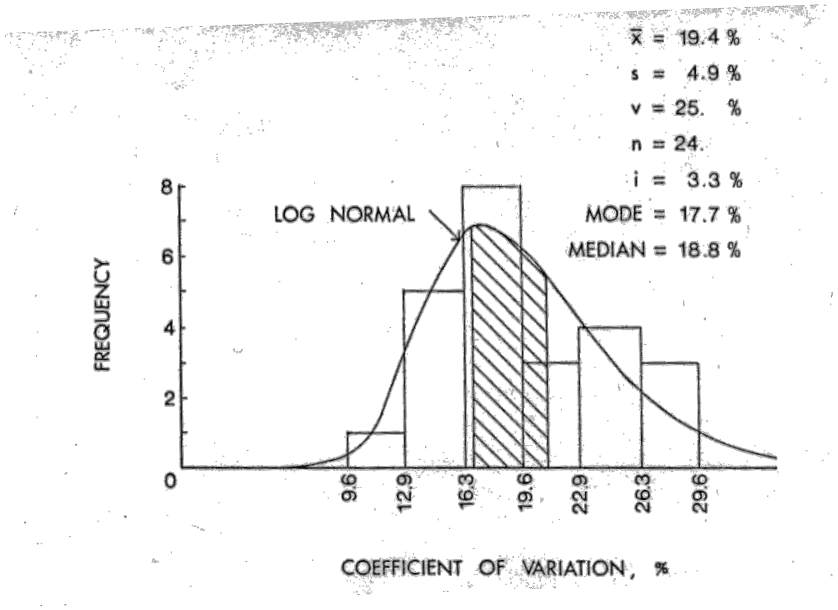

Figure 2-8: coefficient of variation in head joint thickness in brick masonry (Grimm 1988, with permission from ASCE)

Assuming a single level of workmanship (or inspection), as it is in S304, might be reasonable only if appropriate measures were taken to ensure the assumed workmanship quality; otherwise, in a relatively weakly inspected construction practice, any well-inspected construction would be severely penalized. Some standards and authorities for masonry construction, e.g. the British code, Eurocode 6, or the Brick Institute of America, prescribe different partial safety factors for different levels of quality controls (Turkstra and Ojinaga 1980). Despite the fact that workmanship factor needs to be probabilistically identified and be applied accordingly to the reliability analysis, this factor has been selected based on engineering judgement in all studies related to reliability of masonry construction in Canada (Turkstra 1983; Laird et al. 2005). The following is some of the values considered for workmanship effect in different building standards and guidelines.

Partial factors of safety for material strength γ_m from BS 5628 are

γ_m		Category of construction control	
		Special	Normal
Category of manufacturing control	Special	2.5	3.1
	Normal	2.8	3.5

Partial factors of safety for material strength γ_m from EC6 are

γ_m		Category of construction control		
		A	B	C
Category of manufacturing control of masonry units	I	1.7	2.2	2.7
	II	2.0	2.5	3.0

In order to include workmanship effect in the reliability analysis, statistical characteristics for this parameter needs to be known. Based on experimental data, three sets of bias coefficient and CoV were proposed by Turkstra (1989) for the workmanship factor: 1.0 and 0.1 for well inspected, 0.8 and 0.15 for regularly (moderately) inspected, and 0.7 and 0.2 for uninspected masonry. All structural work in Canada is required by the provincial building codes to have periodic review during construction. The level of review has to be such that the designer is satisfied the work is in reasonable conformance with the design. The structural engineer has to sign a form to that effect before the building can be occupied. This level of review would be referred to as "moderate work inspection". The Canadian standard S304.1 however does not recognize other levels of inspection. For the current study, a bias coefficient of 0.85 and a CoV of 0.15 and normal distribution, intended to represent regularly inspected masonry, were used in the analysis based on

the values proposed by Turkstra. Since mortar furrowing does not take place in block masonry construction and the unit height-to-mortar thickness ratio for block masonry is three times that for brick masonry, the slightly higher bias coefficient than that proposed by Turkstra is justified. In an earlier research, Ellingwood (1981) assumed a workmanship factor of 1.0 for inspected workmanship and "slightly conservatively" 0.6 for uninspected workmanship. Also, coefficients of variation of 0.11 and 0.15 were used respectively. Nevertheless, workmanship factor is one of the parameters that needs to be investigated in detail to ensure the statistical information are representative of the current masonry construction practice in Canada.

2.6 STATISTICAL DATA FOR MASONRY CONSTRUCTION

Resistance of a structural member is mainly a function of geometrical and material properties of the member. Resistance parameters considered in this study include

- Masonry compressive strength
- Wall thickness
- Reinforcement location and yield strength
- Masonry workmanship factor
- Rate-of-loading factor

Background for these parameters and statistical values selected for them are explained in Chapter 5.

2.7 STATISTICAL DATA FOR LOADING

The most comprehensive recent study on statistics of different loading types on structures in Canada was reported by (Bartlett et al. 2003). This study was done to support the adoption of companion-action format for load combinations in the 2005 edition of the National Building Code of Canada (NBCC) and also the fact that NBCC was going to specify wind and snow loads based on their 50 year return period values. The study summarized statistics for dead load, live load due to use and occupancy, snow load, and wind load that was used for calibration, and a following paper presented the calibration of load factors. For this study results of the above-mentioned paper is used as it will be seen in Chapter 5.

Chapter 3

Verification of the Behavioural Model

GENERAL

This chapter explains the basics for development of a behavioural model for the analysis of non-slender load-bearing masonry walls; reinforced or unreinforced. The outcome of this model is the interaction diagram between axial compression and out-of-plane bending moment resisted by a given masonry wall.

This model is capable of capturing material nonlinearities, i.e. post-cracking and crushing of masonry and yielding of steel reinforcement. The masonry is presumed to be a homogeneous material with some tension strength. This model is then verified with experimental results in the literature.

3.1. STRESS-STRAIN RELATIONSHIPS

The masonry is treated as a homogeneous material whose mechanical characteristics such as compressive strength and modulus of elasticity are obtained from tests on masonry prisms (assemblages of block units and

mortar). The stress-strain behaviour for masonry and reinforcement steel was presented in Chapter 2. These relationships are both converted to Mathematica® language as functions and then embedded in the main code for reliability analysis. The Mathematica code for steel reinforcement behaviour is written so that considering reinforcement in compression is optional. This is because CSA S304, allows compression in steel reinforcement only if it adequately tied. In this study, compression in steel reinforcement is ignored, as tying reinforcement is not the normal practice in masonry wall construction.

3.2. BEHAVIOURAL MODEL FOR NON-SLENDER WALLS

The P-M interaction diagram is constructed point by point starting from pure bending. The failure criterion which is used is crushing of the masonry at the extreme compression fibre (Figure 3-1). This criterion is applied by assuring that the compression strain at the extreme compression fibre is 0.003 (Drysdale, Hamid et al. 1994).

First, the corresponding neutral axis for pure bending is found by establishing the equilibrium of forces over the section. It is necessary to determine whether the steel reinforcement yield at pure bending.

Then the other points of the diagram are found by gradually increasing the neutral axis distance from the extreme compression fibre until the point of pure axial compression. At each step, the selected distance for the neutral axis and the selected crushing compression strain described above define a strain profile over the section. This strain profile is then used along with the stress-strain relationships to work out internal stresses and finally external forces.

For the purpose of structural reliability analysis, another P-M interaction diagram has to be constructed based on expressions from the masonry standard, CSA S304. The procedure is basically the same; However, rectangular stress block is used for masonry and strength reduction factors are applied on masonry and reinforcement steel. Figure 3-1 briefly illustrates the conversion of the real stress-strain behaviour to an equivalent rectangular stress block with the same resultant force vector. Details can be found in the literature (Hatzinikolas, Korany 2005).

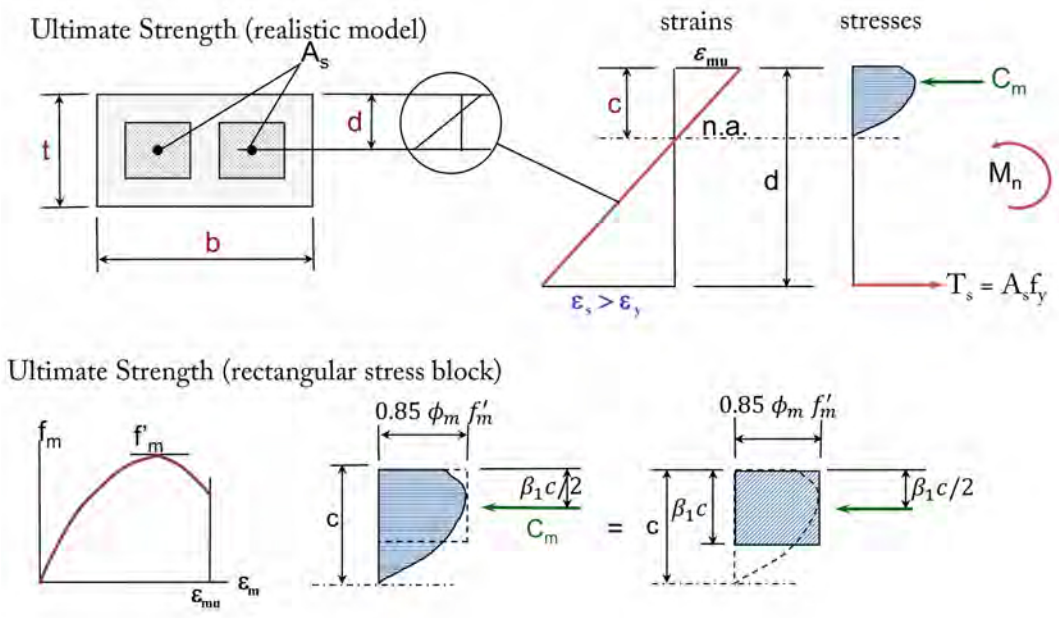

Figure 3-1: Conversion of masonry to equivalent rectangular stress block

3.3. VERIFICATION WITH TEST RESULTS

Although the principle of this behavioural model has been verified elsewhere (e.g. Lu, M. 2003) and only the masonry stress-strain behaviour has been improved in this study, the selected procedure was compared to some previously tested full-scale walls by constructing the corresponding

interaction diagrams. The results are shown in Figures 3-2 to 3-7. In all the following figures the solid line represents the PM interaction diagram based on the explained behavioural model. The dotted line represents the PM interaction diagram based on S304 expressions. Test results are illustrated by points. Specifications for the test specimens are given in the figures.

In Figures 3-2, 3-3, 3-5 and 3-6, the difference between the norms (distance to origin) of experimental results and corresponding points on the interaction diagram with the same eccentricities are within 5%. Experimental points in Figures 3-2 to 3-4 and 3-7 lie in the compression-controlled part of the diagram and points in Figures 3-5 and Figure 3-6 lie in the tension-controlled part of the diagram. For Figures 3-4 and 3-7, the prediction errors are approximately 35% and 50% but still conservative.

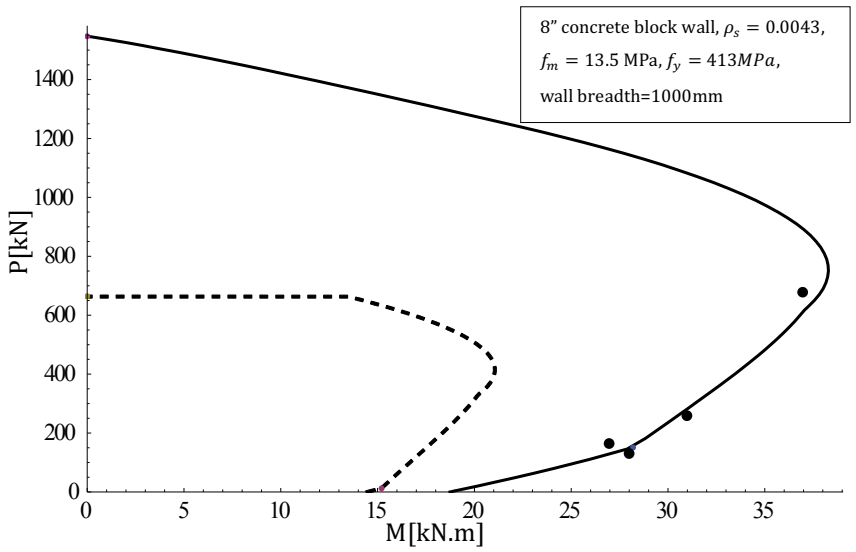

Figure 3-2: Comparison between test results by (Yokel, Mathey et al. 1971) and the behavioural model used in this study

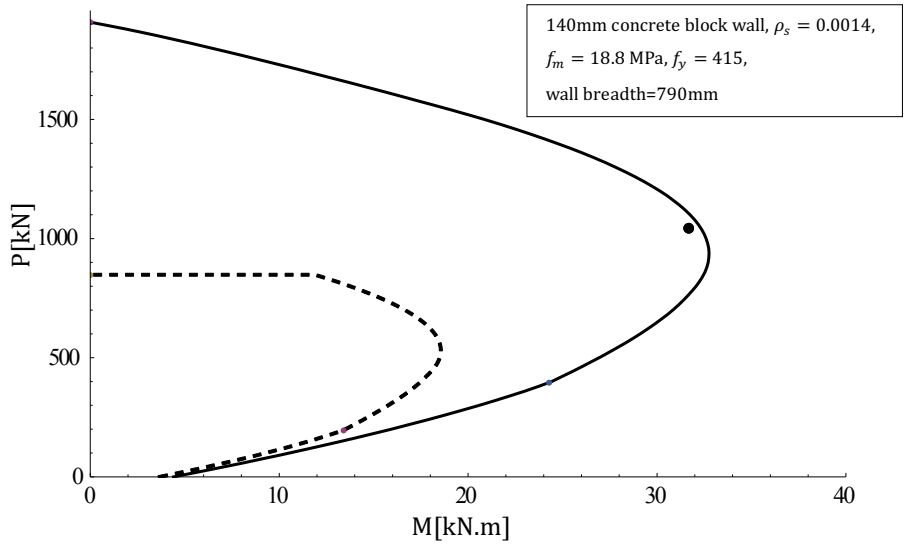

Figure 3-3: Comparison between test results by (Aridru 1997) and the behavioural model used in this study

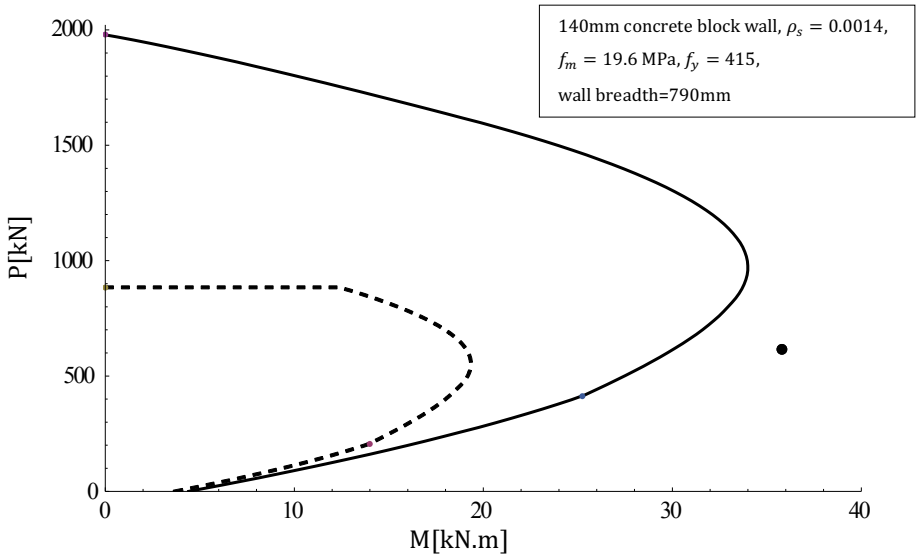

Figure 3-4: Comparison between test results by (Aridru 1997) and the behavioural model used in this study

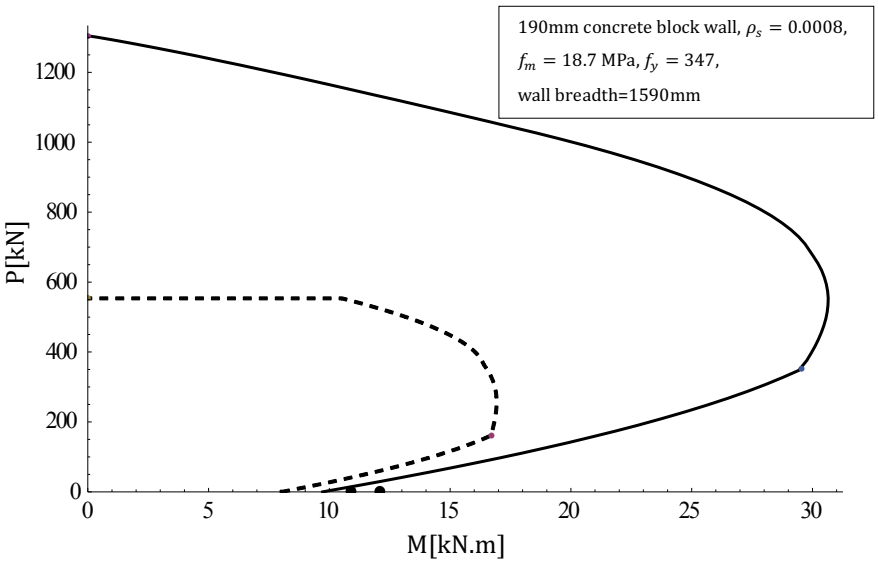

Figure 3-5: Comparison between test results by (Fereig, Hamid 1987) and the behavioural model used in this study

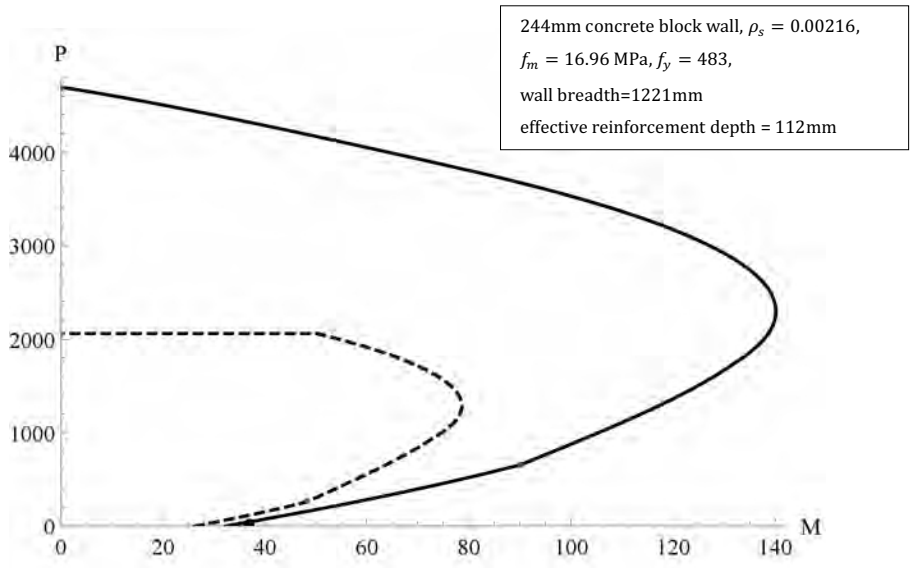

Figure 3-6: Comparison between test results by Athey, J. (1982) and the behavioural model used in this study

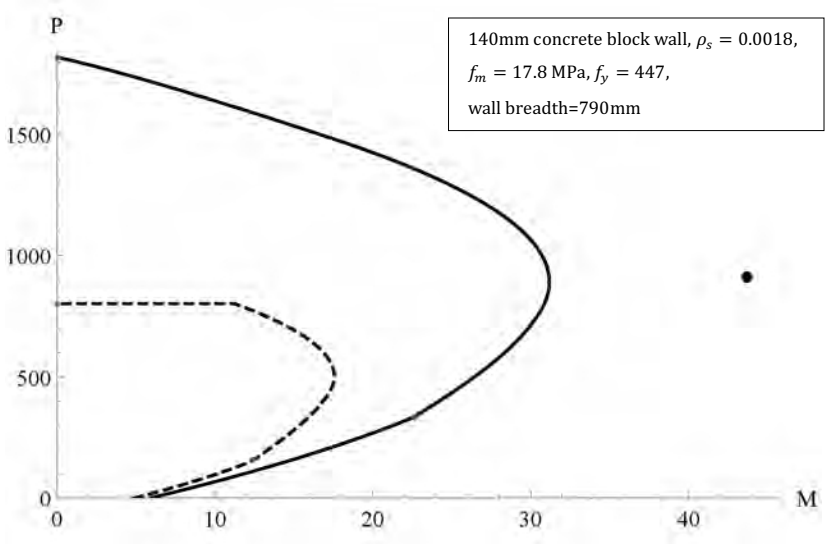

Figure 3-7: Comparison between test results by Hu (2006) and the behavioural model used in this study

Figure 3-8 shows the norm ratio of experimental results to predicted values from Figure 3-2 to Figure 3-7 along with some other experimental results for different eccentricity ratios (Yokel, Dikkers 1971, Aridru 1997, Hu 2006, Olatunji, Warwaruk et al. 1986). The logarithmic scale is chosen for eccentricity ratio to include cases with large eccentricities. Ratios for cases of pure bending are also included (Fereig, Hamid 1987, Sasanian 2009). The average ratio of experimental results to the results from the introduced model is 1.17 with a coefficient of variation of 0.215. Taking into account the variability of experimental results for masonry walls, even for walls with similar material and geometrical properties, the selected behavioural model demonstrates adequate consistency and has been used in several studies. In this study, this model is embedded into reliability analysis algorithm.

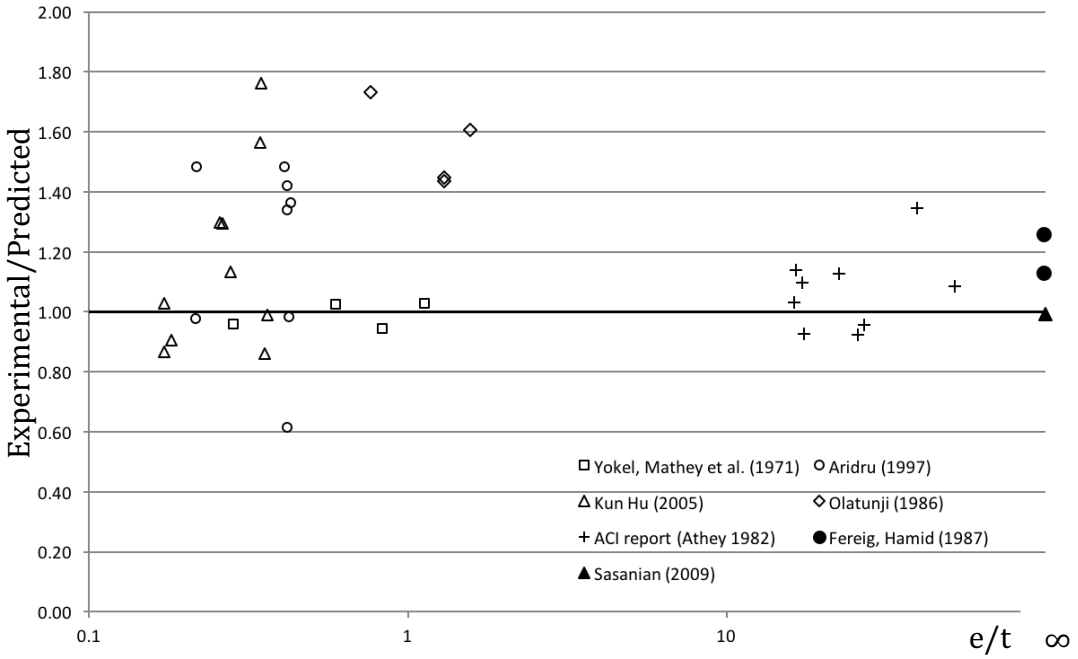

Figure 3-8: Comparison between test results by several investigations and the behavioural model used in this study

3.4. BEHAVIOURAL MODEL FOR MASONRY WALLS CONSIDERING SLENDERNESS EFFECTS

Masonry load-bearing walls usually transmit concentric or eccentric gravity loads combined with lateral loads due to wind or earthquakes. For relatively slender members, strength is reduced by secondary moment caused by axial load acting through a deflected shape. For the case of masonry walls, low tensile strength of masonry causes tension cracking which results in variation of effective sectional properties, like flexural rigidity (EI), over the member height.

There have been many studies on the subject of stability of masonry members where usually specific loading conditions and particular mechanical properties for masonry were considered (Hatzinikolas, Longworth et al. 1978, Frisch-Fay 1975, Sahlin 1971, Maksoud, Drysdale

1993). With complexities related to the interaction of geometric and material nonlinearities, it has been preferred to work out simplified approaches which have limited application. Most analytical equations are for single curvature under eccentric compressive load. Although finite element method is a more comprehensive and still accurate method, there are approximate methods like P-Delta and moment magnifier method which because of their simplicity can be incorporated more suitably in a reliability analysis; where an iterative method is used and a time-exhaustive behavioural model like FEM is not preferred.

In CSA S304-2014, a moment-magnifier method is introduced to account for secondary moment effect by applying a magnification factor to an equivalent uniform primary moment.

$$M_{ftot} = M_{fp}\frac{C_m}{\left(1-\frac{P_f}{P_{cr}}\right)} \text{ but not less than } M_{fp} \qquad \text{(Eq. 3.1)}$$

where

M_{fp}: the maximum factored primary moment of the member due to the end factored moments and lateral loads, N. mm

C_m: factor relating actual moment diagram to an equivalent uniform moment diagram and calculated as follows

$$C_m = 0.6 + 0.4\frac{M_1}{M_2} \text{ but not less than } 0.4 \qquad \text{(Eq. 3.2)}$$

The ratio M_1/M_2 shall be determined

(a) when calculated eccentricities are greater than $0.1t$, by calculating end moments; or

(b) if calculations show that there is essentially no moment at both ends of a compression member, by taking the ratio M_1/M_2 equal to 1.0.

Also where lateral loads occur between the ends of the member such that they contribute more than 50% of the factored moment at the critical section, the ratio of M_1/M_2 shall be taken as equal to 1.0.

$$P_{cr} = \frac{\pi^2 \phi (EI)_{eff}}{[(1 + 0.5\beta_d)(kh)^2]}$$

This method accounts for masonry tensile cracking, by calculating an effective flexural rigidity, EI_{eff} to modify the critical Euler buckling load. This method has the advantage of simplicity and is preferable to use. However, there is some uncertainty and conservatism as to how to include effects of slenderness, tensile cracking, reinforcement and loading conditions for the calculation of critical buckling load. According to CSA S304-2014, EI_{eff} is calculated as follows.

For unreinforced masonry

$$(EI)_{eff} = 0.4E_m I_o \qquad \text{(Eq. 3.3)}$$

For reinforced masonry

$$(EI)_{eff} = E_m \left[0.25I_o - (0.25I_o - I_{cr})(\frac{e - e_k}{2e_k})\right]$$

and $E_m I_{cr} \leq (EI)_{eff} \leq 0.25E_m I_o$

ϕ: resistance factor for member stiffness used in the determination of slenderness effects on the capacity of the masonry. ($\phi_e = 0.65$ for unreinforced masonry and $\phi_{er} = 0.75$ for reinforced masonry)

β_d: ratio of factored dead load moment to total factored moment

k: effective length factor for compression member

h: unsupported height of a wall

E_m: modulus of elasticity of masonry may be taken as $850f_m$ but not greater than 20000 MPa

I_o: moment of inertia of the effective cross-sectional area of a section about its centroidal axis, mm^4

I_{cr}: the transformed moment of inertia of the cracked section calculated ignoring the effects of axial load, mm^4

e: M_{fp}/P_f, mm

e_k: S_e/A_e, mm

S_e: Section modulus of the effective cross-sectional area (A_e), mm^3

For sake of reliability analysis for slender walls, a reliable behavioural model is required. Moment magnifier method has been shown to reveal reliable results provided that an appropriate effective flexural rigidity $(EI)_{eff}$ is utilized (MacGregor et. al. 1975). With the aim of proposing more accurate values for effective flexural rigidity $(EI)_{eff}$, a computerized numerical method was developed by (Liu, Dawe 2003) to study the behaviour of masonry walls with a wide range of physical characteristics and subjected to various loading conditions. The model was verified by comparison of results with test data obtained from the same research and other research reported in the literature. The computer model was then implemented to conduct a comprehensive parametric study to investigate the effects of various

parameters on the strength and behaviour of masonry walls. Load–deflection histories, ultimate load and moment capacities, and $(EI)_{eff}$ values at the time of failure were obtained using the analytical method. These results were compared with those based on the moment-magnifier method recommended by CSA-S304.1-M94 which for calculation of $(EI)_{eff}$ are the same as those based on CSA-S304.1-2014. It was concluded that CSA-S304.1-M94 tends to underestimate $(EI)_{eff}$ values for reinforced walls and this leads to a conservative design over a range of parameters. The following lower bound bilinear limit for the effective rigidity of reinforced masonry walls was established based on about 500 computer model tests.

For $0.0 \leq e/t \leq 0.4$

$$(EI)_{eff}/E_m I_o = 0.80 - 1.95(1.00 - 0.01\,h/t)(e/t), \quad \text{(Eq. 3.4)}$$

For $0.4 < e/t$

$$(EI)_{eff} = 0.022(1.00 + 0.35\,h/t) \quad \text{(Eq. 3.5)}$$

For structural reliability analysis of slender masonry walls it is suggested to use moment magnifier method and using the expressions Equations 3.4 and 3.5 for effective flexural rigidity.

Alternative to using moment-magnifier method with modified parameters to yield more accurate results, is using finite element method, e.g. the procedure used by Liu, Dawe (2003). Using a numerical method such as finite element is assured to provide accurate results at the expense of more computation effort. In Chapter 6, both moment magnifier method and finite element

method are suggested to extend reliability analysis of this investigation to walls with slenderness effects.

3.5. CONCLUSION

The selected behavioural model was presented in form of a computer code in Mathematica® and was verified with experimental results in this Chapter and two methods are suggested to be used for walls with slenderness effects.

The expressions proposed by (Liu, Dawe 2003) for effective flexural rigidity utilized in moment magnifier method provides a working hypothesis for a behavioural model for masonry walls. It should be noted that the reliability analyses will be performed for walls constructed with filled masonry units where the limit state equations are relatively simple. The good agreement between the behaviour of laboratory- tested partially grouted walls and the predictions of strength suggests that the conclusions drawn from a reliability analysis of partially grouted walls would be similar (Ellingwood, Tallin 1985). Extending the analysis to partially-grouted walls will strengthen the results.

Chapter 4

Sensitivity Analysis

GENERAL

Sensitivity of the P-M interaction diagram to different parameters is studied in this chapter. One of the parameters is the method used to construct the P-M interaction diagram; namely, equivalent rectangular stress block versus using the real stress-strain behaviour. Other parameters include steel reinforcement area, wall thickness, masonry compressive strength, steel yield stress and maximum usable strain in masonry.

4.1 P-M INTERACTION DIAGRAM

4.1.1 Equivalent Rectangular Stress Block

According to CSA S304-2014, the interaction diagram for reinforced masonry walls under axial compression and out-of-plane bending moment, may be based on any masonry stress-strain relationship that results in prediction of strength in substantial agreement with results of comprehensive tests (§10.2.5). However, CSA S304-2014 also presents the equivalent rectangular

masonry stress block as a satisfactory tool for working out the wall strength (§10.2.6) and this method is generally used in design approach. Details and examples of this method can be found in CSA S304-2014 and (Hatzinikolas, Korany 2005). Another more realistic stress-strain behaviour for masonry is based on the relationship proposed by (Priestley, Elder 1983) and the maximum usable compression strain for masonry defined by (Drysdale, Hamid 2005). Details for this model were illustrated in Chapter 3, section 3.1.

In order to construct the interaction diagram for a given section, the first step is to find the neutral axis corresponding to pure bending moment. This is done by equating the compression force in masonry and the tension force in the reinforcement in the case of reinforced masonry wall. For unreinforced masonry, the tension force results from tension strength of the masonry. If no tension strength was considered for masonry, the strength of the unreinforced wall under pure bending is considered to be zero. The compression and tension forces are calculated based on a presumed strain profile at failure and the stress-strain behaviour of the materials. The strain profile at failure is usually established by assuming a maximum value for usable strain masonry under compression.

After finding the neutral axis corresponding to pure bending and the strength of the wall under pure bending, the distance between the neutral axis and the compression face is increased step by step. For each step, the corresponding axial force and bending moment about the mid-section can be found by using the stress-strain behaviour of the materials. Therefore, for each step a pair of axial force and bending moment is worked out and by plotting these points, P-M interaction diagram is constructed.

Figures 4-1 and 4-2 provide a comparison between the P-M interaction diagrams based on the above mentioned stress-strain behaviours. The solid

curves correspond to the equivalent rectangular stress block and the dotted curves correspond to the stress-strain behaviour proposed by (Priestley, Elder 1983). Values for axial force and bending moment are normalized by the capacity of the wall under axial load only and pure bending resistance of the wall according to the equivalent rectangular stress block. No material strength reduction factor is used for masonry and reinforcement steel as the goal is the comparison between these behavioural models. The comparison between two methods is done for different reinforcement ratios, wall thicknesses and masonry strengths. It is apparent that in compression controlled zone, the strength defined by CSA S304 is conservative compared to the strength predicted by the behavioural model proposed in this study; about 6 to 15 percent. However, in tension controlled zone, the difference is negligible. This is expected since in the tension-controlled zone, reinforcement has yielded and the tension force is equal for both cases regardless of the masonry behaviour. Also, because the compression zone becomes smaller as we approach to pure bending the difference in moment arm becomes less for two methods and therefore, the effect of the stress block shape becomes less significant. Moreover, it should be noted that the coefficients for equivalent rectangular stress block are calibrated for pure bending and the difference between two methods vanishes approaching pure bending.

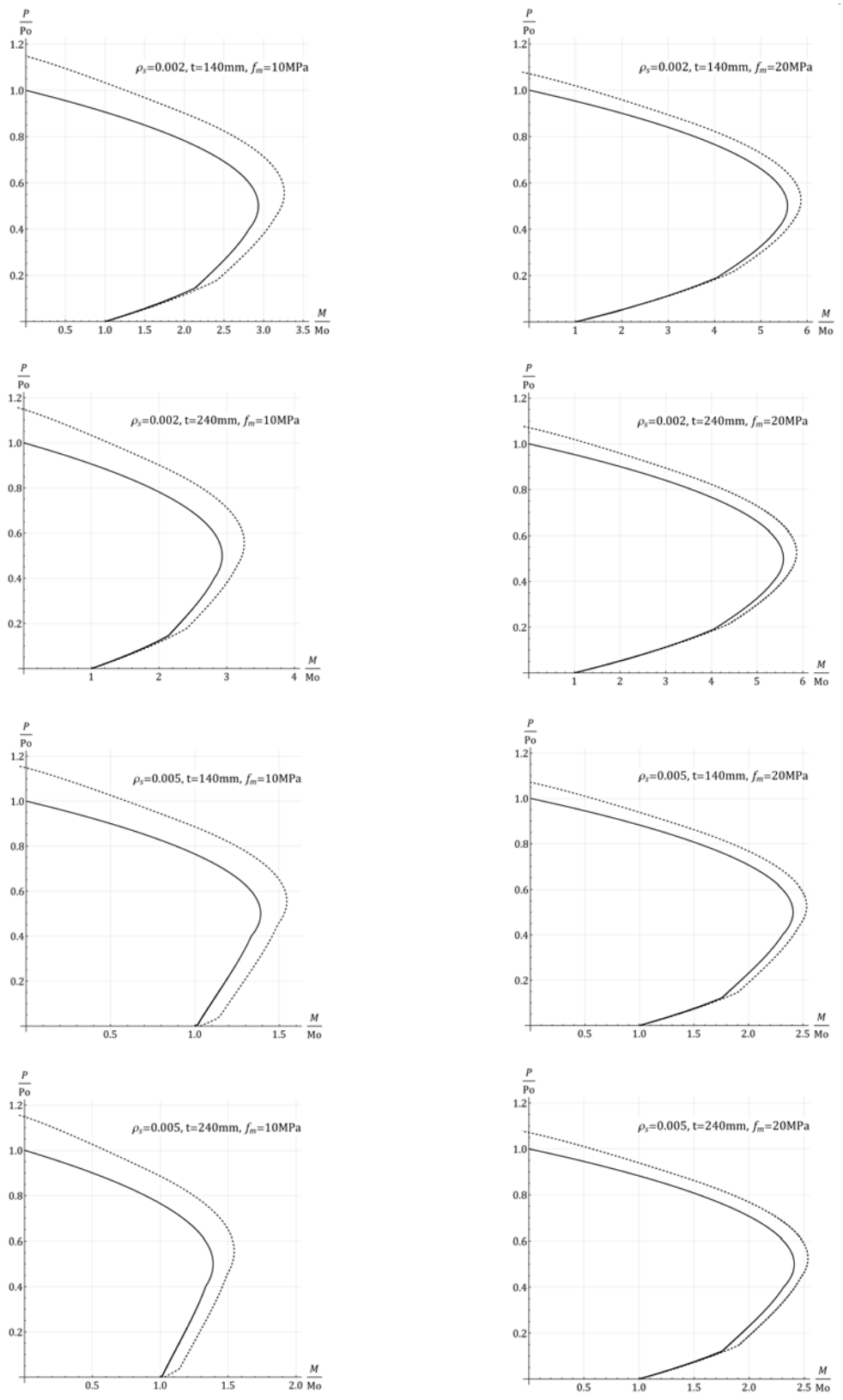

Figure 4-1: Different behavioural models (CSA S304 and proposed model)

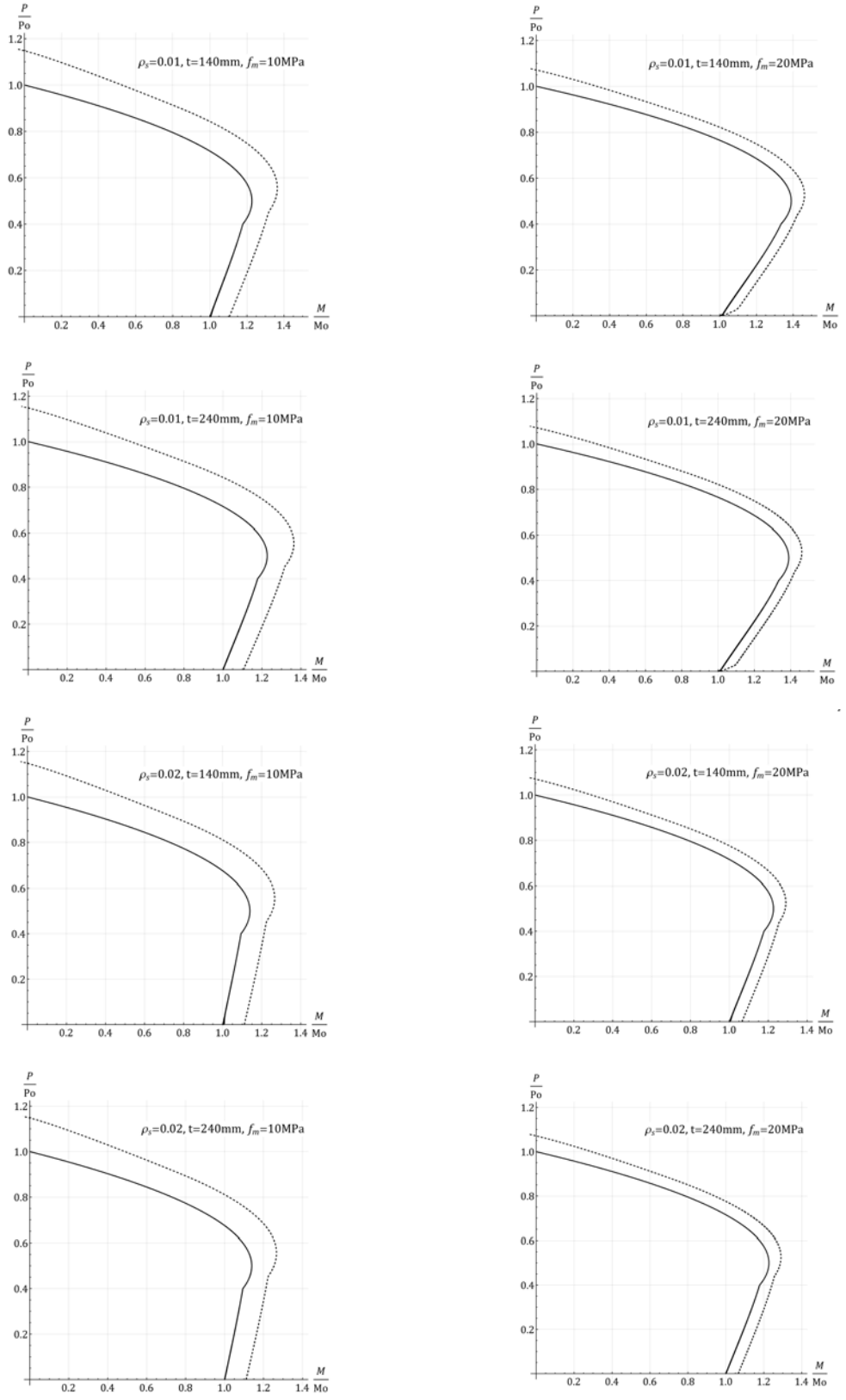

Figure 4-2: Different behavioural models (CSA S304 and proposed model) cont'd

4.2 SENSITIVITY ANALYSIS

4.2.1 Steel reinforcement area

Figure 4-3 shows the effect of 10% change in steel reinforcement area on the P-M interaction diagram. While this effect is only present in the tension-controlled portion of the diagram, since rebar are factory products, not much deviation is expected for this parameter in real world construction. The difference between the curves emerge at a point where the steel reinforcement starts to be in tension at failure which is bit before balanced point.

4.2.2 Wall thickness

As shown in Figure 4-4, the effect of variation in wall thickness on wall strength is significant. However, in the case of concrete masonry walls, masonry blocks are factory made and 10% variation is not expected. As will be discussed in Chapter 5, the coefficient of variation for wall thickness is about 0.01.

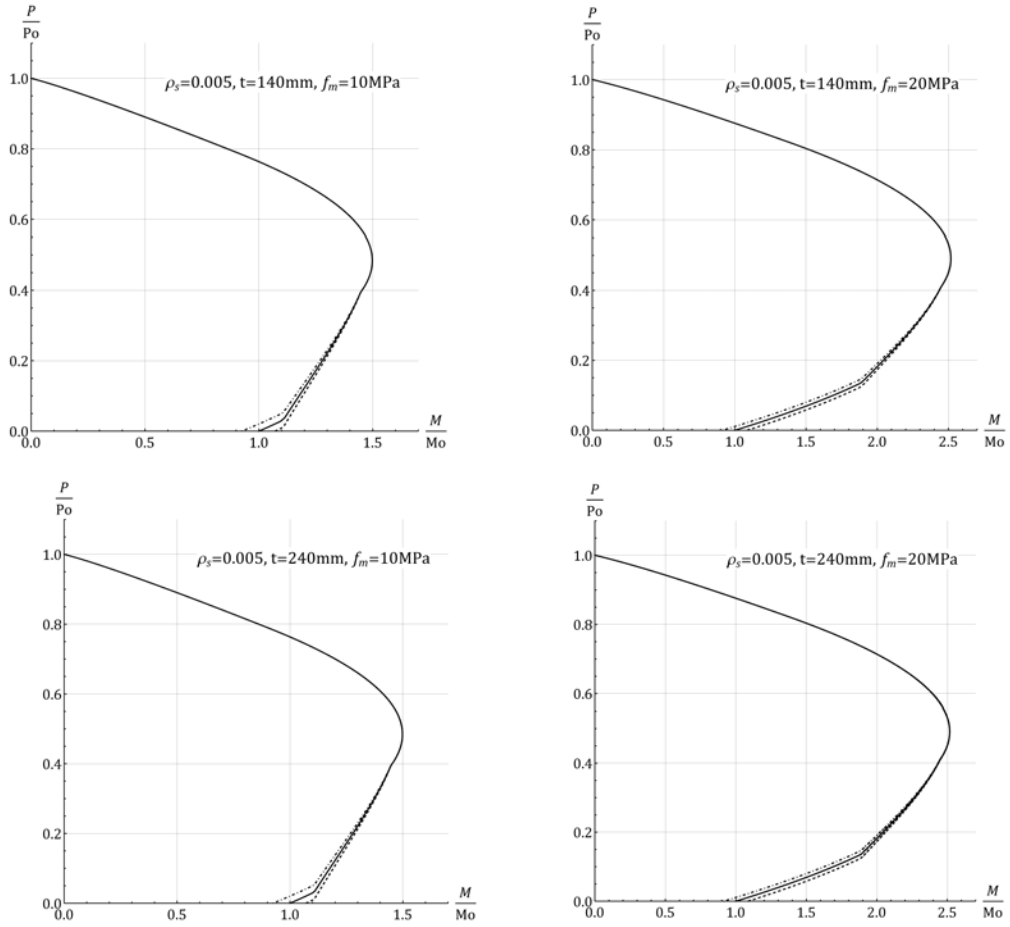

Figure 4-3: Effect of 10% change in reinforcement area

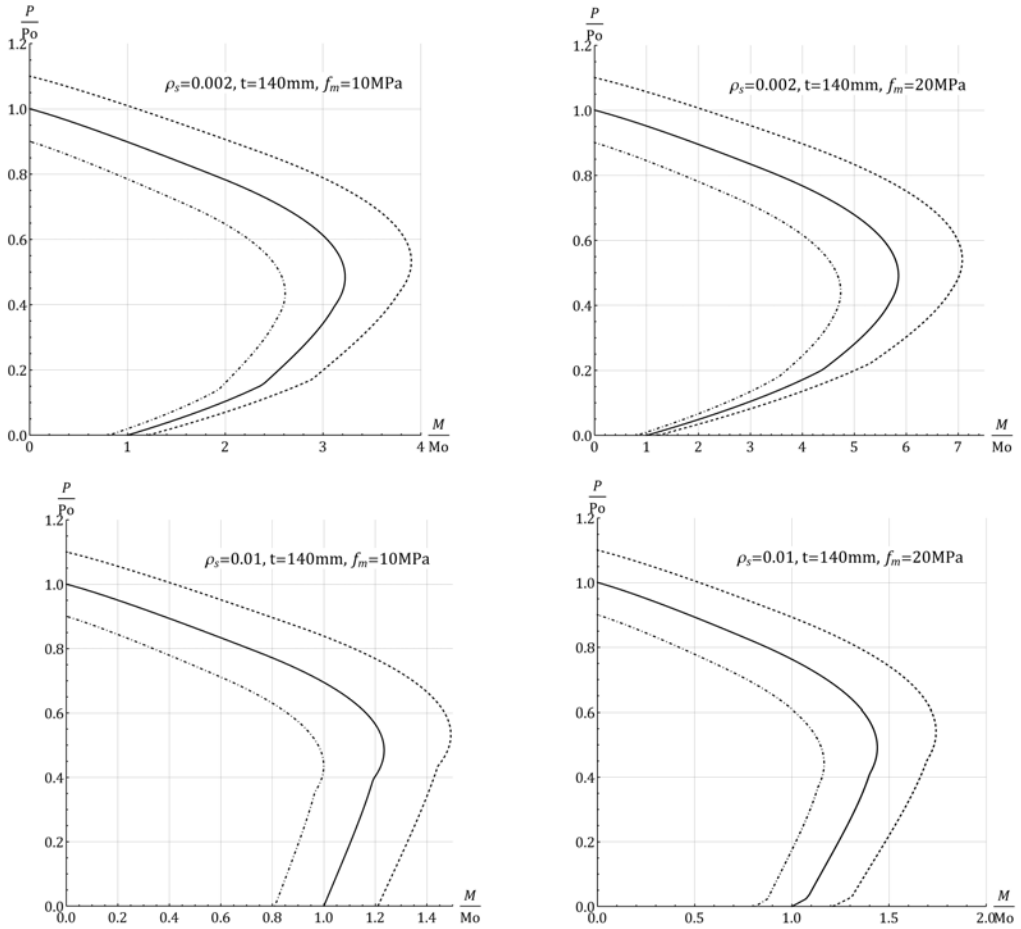

Figure 4-4: Effect of 10% change in wall thickness

4.2.3 Steel yield stress

Figure 4-5 shows the effect of variation in steel yield stress on the interaction diagram. As expected, there are no effect on the compression-controlled part. Also, in the tension-controlled part the effect is not significant. As it will be shown in Chapter 5, reinforcement steel is factory-made and the variation in steel yield stress is much less than 10%. As the graphs show expectedly, the curves diverge exactly after balanced point; where steel reinforcement would have yielded at failure instance.

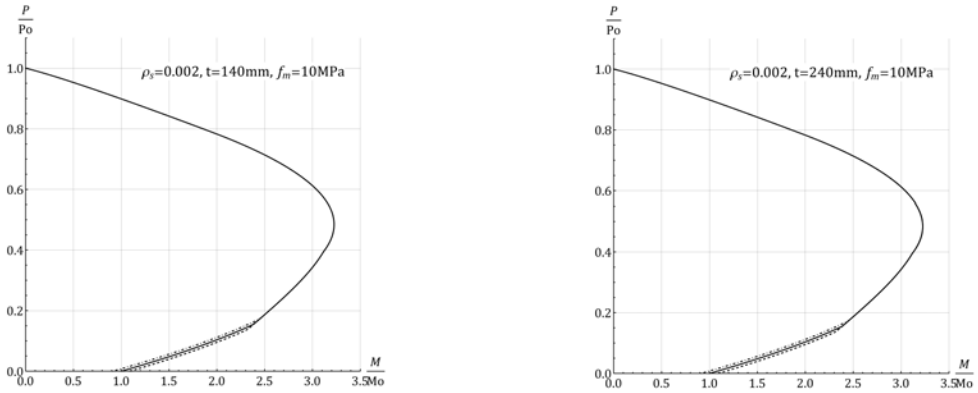

Figure 4-5: steel yield stress

4.2.4 Masonry compressive strength

Masonry compressive strength, f_m, is an important parameter in masonry construction. As it is illustrated in Figure 4-6, the strength of the wall for compression-controlled portion is directly related to masonry compressive strength. However, in the tension-controlled portion of the interaction diagrams, variation in f_m has no effect on the strength as it is expected. Statistical data about uncertainty in masonry strength is given in Chapter 5.

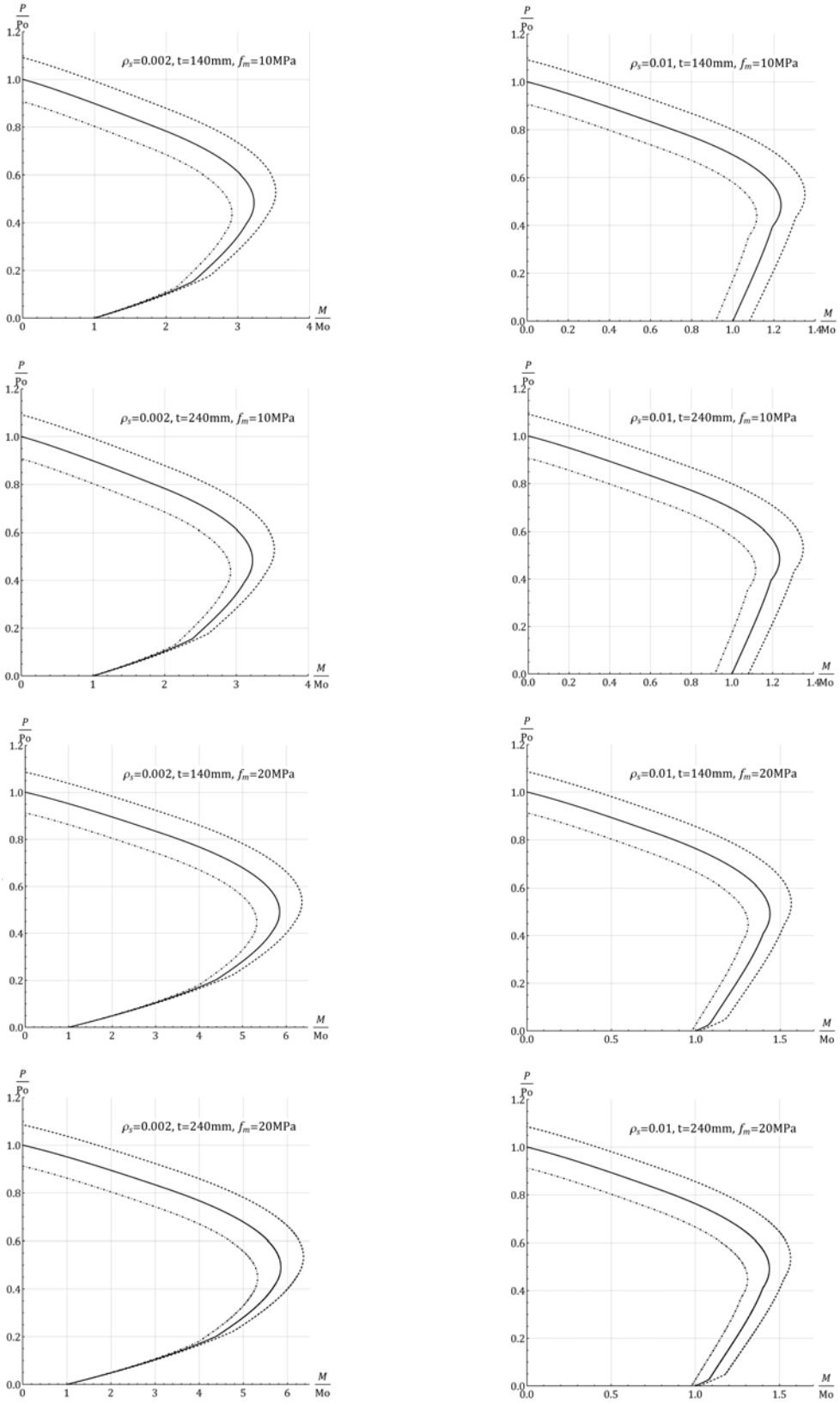

Figure 4-6: Effect of 10% change in masonry compression strength

4.3 CONCLUSION

The effect of changes in important parameters on P-M interaction diagram was investigated in this chapter. These parameters include steel reinforcement area, wall thickness, steel yield stress and masonry compressive strength. Additionally, the effect of the type of the behavioural model was examined. For each parameter $\pm 10\%$ of change was used. However, the real extent for uncertainty for each parameter is reviewed in chapter 5. These diagrams also serve as a verifying tool for the behavioural model selected in terms of comparison to what is expected in response to a parameter change. Table 4–1 shows the summary of the effectiveness of different parameters on different part of the interaction diagram.

Table 4–1 Summary of the sensitivity analysis

Parameter ±10%	**Influence Zone**	
	Compression-Controlled	**Tension-Controlled**
Steel Reinforcement area (ϕ_s)	Partly	✓
Wall Thickness (t)	✓	✓
Masonry Compressive Strength (f'_m)	✓	Partly
Steel Yield Stress (f_y)	-----	✓

Chapter 5

Structural Reliability of Non-Slender Masonry Walls under Combined Axial & Transverse Loads

GENERAL

This chapter illustrates the approach of structural reliability analysis and its findings. First, the ultimate limit state functions are defined for different load combinations and the corresponding random parameters are introduced for both resistance and loading expressions. Statistical information for some random parameters, such as masonry compressive strength, are derived by establishing databases and working out probability density distributions and for the remaining random parameters, statistical information is adopted from recent reliable literature. Consequently, results for structural reliability analysis are illustrated for different cases.

5.1 STRUCTURAL RELIABILITY APPROACH

As mentioned in Chapter 2, the first order reliability method (FORM) (Madsen et al. 1986; Nowak 2000) was used to assess the safety levels of non-slender masonry walls designed to the current Canadian masonry standard S304.1-14 under eccentric axial compression. This method considers the distribution type for all involved parameters in addition to their

mean and coefficient of variation. Rackwitz-Fiessler procedure (Rackwitz and Fiessler 1978) was applied on the ultimate limit state functions described in the following section to determine the Hasofer-Lind reliability index, β, (Nowak 2000) which is a measure of probability of failure for the considered time period. Unlike the mean value reliability index, the Hasofer-Lind reliability index is calculated at a point known as the "design point" instead of the mean values and this guarantees that the evaluated reliability index is the lowest value possible for the limit state function. Since the design point is not known in advance, an iterative approach is required. As recommended by JCSS (2001), for using FORM/SORM, one should give attention to the selection of initial points for the iterative algorithm. Therefore, in this current study, a grid of initial points covering realistic ranges for each variable was considered to make sure of attaining design point with minimum reliability index. Realistic ranges of load type ratios are considered; for live-to-dead from 0.20 to 4.00, for snow-to-dead from 0.25 to 6.00 and for wind-to-dead from 0.25 to 2.50. Also different eccentricities ranging from axial force only to pure out-of-plane bending were considered.

Calculated reliability indices were then compared to the target reliability index (β_T) which is a function of a range of factors including the type of failure, estimated cost of failure and existing levels of safety (Lawrence and Stewart 2009) and serves as an approximate measure of the acceptable probability of failure (CSA S408-11 2011).

It was mentioned in Chapter 2 that Table B.1 of the Canadian standard S408: Guidelines for the Development of Limit States Design (CSA S408-11 2011) suggests that $\beta_T = 4.00$ should be used for normal importance buildings with a sudden (brittle) type of failure, and $\beta_T = 3.50$ should be the minimum index for a gradual (ductile) type of failure. It should be noted that these values are suggested for a 30-year reliability analysis. As β is inversely related with probability of failure, lower values are expected for a 50-year reliability analysis. By calculating the probability of failure for both 30-year and 50-year time periods in terms of the probability of failure in a given year, the equivalent values for 50-year reliability

analysis were calculated as $\beta_T = 3.88$ and $\beta_T = 3.36$ for brittle and ductile failure, respectively.

As an instance for using target reliability indices, Bartlett (2007) discussed a rationale for increasing the material resistance factor for concrete in compression from 0.60 to 0.65 in the 2004 edition of the Canadian concrete design standard A23.3 (CSA-A23. 3-04 2004). The reliability index was calculated for the 0.65 resistance factor and found to be in the 3.9–4.0 range for combinations involving dead plus live or dead plus wind load. It is of note that the reliability indices associated with dead load plus snow load combination tend to be less than the target value, as low as 3.2, regardless of the type of structural material used.

5.2 ULTIMATE LIMIT STATE FUNCTION FOR DEAD LOAD ONLY

For any masonry wall cross section, an axial load versus out-of-plane bending (P-M) interaction diagram can be constructed to represent the section's true strength under different axial load and bending moment combinations, i.e. different virtual eccentricities. This interaction diagram is based on the geometric dimensions of the wall section and the mechanical behaviour of the materials (masonry and reinforcement if any) and does not include any second order effect.

For a given load combination comprising of an axial load and a bending moment, both assumed to be from dead load, (P_D, M_D), the wall design would be safe by ascertaining that (P_D, M_D) is within the true interaction diagram as shown in Figure 5-1.

To assess the reliability level for this design, one can compare the norms (distances to origin) of the load combination point, (P_D, M_D), to the corresponding point on the true strength interaction diagram, (P_r, M_r), for the same virtual eccentricity, i.e. $M_r/P_r = M_D/P_D$ as expressed in Eq. 5-1.

$$G(\boldsymbol{x}) = \sqrt{{M_r}^2 + {P_r}^2} - \sqrt{{M_D}^2 + {P_D}^2} \qquad \text{(Eq. 5-1)}$$

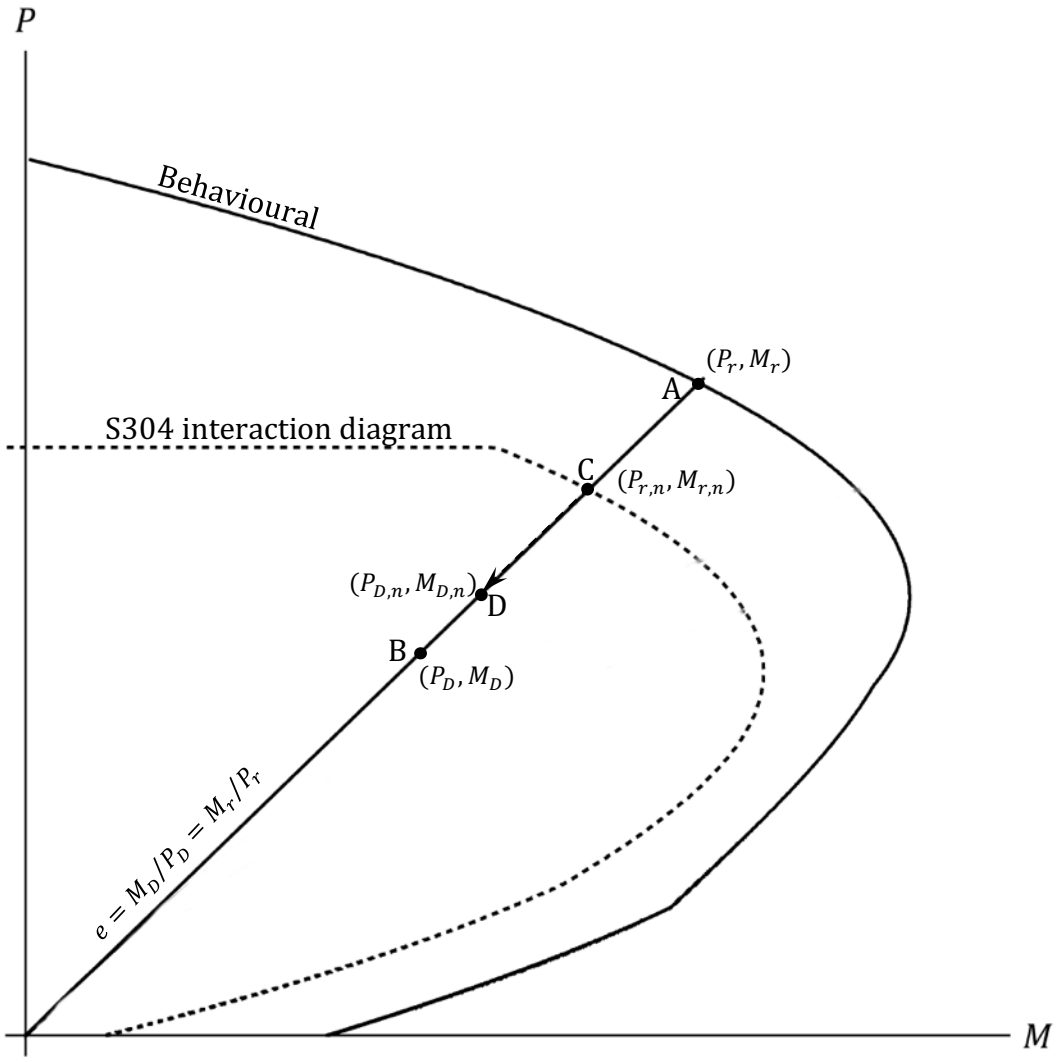

Figure 5-1: Typical interaction diagram showing different points for a given eccentricity (e), true resistance (point A), true load (point B), nominal resistance (point C) and nominal load (point D) which is derived from point C

Where, $G(\boldsymbol{x})$ is the limit state function and is a function of all involved random variables ($P_r, M_r, P_D \; and \; M_D$) represented by the vector $\boldsymbol{x}$. For this case, M_r, P_r, M_D and P_D are the random variables. It is important to note that P_D and M_D are not statistically independent. Dead load is a gravitational load and any present bending moment would be the axial force (in full or in part) multiplied by an eccentricity. Therefore, P_D and M_D are linearly correlated. Also, as will be discussed later, statistical information for different load types include bias mean, coefficient of variation and distribution type and therefore nominal values for loads for each case is calculated assuming that the factored nominal load effect is exactly equal to the strength of the wall calculated according to CSA S304.

5.3 ULTIMATE LIMIT STATE FUNCTION FOR COMBINED LOADS

For load combinations such as dead load plus live load or dead load plus snow load, a similar approach can be taken. The case of dead load plus live load is explained in the following section.

For the load combination of dead load plus live load, the limit state function is expressed as

$$G(\boldsymbol{x}) = \sqrt{{M_r}^2 + {P_r}^2} - \sqrt{(M_D + M_L)^2 + (P_D + P_L)^2} \qquad \text{(Eq. 5-2)}$$

For a wall section with known material properties and dimensions, the nominal resistance ($P_{r,n}, M_{r,n}$) can be worked out for any virtual eccentricity which represents the wall strength capacity according to the design standard. Assuming that the wall is designed so that the factored resistance is equal to the factored loading as per (NBCC 2015) for dead

load and live load with load factors of 1.25 and 1.50, respectively, nominal resistance can be expressed as:

$$P_{r,n} = 1.25\ P_{D,n} + 1.50\ P_{L,n}$$
$$M_{r,n} = 1.25\ M_{D,n} + 1.50\ M_{L,n} \qquad \text{(Eq. 5-3)}$$

Each of the dead and live load has its own statistical properties. Therefore, in order to calculate the nominal load values on the right hand side of Eq. 5-3 in terms of $P_{r,n}$ and $M_{r,n}$, it is necessary to assume that the ratios between $P_{L,n}$ and $P_{D,n}$ and between $M_{L,n}$ and $M_{D,n}$ are known as expressed below.

$$\frac{P_{L,n}}{P_{D,n}} = \alpha_P$$
$$\frac{M_{L,n}}{M_{D,n}} = \alpha_M \qquad \text{(Eq. 5-4)}$$

Substituting in Eq. 5-3 and rearranging, it follows that,

$$P_{D,n} = \frac{P_{r,n}}{1.25 + 1.50\alpha_P}$$

$$P_{L,n} = \frac{\alpha_P \, P_{r,n}}{1.25 + 1.50\alpha_P}$$

$$M_{D,n} = \frac{M_{r,n}}{1.25 + 1.50\alpha_M} \qquad \text{(Eq. 5-5)}$$

$$M_{L,n} = \frac{\alpha_M \, M_{r,n}}{1.25 + 1.50\alpha_M}$$

Similar to the case of dead load only, linear correlations are assumed between P_D and M_D and between P_L and M_L.

5.4 STATISTICAL DATA FOR LOADING

For the random variables corresponding to loading, only the nominal values are needed since the statistical characteristics, namely bias, coefficient of variation and distribution type, can be found in the literature (Bartlett et al. 2003). These statistical characteristics are given in Table 5-1 for different loading types. For example, for dead load the average bias factor (D/D_n) is 1.050 with a coefficient of variation (COV) equal to 0.1 and follows a normal distribution type. The COV of 0.1 includes a COV of 0.07 for the transformation of dead load to dead load effect (Allen 1975; Bartlett et al. 2003)

Nominal values for loading parameters (point D in Figure 5-1) are related to the nominal strength values of the wall determined from the design standard expressions (point C in Figure 5-1). Assuming that the wall was designed to have a resistance exactly equal to the factored dead load with a load factor of 1.4 according to the 2014 version of CSA S304, the nominal load values for axial force and bending moment can then be expressed as

$$P_{D,n} = \frac{P_{r,n}}{1.4} \quad and \quad M_{D,n} = \frac{M_{r,n}}{1.4} \qquad \text{(Eq. 5-6)}$$

Table 5–1 Statistical information for different load types (Bartlett et al. 2003)

Load type	Bias	COV	Distribution type
Dead load	1.050	0.100	Normal
Use and occupancy live load			
50 year maximum load	0.900	0.170	Gumbel
Point-in-time load	0.273	0.674	Weibull
Transformation to load effect	1.000	0.206	Normal
Snow load			
50 year maximum depth	1.100	0.200	Gumbel
Point-in-time depth	0.196	0.882	Weibull
Density	1.000	0.170	Normal
Transformation to load effect	0.600	0.420	Log-normal
Wind Load (Regina)			
50 year maximum velocity	1.039	0.081	Gumbel
Point-in-time velocity	0.156	0.716	Weibull
Transformation to load effect	0.680	0.220	Log-normal

For a given virtual eccentricity, $P_{r,n}$, $M_{r,n}$ can be found from the P-M interaction diagram constructed for the masonry wall section as per CSA S304-2014. Resistance factors for masonry and steel reinforcement, namely $\phi_m = 0.60$ and $\phi_s = 0.85$ are already embodied in this diagram. This interaction diagram is obviously different from the interaction

diagram representing the true strength of the wall. Realizing that reliability levels may not be similar under different combinations of axial load and bending moment (i.e. different load eccentricities) the reliability analysis needs to consider different eccentricities.

5.5 BEHAVIOURAL MODEL FOR RESISTANCE

The resistance part in Eq. 5-1, consisting of M_r and P_r, was worked out from a verified behavioural model explained in Chapter 3. This behavioural model was used to construct the *P-M* interaction diagram that is representative of the true strength of the wall section. This is an efficient model that has been verified and used by other researchers (Ellingwood and Tallin 1985, Liu and Dawe 2003) and was modified in this study. Instead of the idealized rectangular stress block, a more realistic parabolic masonry stress-strain relationship, introduced in Chapter 2, was utilized and subsequently validated against experimental results as shown in Chapter 3. The model can be used to study the behaviour of concrete masonry load-bearing walls under various loading conditions. It accounts for several material nonlinearities, namely masonry tensile cracking, masonry compressive crushing and yielding in steel reinforcement. This model was used in this investigation as a basis for defining the limit state function that is needed to assess the reliability of masonry walls. Reliability analyses were performed on hollow and fully-grouted unreinforced walls as well as fully grouted reinforced walls. The reported good agreement between the behaviour of experimentally tested partially grouted masonry walls and strength predictions suggests that the conclusions drawn from a reliability analysis on partially grouted walls would be similar to those drawn for fully grouted walls (Ellingwood and Tallin 1985).

5.6 STATISTICAL INFORMATION FOR THE RESISTANCE PARAMETERS

In addition to the statistical information for different types of load presented in Table 5-1 the statistical information for the mechanical and geometrical parameters involved in the behavioural model are needed carry out the reliability analysis. The statistical characteristics of such parameters are summarized in Table 5–2 and explained in the following sections.

Table 5–2 Statistical information for resistance parameters

parameter	Mean	COV	Dist. type	Reference
grouted masonry compressive strength ($\boldsymbol{f_m}$)	1.60 f'_m	0.236	Gumbel	Moosavi & Korany 2014
hollow masonry compressive strength ($\boldsymbol{f_m}$)	1.46 f'_m	0.205	Normal	Moosavi & Korany 2014
wall thickness ($\boldsymbol{t}$)	1.00 t_n	0.010	Normal	Moosavi & Korany 2014
reinforcement location ($\boldsymbol{d}$)	1.00 d_n	$4mm/d_n$	Normal	Ellingwood 1980
reinforcement yield stress ($\boldsymbol{f_y}$)	1.14 f_{yn}	0.070	Normal	Bournonville et al. 2004
workmanship factor ($\boldsymbol{\rho_w}$)	0.85	0.150	Normal	Moosavi & Korany 2014
rate of loading ($\boldsymbol{\rho_{r(D+L)}}$) *	0.88			Jones and Richart 1936
rate of loading ($\boldsymbol{\rho_{r(D+S)}}$) *	0.79			Jones and Richart 1936
rate of loading ($\boldsymbol{\rho_{r(D+W)}}$) *	0.94			Jones and Richart 1936

*considered as a reduction factor on f_m

Masonry compressive strength

In a preceding study by the author, 860 compressive strength data points were collected from concrete masonry prism tests under axial compression (Moosavi and Korany 2014). These data points include neither units having compressive strength values outside the range of Table 4 in the Canadian masonry design standard CSA S304-2014 nor grout strength not meeting the requirements of CSA A179-14. Prism compressive resistance was

adjusted for the height-to-thickness ratio effect according to Table D1 of Annex D in CSA S304-2014.

As shown in Figure 5-2, the bias factor was determined for both hollow and grouted masonry by comparing the measured axial load resistance from prism testing to the nominal resistance based on unit strength and mortar type according to Table 4 in S304-14.

In previous studies, the distribution type for bias factor of masonry compressive strength, f_m, was assumed to be either normal (Turkstra 1989) or log-normal (Ellingwood and Tallin 1985). Also in an online publication from JCSS, (2001), log-normal distribution with bias mean of 1.0 and CoV of 0.2 is suggested for compression strength of masonry made of regular concrete blocks with thin mortar layers. In this current investigation, the maximum likelihood method (Ang and Tang 2007) was used to fit different distributions to the collected test data. Then, the Anderson-Darling test for goodness-of-fit (Ang and Tang 2007) was used to select the best fit. Normal and Gumbel distributions were found to be the most appropriate for hollow and grouted masonry, respectively. As can be seen in Figure 5-3, Gumbel distribution presents a good fit to the lower tail of the grouted masonry data which is important from a reliability analysis point of view.

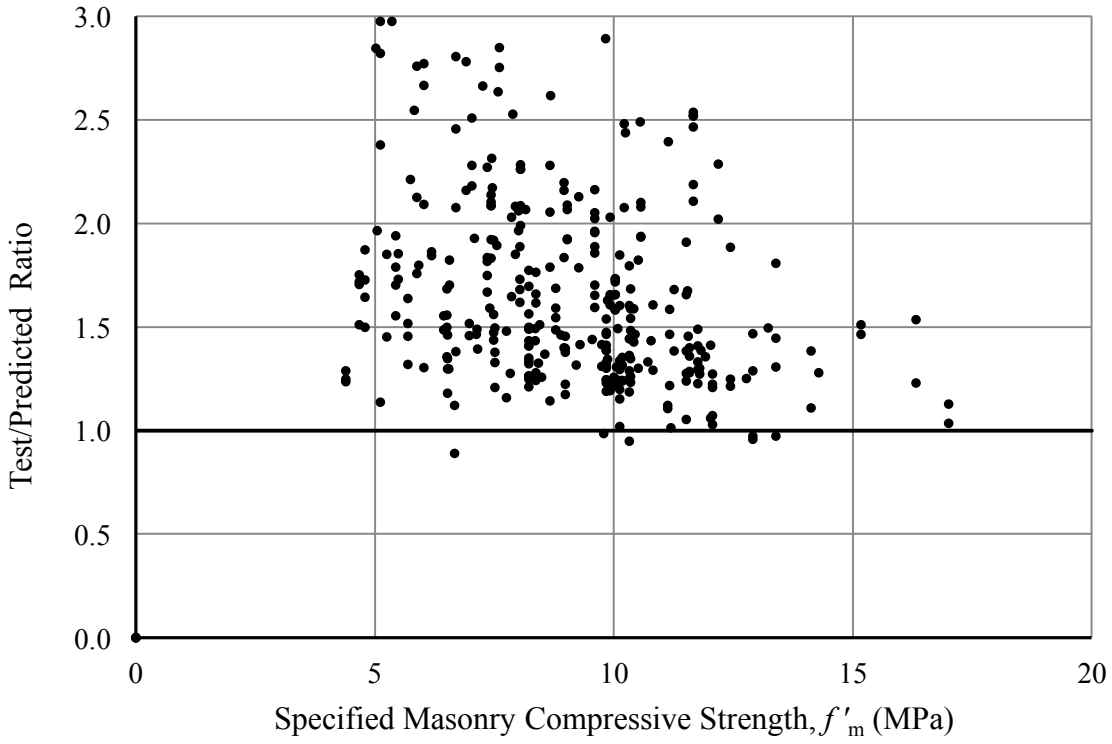

Figure 5-2: Test-to-specified compressive force ratios for grouted prism test (Moosavi and Korany 2014)

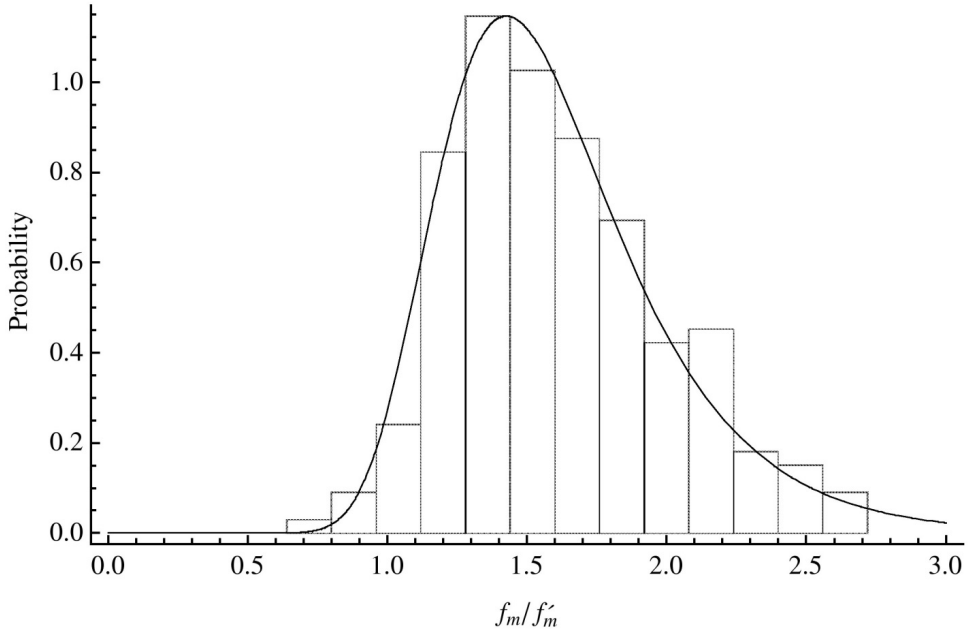

Figure 5-3: Gumbel distribution fit for f_m/f'_m for grouted masonry

It is well established (Stewart and Lawrence 2006; Ellingwood 1981) that the bias computed from different test results, known as model error, includes variations in the test procedures, V_{test}, and specimen variability, V_{spec}, in addition to variations in the strength prediction error or professional factor. Therefore, the variability in the professional factor can be expressed as:

$$V_P = \sqrt{{V_{model}}^2 - {V_{test}}^2 - {V_{spec}}^2} \qquad \text{(Eq. 5-7)}$$

where, V_P is the coefficient of variation (CoV) of the professional factor, V_{model} is the CoV of the strength prediction model (Table 4 in CSA S304-2014), which was found from test results to be 0.21 and 0.24 for hollow and grouted masonry, respectively. V_{test} represents the CoV of the measured capacity due to inaccuracies in the test measurements and/or the definition of failure, and V_{spec} represents CoV related to the differences between the measured and actual parameters of the test specimens. Ellingwood (1981) suggested a value of 0.02 for V_{test} and 0.04 for V_{spec}. These values were used in this study to compute the CoV for the professional factor for both hollow and grouted masonry. Therefore,

$$V_P = \sqrt{0.24^2 - 0.02^2 - 0.04^2} = 0.236 \text{ grouted}$$

$$V_P = \sqrt{0.21^2 - 0.02^2 - 0.04^2} = 0.205 \text{ hollow} \qquad \text{(Eq. 5-8)}$$

Wall thickness

For concrete masonry unit, the wall thickness is typically equal to concrete unit thickness. Therefore, in this investigation, the variability in the thickness of the masonry wall section was assumed to be equal to the variability in the masonry unit thickness and the statistical parameter for the unit geometry reported by Moosavi and Korany (2014) were used as shown in Table 5–2.

Reinforcement location and yield strength

Ellingwood (1980) summarized the statistical data for the location and strength of steel reinforcing bars. For effective reinforcement depth, d, a normal distribution with mean of $d_n$and COV of $^{4\ mm}/_{d_n}$was estimated by Ellingwood. This implies that the standard deviation for steel rebar location is independent from its effective depth. These statistical data have been used in many reliability studies (e.g. Nowak et al. 2008; Nowak and Szerszen 2003) and were, therefore, adopted.

MacGregor (1976) reported a mean value of 1.03 f_{yn} for grade 60 reinforcement to be used in reliability analysis for reinforced concrete. The coefficient of variation was assumed to be 0.07 according to Allen (1972). For common Grade 60 steel reinforcement, Ellingwood (1980) reported a mean value of 1.12 f_{yn} and a coefficient of variation of 0.11 for the reinforcement yield strength. Nowak and Szerszen (2003) did an investigation on steel reinforcing bar 420 MPa grade with bar diameters from 9.5 to 34.5 mm. The recommended bias factor for f_y was 1.145 with a coefficient of variation of 0.05. In a more comprehensive study (Bournonville et al. 2004), the variability of mechanical properties and weight of steel reinforcing bars produced in the United States and Canada was evaluated. For grade 428 MPa reinforcement, a bias factor of 1.14 with cov = 0.07 was concluded from this study. Both normal and beta distributions were reported as appropriate. In the current investigation, a normal distribution was assumed for the bias of the reinforcing steel yield strength and the bias factor and COV reported by Bournonville et al. (2004) were adopted as it is more recent and comprehensive.

Masonry Workmanship Factor

The effect of workmanship on the reliability of structural masonry is well acknowledged and the documented in literature. The bias coefficient and CoV of 0.85 and 0.15 (normal distribution) for workmanship reported by Moosavi and Korany (2014) were used in this study. As stated before, it is suggested that statistical information for workmanship factor be supported with more test results to represent current masonry construction practice in Canada.

Rate-of-Loading Factor

The effect of loading rate on the mechanical response of concrete masonry walls cannot be ignored. (Jones and Richart 1936) suggested the following relation between concrete compressive strength and the rate of loading.

$$f_{cr} = f_{c1}[1 + K \log_{10}(r)] \quad 0.1 \text{ psi/sec} < r < 10{,}000 \text{ psi/sec} \qquad \text{(Eq. 5-9)}$$

Where,
f_{cr} is the strength at a given rate of loading r in psi/sec;
f_{c1} is the strength at a rate of loading of 1 psi/sec; and
K is a constant, roughly equal to 0.08 for 28-day compressive strength

It is desired to relate the 28-day compressive strength of concrete masonry to the prescribed testing speed at which masonry prisms are generally tested, namely around 22 psi/sec. Therefore, for 28-day masonry compressive strength, the rate of loading factor, ρ_r, is

$$\rho_r = \frac{f_{cr}}{f_{c22}} = 0.90[1 + 0.08 \log_{10}(r)] \qquad \text{(Eq. 5-10)}$$

Where,

r is the rate of loading in psi/sec; and

f_{c22} is the strength at a rate of loading of 22 psi/sec.

In this analysis, r values were computed for masonry having compressive strength in the range from 5 MPa to 25 MPa (725– 3625 psi) to cover the spectrum of masonry compressive strength values in CSA S304-2014. The loading time to failure was taken as one hour for live load, 10 minutes for wind load and one day for snow load (Bartlett 2007). The average values for dead plus live, dead plus snow and dead plus wind load combinations were 0.88, 0.79 and 0.94, respectively. The variability in the rate of loading is negligible compared to the large coefficients of variation for the other parameters and therefore ignored in this analysis.

5.7 PROPERTIES OF ANALYZED WALLS

Wall thickness values of 190mm and 290mm were considered to investigate the effect on reliability levels. For masonry strength, f_m, the upper and lower values recognized by the standard (CSA S304.1 2014) in Table 4, namely 5MPa and 17MPa, were selected to observe the corresponding effect. Reinforcement ratios of ρ_s =0.0013 and ρ_s =0.0025 were considered. Reinforcement ratio of 0.0013 is the minimum ratio allowed by the standard and 0.0025 is a value very close to the balanced reinforcement ratio in pure bending for the range of f_m considered. At larger reinforcement ratios, the whole interaction diagram will involve compression failure mode and the reliability levels would not be affected. From a

practical point of view, ρ_s=0.0013 and ρ_s=0.0025 for a wall with t =190mm can be related to 15M bars spaced at s=800mm and 15M bars spaced at s=400mm respectively. Also for a wall with t =290mm, ρ_s=0.0013 and ρ_s=0.0025 can be related to 20M bars spaced at s=800mm and 15M bars spaced at s=400mm respectively.

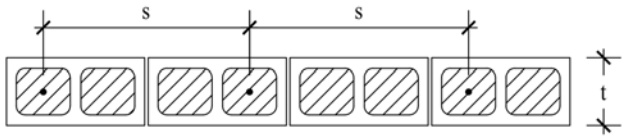

Figure 5-4: Schematic plan for grouted reinforced masonry wall

5.8 RESULTS OF RELIABILITY ANALYSIS AND DISCUSSION

Reliability levels associated with the current masonry design practice were calculated by analysing concrete masonry walls under out-of-plane bending and axial compression with different reinforcement ratios and virtual eccentricities.

5.8.1 REINFORCED MASONRY UNDER DEAD LOAD ONLY

The first set of the reliability analysis was performed for the case of dead load only. Figure 5-5 shows the variation of β with respect to normalized virtual eccentricity for the case of DL only. The first observation is that the reliability index barely falls under 4.0. Also, the effect of considering a minimum eccentricity of $e/t = 0.1$ prescribed by CSA S304 is apparent in the larger values in all the diagrams before $e/t = 0.1$.

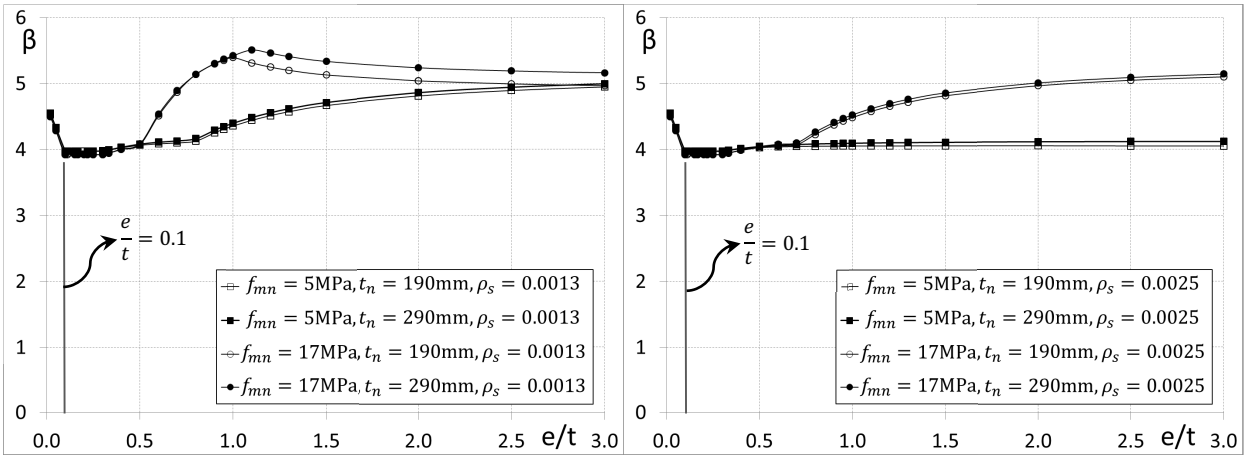

(a (b

Figure 5-5: β versus normalized virtual eccentricity for dead load only (DL)

But regardless of the reliability levels, the other observation is that the reliability levels for small eccentricities (compression failure) are not affected much by masonry strength, wall thickness and reinforcement ratio. This is because in compression failure mode, masonry strength is the dominant parameter and interaction of uncertainties from masonry strength and reinforcement properties is not present.

Another important observation is the fact that for the same masonry strength and reinforcement ratio, reliability levels are very close for different wall thickness values. In fact, reliability levels for small wall thickness values are slightly lower. The reason for this is that the coefficient of variation for reinforcement location is introduced as $4mm/d_n$ which implies that for smaller wall thickness values, reinforcement depth has a larger coefficient of variation causing lower reliability levels. It is concluded that performing reliability analysis for the smaller wall thickness values gives lower bounds for reliability levels.

Another important observation is that reliability levels for tension failure mode are generally higher than compression failure mode. For instance, looking at Figure 5-5(a) it can be seen that for the same steel reinforcement ratio, reliability levels drop for lower masonry strength values. There are two facts to consider: 1) Balanced reinforcement ratio,

for which both reinforcement yielding and masonry crushing occur at the same time in case of pure bending, directly relates to masonry strength; i.e. stronger masonry material leads to a larger balanced reinforcement ratio. For instance, in Figure 5-5(a) $\rho_s = 0.0013$ is closer to ρ_b for $f_{mn} = 5$MPa than for $f_{mn} = 17$MPa and similarly for Figure 5-5(b) 2) Balanced eccentricity, where failure mode moves from compression to tension, increases as reinforcement ratio moves closer to the balanced reinforcement ratio. Therefore, in Figure 5-5(a) balanced eccentricity for $f_{mn} = 5$MPa is much larger than that for $f_{mn} = 17$MPa. This means that the graphs for $f_{mn} = 5$MPa mostly involve compression failure mode. And in the graphs for $f_{mn} = 17$MPa the change from compression to tension failure mode is apparent.

It is worth mentioning that high reliability levels for tension failure zones in Figure 5-5 is just partly because of less uncertainty in steel material characteristics. Another reason for this observation relates to the fact that these results are for the case of dead load only; the axial force and the bending moment are correlated. Since axial force improves the bending moment capacity of the wall in tension failure zone, this correlation leads to high reliability levels.

5.8.2 RESULTS FOR REINFORCED MASONRY WALLS FOR OTHER LOAD COMBINATIONS

As discussed in derivation of the limit state function for the combination of dead and live loads, the analyses need to be performed for different live load to dead load ratios. Since, bending from gravitational load types are actually the corresponding axial load multiplied by eccentricity, it is assumed that this ratio for axial load and bending moment are the same (Eq. 5-11).

$$\frac{P_{L,n}}{P_{D,n}} = \alpha_P = \frac{M_{L,n}}{M_{D,n}} = \alpha_M \qquad \text{(Eq. 5-11)}$$

Different types of flooring and roofing systems along with ranges for transient loads were considered. If only loads on floor and roof are considered, for the combination of $dead + live$, α_P (or α_M) may range to around 4.00 for light wood flooring and for the combination of $dead + snow$, α_P (or α_M) may range to around 6.00 for light-frame wood roof and metal roofing. However, self-weight of masonry walls affect these ratios considerably. Concurrent large values for α_P and α_M only can happen for eccentricities less than $e/t = 1.00$. For eccentricities more than $e/t = 1.00$, α_P barely exceeds 2.50 but α_M might still range up to 4.00 and 6.00 for $dead + live$ and $dead + snow$ load combinations, respectively. For the combination of $dead + wind$, α_M might range to very large values for cantilever masonry walls but as will be seen in the reliability analysis results, changes in reliability index is negligible beyond $\alpha_M = 2.50$. Also, this load combination is not as detrimental as other combinations. Lower bound ratio of 0.25 was considered for both α_P and α_M. Similar ranges are considered in other studies (Ellingwood 1980; Bartlett 2007).

The same approach is valid for dead plus snow load since they are both gravitational load types. However, for the combination of dead and wind load types, $\alpha_P = P_{W,n}/P_{D,n}$ may be presumed negligible as wind is a transverse load and contributes mostly in the out-of-plane moment. Therefore, only $\alpha_M = M_{W,n}/M_{D,n}$ was taken as a variable. The following figures show the reliability analysis results for load combinations including $DL + LL$, $DL + SL$ and $DL + WL$.

Figure 5-6 illustrates the variation of reliability index with respect to normalized virtual eccentricity for $DL + LL$ combination for different values of α_P and α_M. In general, the minimum β for all cases is 3.40. However, it can be realized that for all cases the minimum β happens when the wall is designed for eccentricities in compression controlled region. In this region the strength relies merely on masonry strength and this means that, from a

strength point of view, ϕ_m establishes the reliability levels. For sake of comparison, it is worth mentioning that the minimum reliability level for reinforced concrete under combined compression and bending has been calculated to be about 3.77 (Bartlett 2007).

For the case of $\alpha_P = \alpha_M = 0.25$ in Figure 5-6, when dead load has the larger contribution compared to live load, the behaviour of the curves is similar to Figure 5-5 for the case of dead load only. Although, the smaller dead load factor of 1.25 compared to 1.40 has yielded lower reliability levels in Figure 5-6. As α_P and α_M ratios, i.e. live load contribution increase, an apparent decrease in reliability levels is observed in the curves mainly in the tensioned controlled region. However, this decrease barely passes the minimum reliability levels already seen in compression controlled regions. The decrease can be attributed to the larger uncertainty in live load compared to dead load, nevertheless this decrease is only observed in the tension region. It is worth mentioning that other than ϕ_m, there are three other safety factors in this analysis which have been calibrated over time to yield relatively consistent levels of safety. Each of these safety factors are more effective for different cases but as it can also be seen in Figure 5-6, for critical cases they tend to result in relatively consistent reliability indices.

Figure 5-7 illustrates the variation of reliability index with respect to normalized virtual eccentricity for $DL + SL$ combination for different values of α_P and α_M. The minimum β for all cases is 2.82. It must be noted that regardless of the structural material, the reliability levels associated with snow loading tend to be less than the target values. For example, for reinforced concrete under combined compression and bending, β falls as low as 3.20 (Bartlett 2007). Lower reliability indices for snow load combination corresponds to the larger coefficient of variation of this type of load compared to other loads (Table 5–1).

Figure 5-8 illustrates the variation of reliability index with respect to normalized virtual eccentricity for $DL + WL$ combination for different values of α_P and α_M. The minimum β for all cases is 3.45. As for comparison, the minimum reliability level for reinforced concrete

under combined compression and bending has been calculated to be about 3.88 (Bartlett 2007).

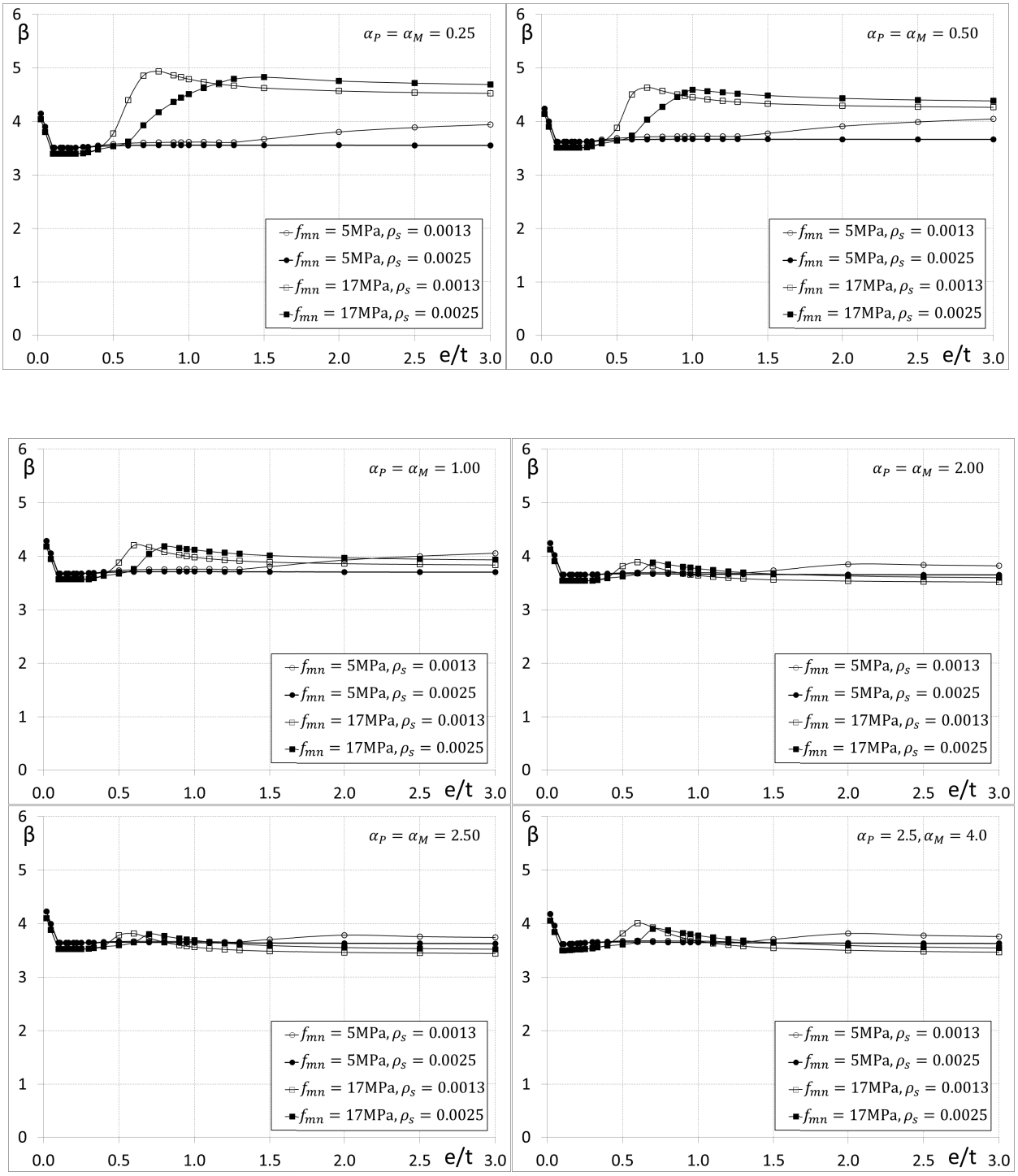

Figure 5-6: β versus normalized virtual eccentricity for $DL + LL$ for different values of α_P and α_M (reinforced)

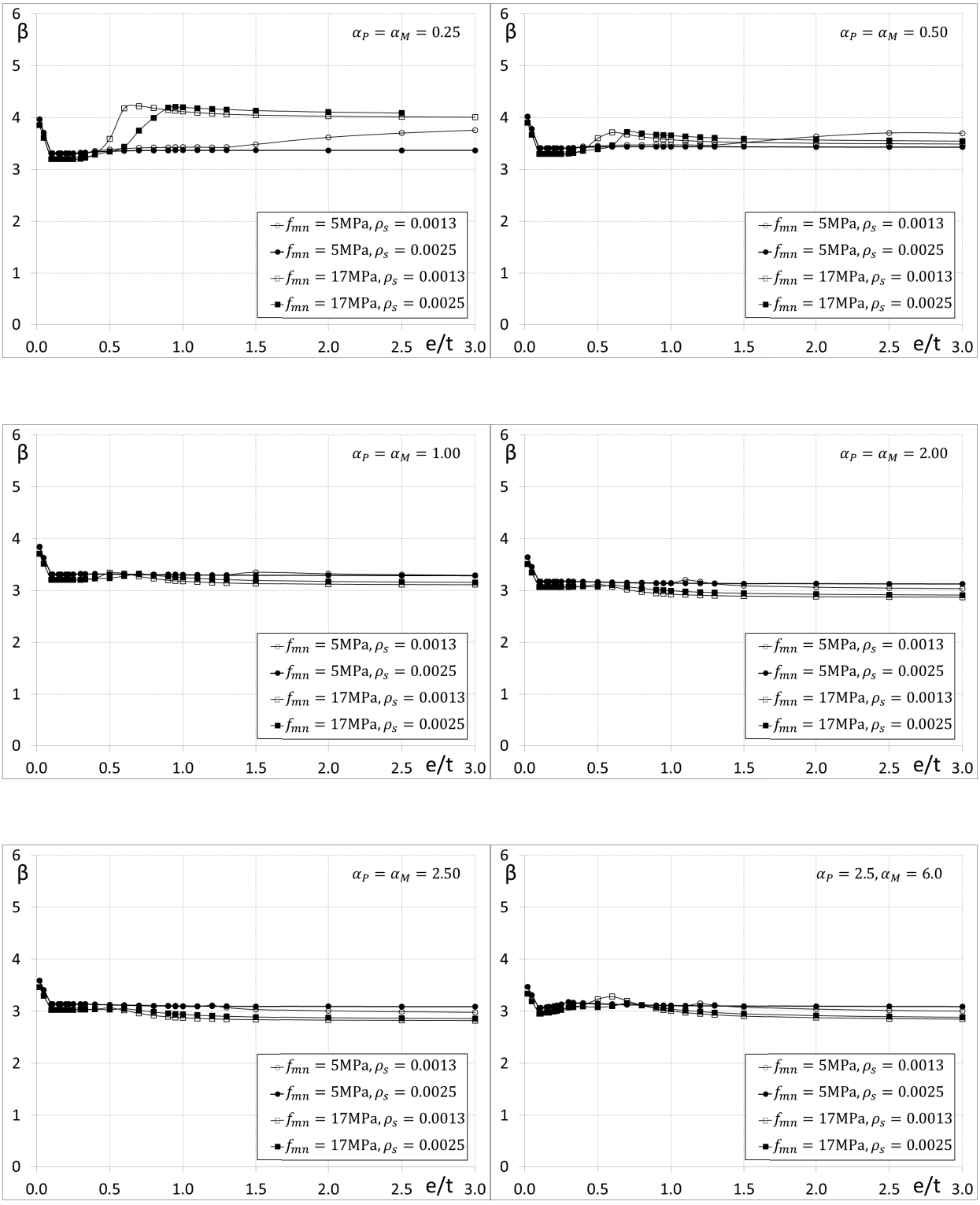

Figure 5-7: β versus normalized virtual eccentricity for $DL + SL$ for different values of α_P and α_M (reinforced)

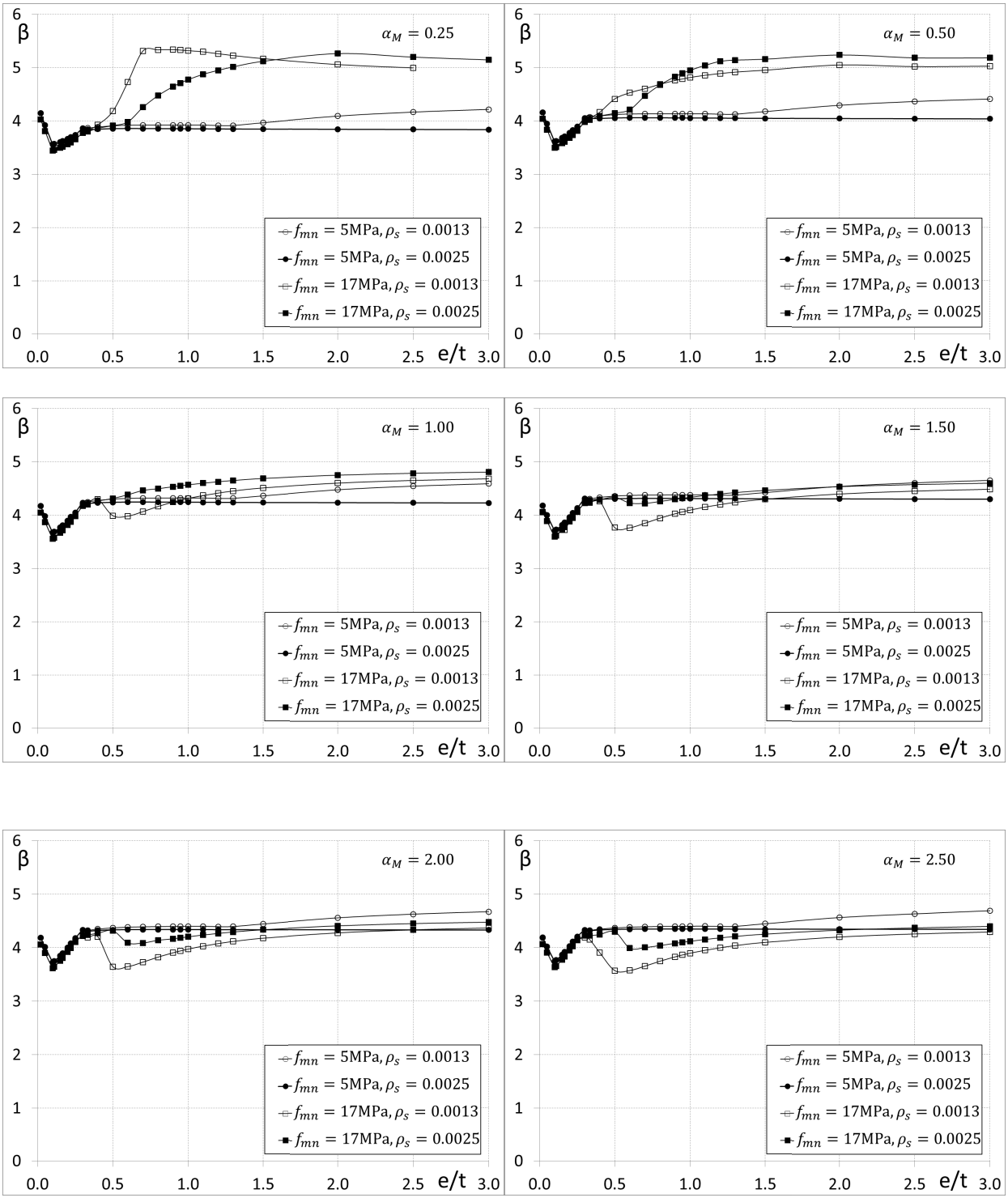

Figure 5-8: β versus normalized virtual eccentricity for dead plus wind load types for different values of α_P and α_M (reinforced)

5.8.3 RESULTS FOR FULLY GROUTED AND HOLLOW UNREINFORCED MASONRY WALLS

Reliability analysis was also performed for non-slender fully grouted unreinforced masonry walls. For the case of dead load only, as shown in Figure 5-9, the analysis was done for different masonry strength and wall thickness values. It is observed that wall thickness does not have any influence on reliability levels and the effect of masonry strength is negligible and reliability levels for $f_{mn} = 17$ MPa are slightly lower than reliability levels for $f_{mn} = 10$ MPa. Analysis was also performed for $f_{mn} = 5$ MPa to yield results slightly higher than $f_{mn} = 10$MPa. Points for $f_{mn} = 5$ MPa are not shown for legibility. So for all other load combinations, reliability analysis was run for $f_{mn} = 17$MPa and $t = 190mm$.

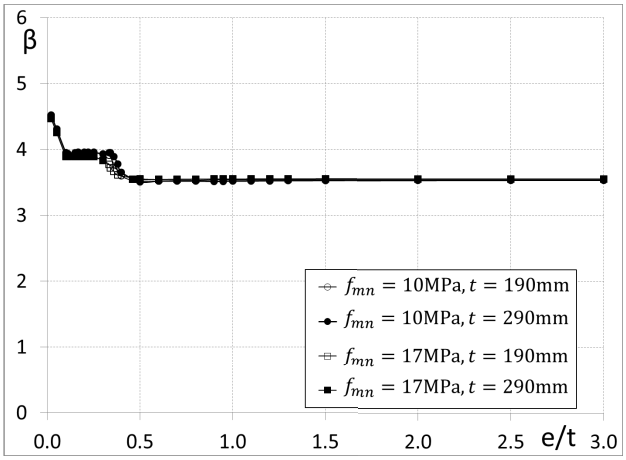

Figure 5-9: β versus normalized virtual eccentricity for DL (unreinforced, grouted)

Figure 5-9 through Figure 5-12 show reliability levels for unreinforced masonry wall for DL, $DL + LL$, $DL + SL$, $DL + WL$ combinations, respectively. The minimum reliability indices are 3.47, 3.04, 2.82 and 3.35, respectively. This numbers compare to 3.00, 3.40, 2.82, 3.45 for reinforced masonry.

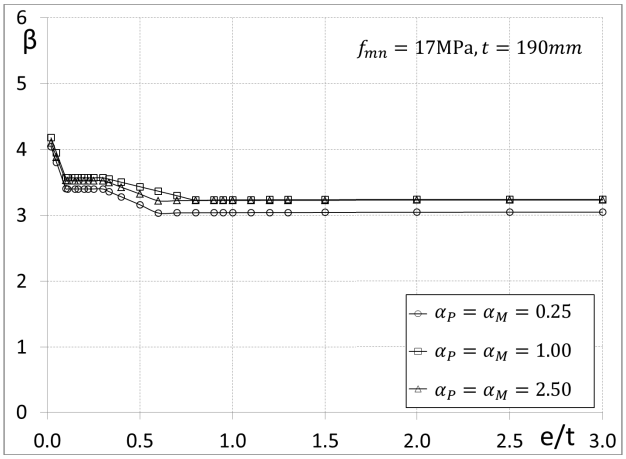

Figure 5-10: β versus normalized virtual eccentricity for $DL + LL$ (unreinforced, grouted)

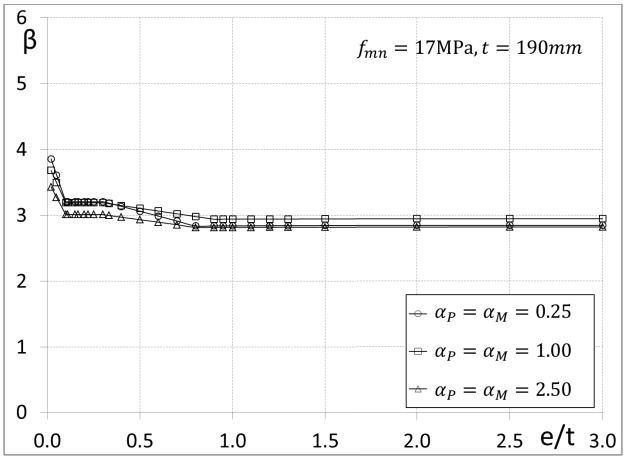

Figure 5-11: β versus normalized virtual eccentricity for $DL + SL$ (unreinforced, grouted)

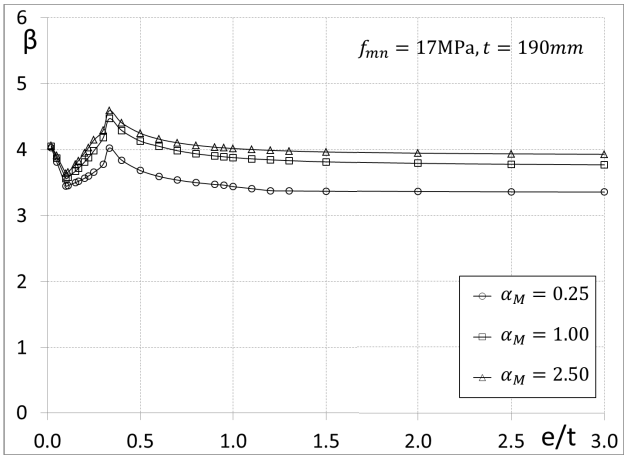

Figure 5-12: β versus normalized virtual eccentricity for $DL + WL$ (unreinforced, grouted)

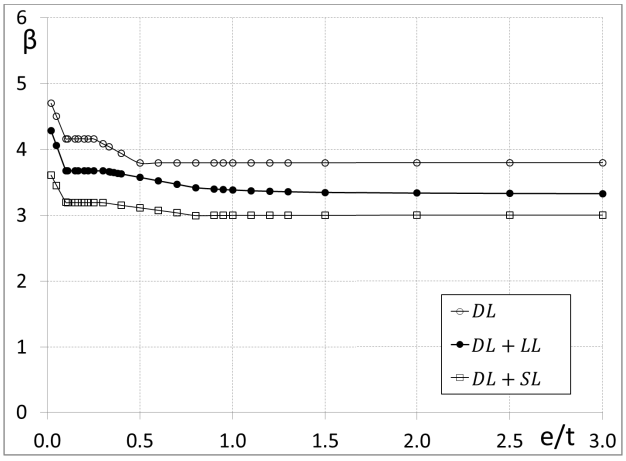

Figure 5-13: β versus normalized virtual eccentricity with $\phi_m = 0.55$ for DL, $DL + LL$, $DL + SL$ (unreinforced, grouted)

As mentioned before, ϕ_m should be considered 0.60 according to (CSA S304.1 2014). The value for ϕ_m used to be 0.55 and was increased to 0.60 in the 2004 edition of the standard (CSA S304.1 2004). In order to observe, how this change has affected the reliability levels for unreinforced masonry, analysis was repeated with $\phi_m = 0.55$ for curves with lowest β for DL, $DL + LL$ and $DL + SL$ from Figures 5-9 to 5-11 and the result is given in Figure 5-13.

The minimum reliability indices are improved from 3.47 to 3.79 for DL, from 3.04 to 3.33 for $DL + LL$ and from 2.82 to 3.00 for $DL + SL$.

Reliability analyses were also performed for hollow unreinforced walls. Figure 5-14 shows the results for DL only for both fully grouted and hollow unreinforced masonry walls. Figure 5-15and Figure 5-16 contain the results for cases of $DL + LL$ and $DL + SL$ for hollow unreinforced masonry walls. It is observed that reliability levels are generally higher for hollow masonry than for fully grouted masonry. This can be partly attributed to the effect of a lower CoV for hollow masonry. Also, it should be noticed that the distribution type for f_m in grouted masonry is Gumbel distribution, while for hollow masonry it is a normal distribution. By looking at a Gumbel distribution formulation, it becomes apparent that the median of the distribution is less than the mean. This implies that even though the mean for grouted masonry is higher than hollow masonry, the probability for values less than mean is higher than for the values higher than mean. In other words, strength distribution for hollow masonry reveals more reliable behaviour than fully grouted masonry. This difference can be attributed to the fact that the strength measured for hollow masonry comes from face shells spaced by mortars that is a very clear explanation of the material and that strength is used exactly at the same location for analysis. However, for grouted masonry, the strength is measured for the whole assembly, which is face shell spaced by mortar at some region and only grout at some other region and variation in grout strength adds to the uncertainty.

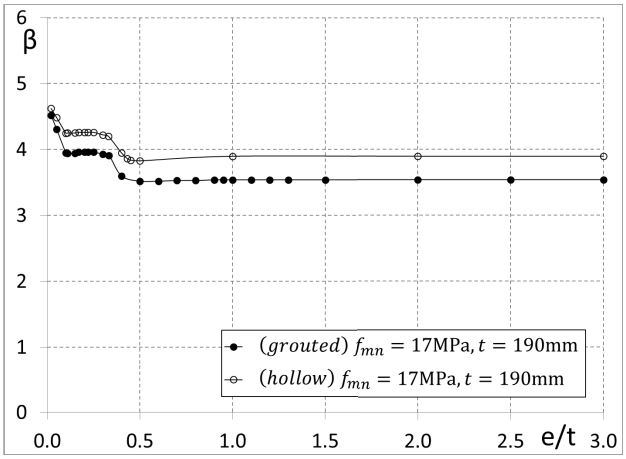

Figure 5-14: β versus normalized virtual eccentricity with $\phi_m = 0.60$ for DL (unreinforced, grouted & hollow)

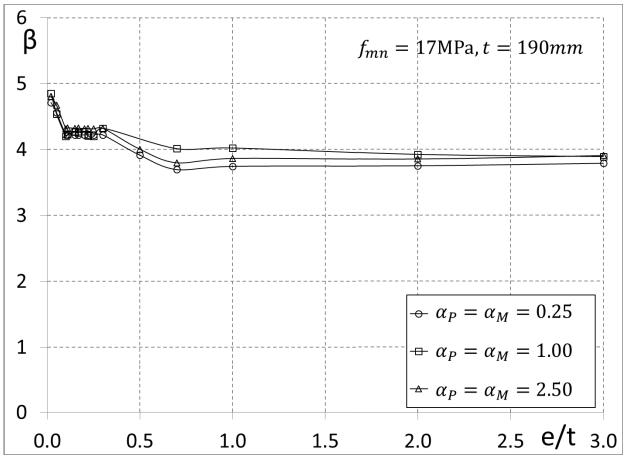

Figure 5-15: β versus normalized virtual eccentricity with $\phi_m = 0.60$ for $DL + LL$ (unreinforced, hollow)

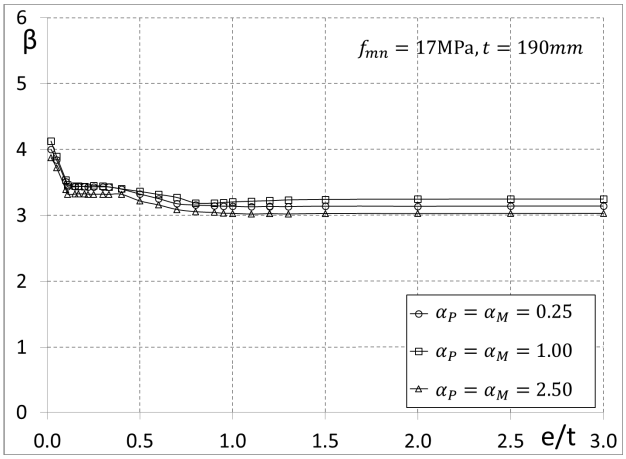

Figure 5-16: β versus normalized virtual eccentricity with $\phi_m = 0.60$ for $DL + SL$ (unreinforced, hollow)

5.9 SUMMARY AND CONCLUSION

A comprehensive limit state function is proposed for calculation of reliability indices for non-slender masonry walls under axial load and out-of-plane bending moment. Both unreinforced and reinforced walls were considered. Analysis was done for different load combinations, namely, DL, $DL + LL$, $DL + SL$ and $DL + WL$. Wherever possible, results are compared with reliability levels for reinforced concrete.

It is observed that reliability levels for $DL + SL$ are the most critical due to larger CoV in snow load. For both reinforced and unreinforced masonry walls reliability indices fall under 3.0 for this load combination.

Extending the analysis from dead-load-only to dead load plus a transient load is inevitable because the nature of these loads are different. For example, uncertainty in dead load is practically not a function of time and relates to uncertainties in material and geometrical properties, construction procedures, etc. However, uncertainty in transient loads is a function of time and the nominal values are related to maximum values over periods of

time. Therefore, the distribution type for dead load and transient loads are different and thus structural reliability analysis should include dead-load plus transient loads.

Load factors for companion loads (transient loads other than the main transient load) are selected to yield reliability levels not lower than the combinations with only one transient load. Thus, although a comprehensive reliability analysis should include all possible load combinations, considering dead-plus-one-transient load still reveals the essential information for investigating the appropriateness of the parameters affecting the resistance part of the limit state function; including the sufficiency of the strength reduction factors and adequacy of the procedures for member strength evaluation. Accordingly, the recent changes in the companion load factors NBCC 2015 do not affect the results of this analysis.

5.10 APPENDIX: P-M INTERACTION DIAGRAMS FOR THE WALLS UNDER STUDY

The following are the P-M interaction diagrams for the walls studied here. Values for axial force and bending moment are in kN and kN.m respectively. In all figures, the diagrams with the solid line represent the verified behavioural model used in this research and the dotted line represents the interaction diagram according to CSA-S304.

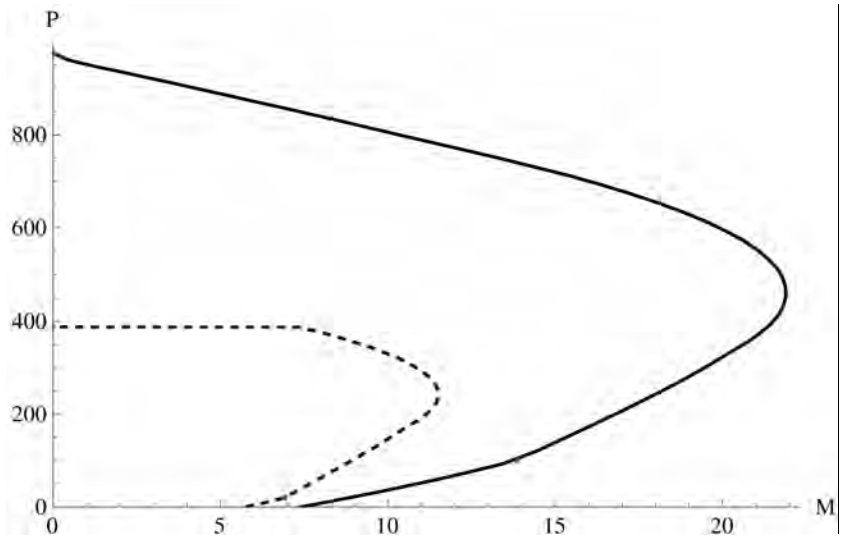

Fig. 5-A1. P-M interaction diagram for a wall with $f_m = 5$ MPa, $t = 190$ mm, $\rho_s = 0.0013$

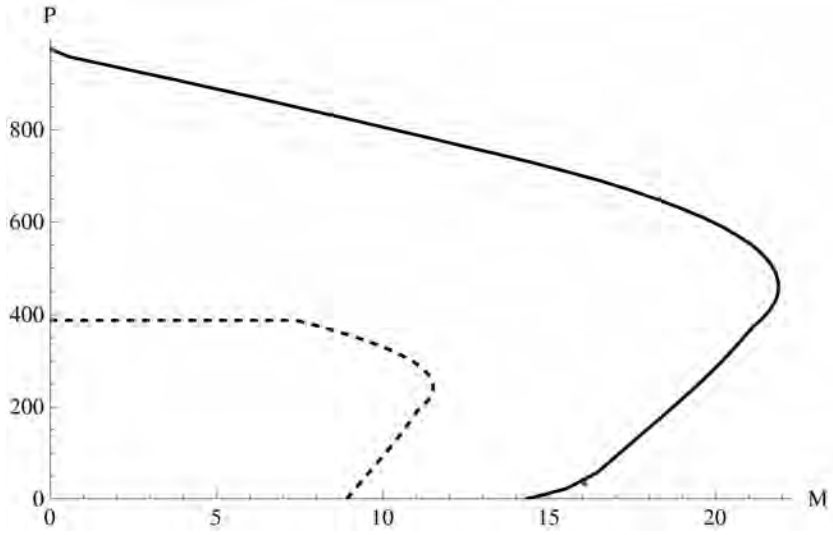

Fig. 5-A2. P-M interaction diagram for a wall with $f_m = 5$ MPa, $t = 190$ mm, $\rho_s = 0.0025$

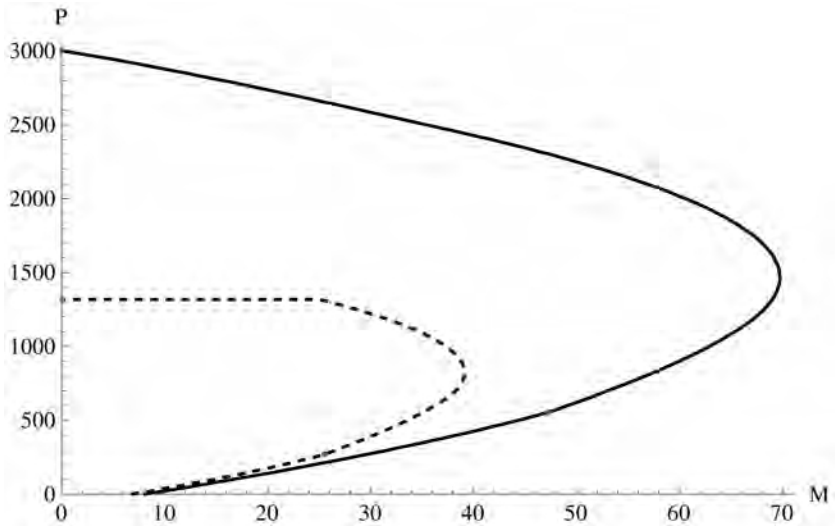

Fig. 5-A3. P-M interaction diagram for a wall with $f_m = 17$ MPa, $t = 190$ mm, $\rho_s = 0.0013$

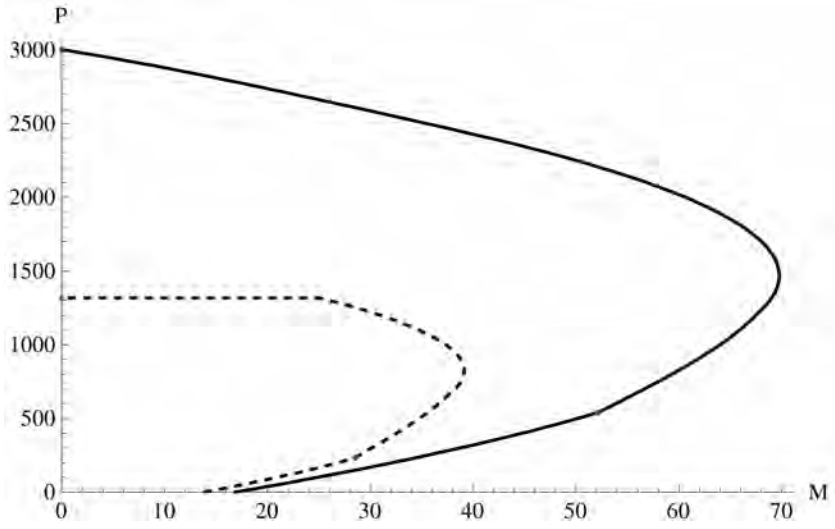

Fig. 5-A4. P-M interaction diagram for a wall with $f_m = 17$ MPa, $t = 190$ mm, $\rho_s = 0.0025$

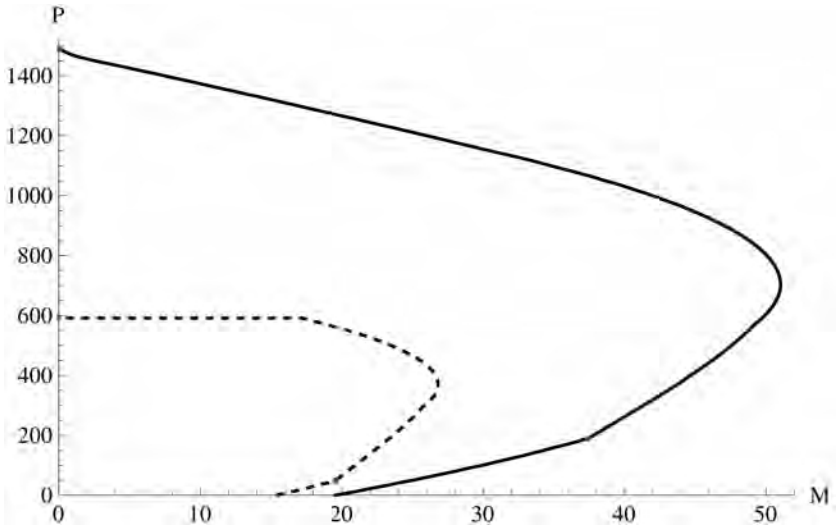

Fig. 5-A5. P-M interaction diagram for a wall with $f_m = 5$ MPa, $t = 290$ mm, $\rho_s = 0.0013$

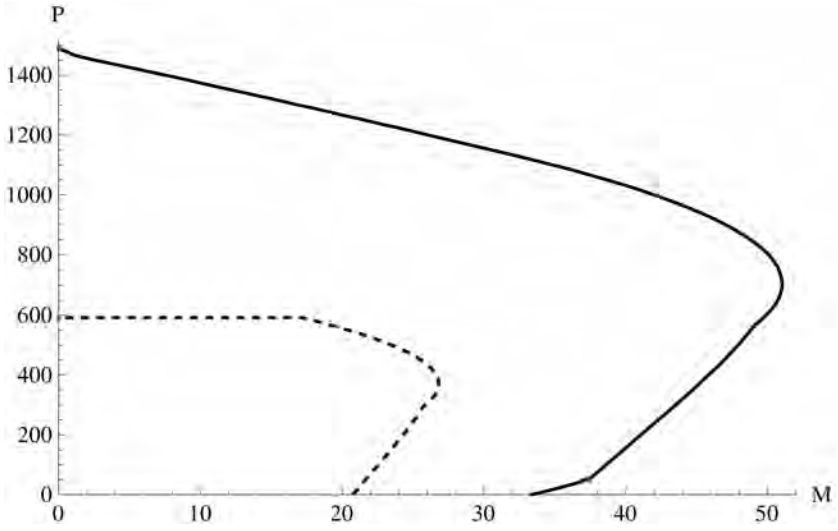

Fig. 5-A6. P-M interaction diagram for a wall with $f_m = 5$ MPa, $t = 290$ mm, $\rho_s = 0.0025$

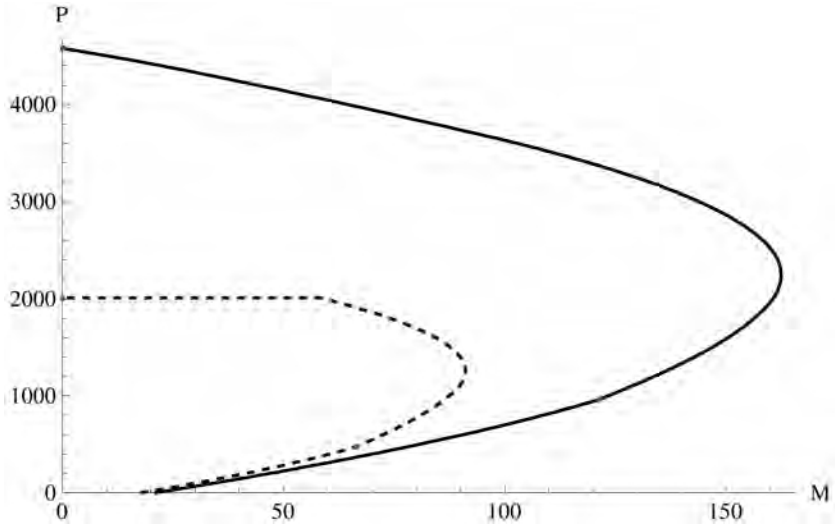

Fig. 5-A7. P-M interaction diagram for a wall with $f_m = 17$ MPa, $t = 290$ mm, $\rho_s = 0.0013$

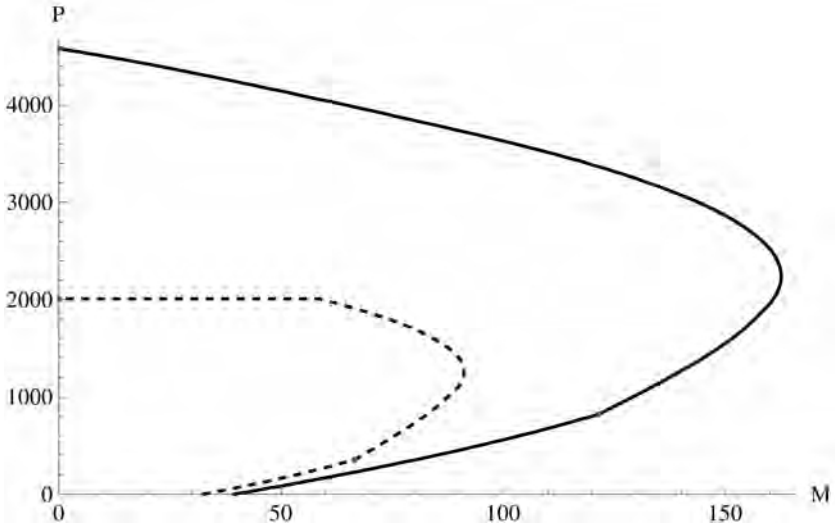

Fig. 5-A8. P-M interaction diagram for a wall with $f_m = 17$ MPa, $t = 290$ mm, $\rho_s = 0.0025$

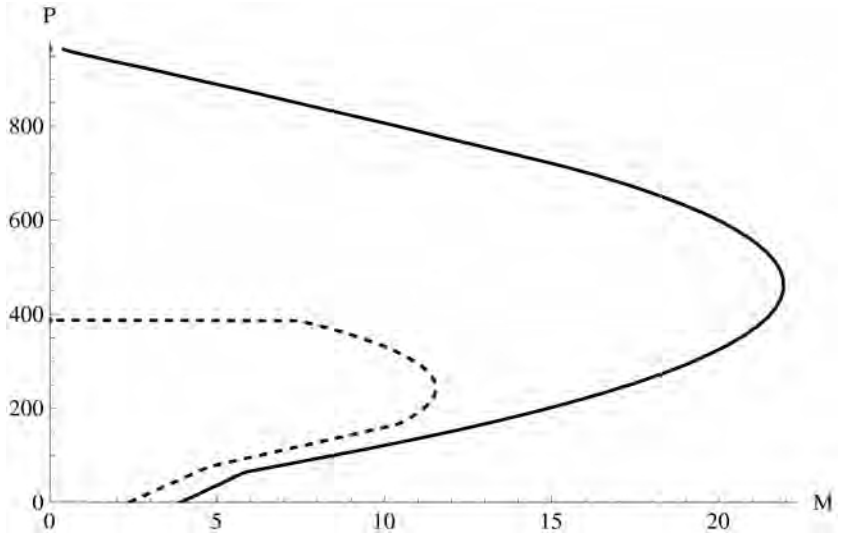

Fig. 5-A9. P-M interaction diagram for a wall with $f_m = 5$ MPa, $t = 190$ mm

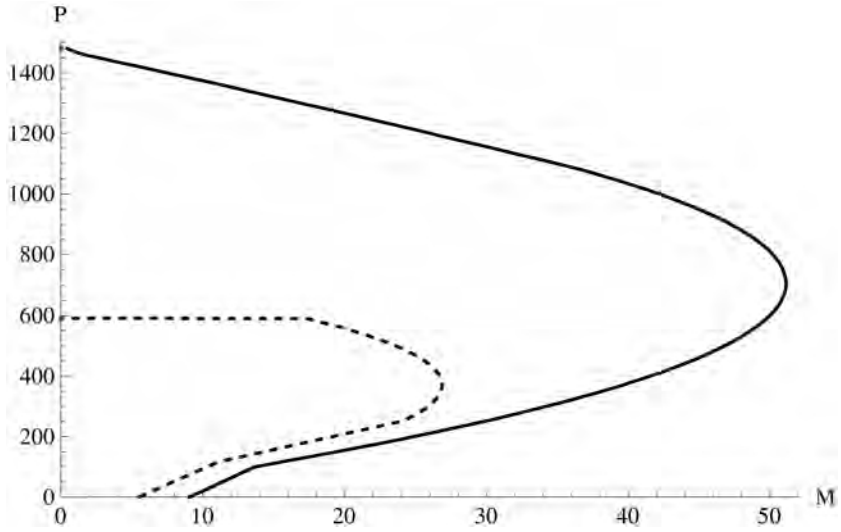

Fig. 5-A10. P-M interaction diagram for a wall with $f_m = 5$ MPa, $t = 290$ mm

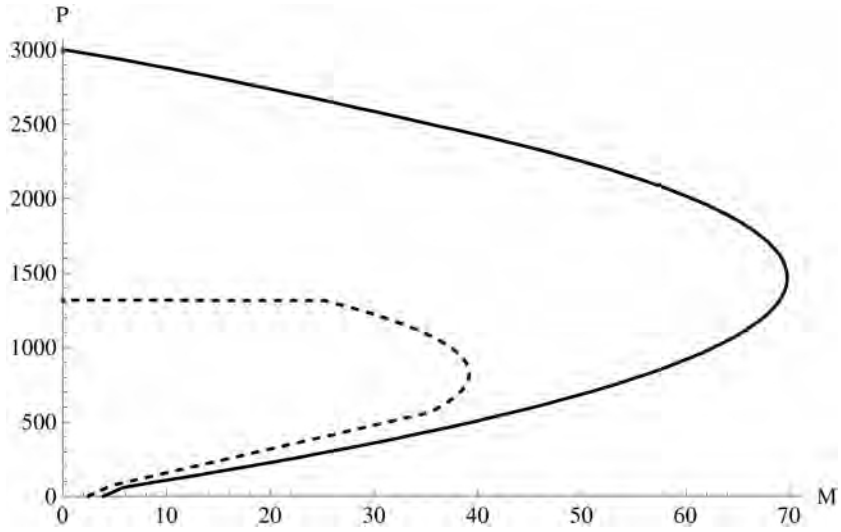

Fig. 5-A11. P-M interaction diagram for a wall with $f_m = 17$ MPa, $t = 190$ mm

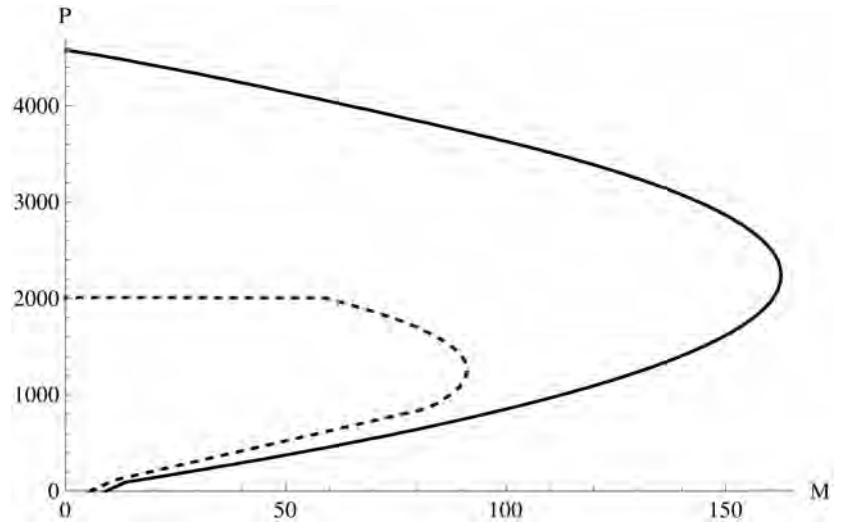

Fig. 5-A12. P-M interaction diagram for a wall with $f_m = 17$ MPa, $t = 290$ mm

Chapter 6

Steps Towards Reliability Analysis Considering Slenderness Effects

GENERAL

This chapter introduces the steps for the structural reliability analysis of masonry walls for which slenderness effects are considerable. Two techniques are discussed in the following; an approximate and time-saving procedure using moment-magnifier method and a more accurate procedure which is more computation exhaustive. The framework and scope of the analysis are also discussed.

6.1 DEFINITION OF LIMIT STATE FUNCTION FOR MASONRY WALLS WITH SLENDERNESS EFFECTS USING MOMENT MAGNIFIER METHOD

Moment magnifier method is a time-saving method to approximately assess the strength of columns and load-bearing walls considering second-order or slenderness effects. Steps and details for this method are widely available in literature and design handbooks (e.g. Drysdale & Hamid, 2005). Basically, for any masonry wall, ultimate strength of the wall under axial load with a

known virtual eccentricity can be calculated by intersecting equation for moment-magnifier method and the $P-M$ interaction diagram for the cross section of the wall. Figure 6-1 illustrates an example for a given axial force and out-of-plane bending moment caused by dead load (P_{Dn}, M_{Dn}). The accuracy of this method depends partly on what equations are used to construct $P-M$ interaction and moment-magnifier curves. Figure 6-1 illustrates two sets of formulations for assessing the wall strength according to moment-magnifier principle. One set of formulations are based on expressions from CSA S304 (P_{rn}, M_{rn}). and the other set includes a $P-M$ interaction curve based on a realistic material behaviour, introduced in Chapter 3 and a moment magnifier curve based on a more realistic effective flexural stiffness, EI_{eff}, (P_r, M_r) which is also explained in Chapter 3 based on a study by (Liu, Dawe 2003).

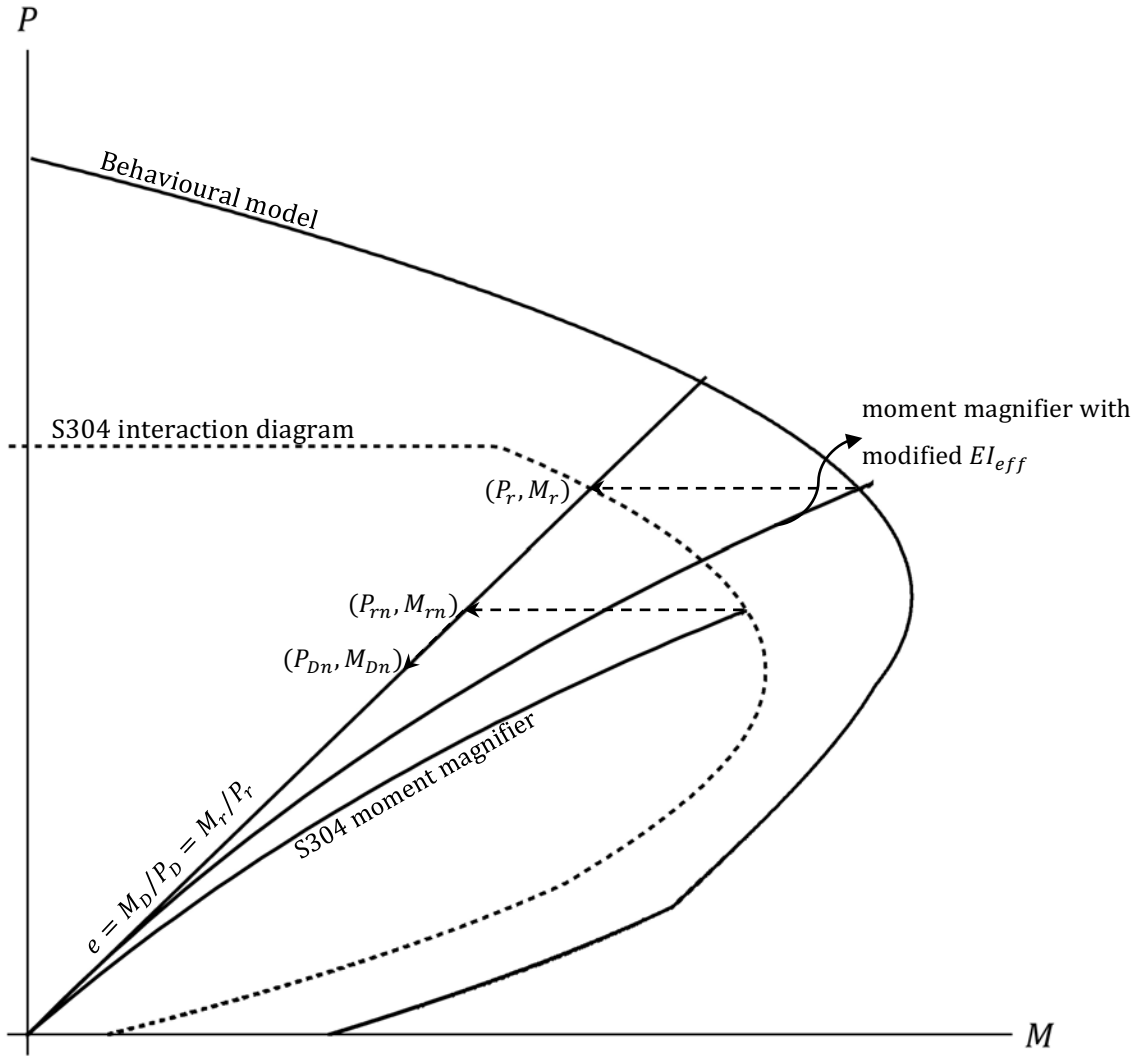

Figure 6-1: Illustration of limit-state function for slender walls

The case for dead load only for deriving the limit state function will be considered as an example.

Similar to what we had for non-slender walls, limit state function is defined as

$$G(\boldsymbol{x}) = \sqrt{{M_r}^2 + {P_r}^2} - \sqrt{{M_D}^2 + {P_D}^2} \qquad \text{(Eq. 6.1)}$$

Since nominal values for loading parameters (P_D, M_D) are related to nominal strength values of the wall by design expressions. Assuming that the wall under study is exactly designed for factored dead load with a load factor of 1.4 according to (CSA S304.1 2014), nominal load values for axial force and bending moment can be worked out as

$$P_{D,n} = \frac{P_{r,n}}{1.4}$$
$$M_{D,n} = \frac{M_{r,n}}{1.4} \qquad \text{(Eq. 6.2)}$$

As shown in Figure 6-1, for a given virtual eccentricity, ($P_{r,n}$, $M_{r,n}$) can be calculated in two steps as follows.

1. Intersecting the moment-magnifier equation constructed for the given eccentricity and the P-M interaction diagram constructed for the given masonry wall as per (CSA S304-2014).
2. Projecting that intersection point on the line representing the given eccentricity in the direction parallel to moment axis.

Resistance factors for masonry, steel reinforcement and member stiffness, namely $\phi_m = 0.60$, $\phi_s = 0.85$ and $\phi_{er} = 0.75$ (or $\phi_e = 0.65$) are already embodied in these steps. The corresponding formulations for these curves are explained elsewhere, e.g. Drysdale & Hamid, (2005).

Resistance part in Eq. 6.1, consisting of M_r and P_r, might be worked out using the same two steps introduced above, except that equations for $P - M$ interaction diagram and moment-magnifier are based on more realistic behavioural models and represent a more accurate model for the wall strength (Figure 6-1). As a clarification, it should be noted that the point representing M_r and P_r in Figure 6-1 seems to also lie on S304 interaction

diagram. This is only a coincidence. The corresponding principles for $P - M$ interaction curve and moment-magnifier curve are explained in Chapter 3. The subsequent steps for reliability analyses are the same as what was explained in Chapter 5. This method is essentially mapping the magnified moment to a straight line representing the eccentricity and using norm values (distance to origin) to define the limit state function. This provides a means for expanding the results of this research to cover a wider range of masonry walls.

Similar to non-slender masonry walls, the reliability levels might not be similar for different combinations of axial load and bending moment, i.e. different load eccentricities. Therefore, reliability analysis needs to be done for different eccentricities.

6.2 DEFINITION OF LIMIT STATE FUNCTION FOR MASONRY WALLS WITH SLENDERNESS EFFECTS USING FINITE ELEMENT METHOD

As pointed out in Chapter 3, a more accurate procedure to derive resistance part of the limit state function in Eq. 6-1 is to use finite element method.

Masonry load-bearing walls are generally long enough to be analyzed or tested ideally as wide columns with free side edges that are under uniform axial load and lateral loading. (Ganduscio and Romano 1997) stated that if the effects of lateral edge restraints are negligible, the analysis of masonry wall can be advantageously carried out by idealizing the member as a beam-column. This fact has been used in many numerical studies afterwards.

Therefore, a two-dimensional finite element model with beam-column elements can be used for the purpose of reliability analysis. A nonlinear step-by-step analysis (push-over analysis) must be used so that material and geometrical nonlinearities are reflected at every step until failure of the wall.

6.3 FRAME WORK FOR RELIABILITY ANALYSIS OF MASONRY WALLS WITH SLENDERNESS EFFECTS

Scope of a comprehensive reliability analysis for masonry walls with slenderness effects will include the following.

- Reinforced & unreinforced walls
- Load combinations: *DL, DL+LL, DL+ SL, DL+WL*
- Single curvature, double curvature and cantilever case
- Range of eccentricities from axial load only to dominant bending moment
- Range of slenderness ratios from $(k\ h)/t$ where slenderness effects are negligible to maximum $(k\ h)/t$ allowed in CSA S304.
- Current resistance factors are $\phi_m = 0.60$, $\phi_s = 0.85$ and $\phi_{er} = 0.75$ (for unreinforced masonry $\phi_e = 0.65$), the previous factors in CSA S304 1994 were $\phi_m = 0.55$, $\phi_s = 0.85$ and $\phi_{er} = \phi_e = 0.65$. Reliability analysis for both of these set of factors needs to be performed to assess the change in reliability levels.

CSA S304 standard uses the format of partial safety factors to isolate the main sources of uncertainty and deals with them separately with different safety factors. Therefore, it is good practice to calibrate ϕ_m for non-slender masonry walls to a target reliability defined by standard authority, assuming ϕ_s is the same as ϕ_s in reinforced concrete standard and then expanding the analysis and calibration to ϕ_{er} and ϕ_e for masonry walls with slenderness effects. The results from this study provides a means for calibration of ϕ_m. Although, CSA S408 recommends values for target reliability levels, the final decision for target values is made by standard committees.

Chapter 7

Summary of Results & Discussions

GENERAL

This chapter contains summary of the results for this research work along with discussion of the findings.

7.1 STEPS TAKEN & ACCOMPLISHED OBJECTIVES

The objectives defined in Chapter 1 were addressed as followed.

Objective 1: After selection of the behavioural model in Chapter 2, this model was coded in Mathematica® and compared with several experimental results for accuracy and consistency verification (Chapter 3). Sensitivity of the model to geometrical and material parameters was also investigated (Chapter 4).

Objective 2: A new limit state function was proposed for non-slender walls under axial compression only and under axial compression combined with out-of-plane bending moment (Chapter 5). This limit-state function can be used for all eccentricities.

Objective 3: Statistical data for load and resistance parameters are inputs for reliability analysis. Effort was made to collect the most recent statistical information for loads in Canada and for resistance parameters representing Canadian practice of masonry construction (Chapter 5);

Objective 4 & 5: Reliability analysis was performed for both reinforced and unreinforced masonry walls under axial load and out-of-plane bending moment. Effort was made to include all eccentricities, critical load combinations, different transient to dead load ratios and the effect of the recent change of masonry resistance reduction factor. (Chapter 5). Results were presented and discussed.

Objective 6: The limit-state function was generalized so that it can be used for reliability analysis of masonry walls with slenderness effects to assess the reliability levels provided by the design expressions and material resistance factors in the 2014 edition of CSA S304 for this category of walls (Chapter 6).

7.2 SUMMARY OF THE CONCLUSIONS

A comprehensive limit state function is proposed for calculation of reliability indices for non-slender masonry walls under axial load and out-of-plane bending moment. Both unreinforced and reinforced walls were considered. Analysis was done for different load combinations, namely, DL, $DL + LL$, $DL + SL$ and $DL + WL$. Wherever possible, results are compared with reliability levels for reinforced concrete.

It is noteworthy, that extending the analysis from dead-load-only to dead load plus a transient load is inevitable because the nature of these loads is different. For example, uncertainty in dead load is practically not a function of time and relates to uncertainties in material and geometrical properties, construction procedures, etc. However, uncertainty in transient loads is a function of time and the nominal values are related to maximum values over periods of time. Therefore, the distribution type for dead load and transient loads are different and thus structural reliability analysis should include dead-load plus transient loads.

On the other hand, load factors for companion loads (transient loads other than the main transient load) are selected to yield reliability levels not lower than the combinations with only one transient load. Thus, although a comprehensive reliability analysis should include all possible load combinations, considering dead-plus-one-transient load still reveals the essential information for investigating the appropriateness of the parameters affecting the resistance part of the limit state function; including the sufficiency of the strength reduction factors and adequacy of the procedures for member strength evaluation. Accordingly, the recent changes in the companion load factors NBCC 2015 do not affect the results of this analysis.

Findings of this investigation reveals that reliability levels for $DL + SL$ are the most critical. For both reinforced and unreinforced masonry walls reliability indices fall under 3.0 for this load combination.

Table 7–1 is a comparison of reliability indices between reinforced masonry and reinforced concrete for current resistance factors, i.e $\phi_m = 0.60$. and $\phi_c = 0.65$. It is observed that reliability levels are noticeably less for reinforced masonry. Specifically, β_{min}= 2.82 for *DL+SL* combination is very low. Even though for this load combination relatively lower β has been accepted for reinforced concrete, i.e. β_{min}= 3.20, β_{min}= 2.82 for masonry does not look acceptable.

Table 7–1 Comparison of current minimum reliability indices ($\boldsymbol{\beta}_{min}$) between reinforced masonry & reinforced concrete

Transient Load	**Masonry**	**Concrete (Bartlett 2007)**
Live Load	β_{min}= 3.40	β_{min}= 3.77
Snow Load	β_{min}= 2.82	β_{min}= 3.20
Wind Load	β_{min}= 3.45	β_{min}= 3.88

The effect of the change in ϕ_m from 0.55 to 0.60 on reliability levels of unreinforced masonry is also presented in Table 7–2. According to CSA S408 (2011) for normal buildings with gradual failure the target reliability index is 3.4. It can be seen with $\phi_m = 0.60$, reliability levels are not even close to this target value.

Table 7–2 Effect of the recent change in ϕ_m on $\beta_{\min}$ unreinforced masonry

Load Comb.	$\phi_m = 0.55$	$\phi_m = 0.60$
DL	$\beta_{min} = 3.79$	$\beta_{min} = 3.47$
DL+LL	$\beta_{min} = 3.33$	$\beta_{min} = 3.04$
DL+SL	$\beta_{min} = 3.00$	$\beta_{min} = 2.82$

The results show that the recent increase in ϕ_m from 0.55 to 0.60 has caused relatively lower reliability levels for masonry construction compared to other structural materials such as reinforced concrete and also less than recommended values in CSA S408. The findings of this research gives a tool to better understand the current reliability levels of the standard. It is apparent that this study has to be extended to walls for which slender effects are sizeable to investigate also the recent change in ϕ_e in CSA S304 and then decide what value for ϕ_m would yield the desired reliability levels. Proposing the algorithm and the framework for this analysis in Chapter 6 is a step toward this goal. Any further change to resistance factors for masonry should be done after comprehensive reliability analysis.

The following is a list of recommendations for future work: (1) To revisit the workmanship factor for better reflecting the current practice; (2) To extend the study to walls with slenderness effects; (3) To extend the study to partially grouted walls; (4) to verify results with using SORM (as an alternative reliability analysis approach) and FEM (as an alternative behavioural model).

References

ACI 530, 2011. Building Code Requirements & Specification for Masonry Structures: Containing Building Code Requirements for Masonry Structures (TMS 402-11/ACI 530-11/ASCE 5-11) & Specification for Masonry Structures (TMS 602-11/ACI 530.1-11/ASCE 6-11) & Companion Commentaries. Masonry Society; American Concrete Institute; Structural Engineering Institute of the American Society of Civil Engineers, Boulder, CO; Farmington Hills, MI; Reston, VA.

Ahmad, S., Mital, V., & Abbas, H. 1987. Discussion of "Mechanics of Masonry in Compression" by W. Scott McNary & Daniel P. Abrams (April, 1985, vol. 111, no. 4), *Journal of Structural Engineering*, **113**: 190-191.

Allen, D. E. (1972). "Statistical Study of the Mechanical Properties of Reinforcing Bars." *Building Research Note,* 85 22.

Allen, D. E. (1975). "Limit States Design: A Probabilistic Study." *Canadian Journal of Civil Engineering,* 2(1), 36-49.

Ang, A. H., & Tang, W. H. (2007). *Probability Concepts in Engineering Planning & Design: Emphasis on Applications in Civil & Environmental Engineering.* Wiley.

Aridru, G., 1997. *Effective Flexural Rigidity of Plain & Reinforced Concrete Masonry Walls*, The University of New Brunswick.

Athey, J., 1982. Test Report on Slender Walls. *Los Angeles, California PCA, PC (2008). Notes on ACI,* pp. 318-308.

AS 5104. (2005). "General Principles on Reliability for Structures.".

Bartlett, F., Hong, H., & Zhou, W. (2003). "Load Factor Calibration for the Proposed 2005 Edition of the National Building Code of Canada: Statistics of Loads & Load Effects." *Canadian Journal of Civil Engineering*, 30(2), 429-439.

Bartlett, F. M. (2007). "Canadian Standards Association, Standard A23.3-04 Resistance Factor for Concrete in Compression." *Canadian Journal of Civil Engineering,* 34(9), 1029-1037.

Bournonville, M., Dahnke, J., & Darwin, D. (2004). "Statistical Analysis of the Mechanical Properties & Weight of Reinforcing Bars." *University of Kansas Report*.

Brehm, E., Lissel, S. 2012. Reliability of Unreinforced Masonry Bracing Walls. 15th International Brick & Block Masonry Conference. Florianópolis, Brazil.

Brick Institute of America. 1969. Recommended Practice for Engineered Brick Masonry. In Edited by McLean, USA, pp. 250-253.

Chen, W.F. & Atsuta, T. 1973. Strength of Eccentrically Loaded Walls, *International Journal of Solids & Structures*, **9**: 1283-1300.

CSA A179 (2004). "Mortar & Grout for Unit Masonry." 30.

CSA A23. 3 (2004) Design of Concrete Structures. Canadian Standards Association.

CSA S304 (2014) Design of Masonry Structures. Canadian Standards Association, Mississauga, Canada.

CSA S408 (2011). Guidelines for the Development of Limit States Design. Canadian Standards Association, Ontario, Canada.

De Falco, A. & Lucchesi, M. 2002. Stability of Columns with No Tension Strength & Bounded Compressive Strength & Deformability. part I: Large Eccentricity, *International Journal of Solids & Structures*, 39: 6191-6210.

Ditlevsen, O. 1976. A Code Model for Combination of Actions. *In* International Workshop on Structural Reliability, Mexico, Vol. 2, pp. 110-123.

Drysdale, R.G. & Hamid, A.A. 2005. Masonry Structures: Behaviour & Design. Englewood Cliffs, NJ.

Ellingwood, B. (1980). Development of a Probability Based Load Criterion for American National Standard A58: Building Code Requirements for Minimum Design Loads in Buildings & Other Structures. US Department of Commerce, National Bureau of Standards.

Ellingwood, B. 1981. Analysis of Reliability for Masonry Structures, *Journal of the Structural Division*, **107**: 757-773.

Ellingwood, B. & Tallin, A. 1984. Probability-Based Design for Masonry Construction. *In* Proceedings of the 4th ASCE Specialty Conference on Probabilistic Mechanics & Structural Reliability, Berkeley, USA, pp. 82-85.

Ellingwood, B.M. & Tallin, A.A. 1985. Limit States Criteria for Masonry Construction, *Journal of Structural Engineering*, 111: 108.

Eamon, Christopher D. "Reliability of Concrete Masonry Unit Walls Subjected to Explosive Loads." *Journal of structural engineering* 133.7 (2007): 935-944.

Felippa, C. 2012. The TL Plane Beam Element: Formulation [online]. Available from http://www.colorado.edu/engineering/cas/courses.d/NFEM.d/NFEM.Ch10.d/NFEM.Ch10.pdf.

Ferry-Borges, J. & Castanheta, M. 1971. Structural Safety.

Fereig, S. & Hamid, A., 1987. Flexural Strength of Reinforced Block Masonry Walls, *Proceedings of the 4th North American masonry conference, Los Angeles, California* 1987.

Francis, A.J., Horman, C.B., & Jerrems, L.E. 1971. The Effect of Joint Thickness & Other Factors on the Compressive Strength of Brickwork. *In* proceedings of the 2nd International Brick Masonry Conference, Stoke-on-Trent, UK, pp. 31-37.

Frisch-Fay, R. 1975. Stability of Masonry Piers, International Journal of Solids & Structures, **11**: 187-198.

Frisch-Fay, R. 1977. Stability Functions for Structural Masonry, *International Journal of Solids & Structures*, **13**: 381-393.

Frisch-Fay, R. 1980. Buckling of Masonry Pier Under Its Own Weight, *International Journal of Solids & Structures*, **16**: 445-450.

Fyfe, A.G. 2000. Numerical Modelling of Workmanship in Masonry Structures. Ph.D. dissertation, University of Wales Swansea, UK.

Fyfe, A.G., Middleton, J., & Pande, G.N. 2000. Numerical Evaluation of the Influence of Some Workmanship Defects on the Partial Factor of Safety for Masonry, Masonry International, **13**: 48-53.

Ganduscio, S. & Romano, F. 1997. FEM & Analytical Solutions for Buckling of Nonlinear Masonry Members, *Journal of Structural Engineering*, ASCE, **123**: 104-111.

Grimm, C.T. 1988. Some Brick Masonry Workmanship Statistics, *Journal of Construction Engineering, & Management*: 147-149.

Hatzinikolas, M. & Korany, Y. 2005. Masonry Design for Engineers & Architects. Canadian Masonry Publications, Edmonton, AB, Canada.

Hatzinikolas, M., Longworth, J., Warwaruk, J., 1978. *Concrete masonry walls.* Edmonton: Dept. of Civil Engineering, University of Alberta.

Hendry, A.W. 1990. Masonry Materials & the Effect of Workmanship. *In* Proceedings of the 3rd International Seminar on Structural Masonry for Developing Countries, University of Edinburgh, Scotland, pp. 23-29.

Hendry, A.W. 1976. The Effect of Site Factors on Masonry Performance. *In* proceedings of the 1st Canadian Masonry Symposium, Calgary, pp. 182-198.

Hu, K. 2006. Behaviour of Reinforced Concrete Masonry Walls Subjected to Combined Axial Loading & Out-of-Plane Bending. Dalhousie University.

JCSS (2001a) Report 32: Probabilistic Assessment of Existing Structures, A Publication for the Joint Committee on Structural Safety (Vol. 32). RILEM publications, Edited Diamantidis, D.

JCSS (2001b) Probabilistic Model Code, Zurich, Joint Committee on Structural Safety, 2001. ISBN 978-3-909386-79-6.

Jones, P. G., & Richart, F. (1936). "The Effect of Testing Speed on Strength & Elastic Properties of Concrete." *Proceedings,* 380-392.

Laird, D.A., Drysdale, R.G., Stubbs, D.W., & Sturgeon, G.R. 2005. The New CSA S304.1-04 “Design of Masonry Structures”. In proceedings of the 10th Canadian Masonry Symposium, Banff, Alberta, pp. 10.

Lawrence, S.J. & Stewart, M.G. 2009. Structural Reliability & Partial Safety Factors for Unreinforced Masonry in Vertical Bending. 274.01.2009, The University of Newcastle, Australia.

Lind, N.C. 1971. Consistent Partial Safety Factors, *Journal of the Structural Division,* **97**: 1651-1669.

Liu, Y. 2002. Beam-Column Behaviour of Masonry Structural Elements.

Liu, Y. & Dawe, J., 2003. Analytical Modeling of Masonry Load-Bearing Walls. *Canadian Journal of Civil Engineering*, 30(5), pp. 795-806.

Lotfi, H.R. & Shing, P.B. 1994. Interface Model Applied to Fracture of Masonry Structures, *Journal of Structural Engineering*, **120**: 63-80.

Liu, Y. & Dawe, J., 2003. Analytical Modeling of Masonry Load-Bearing Walls. *Canadian Journal of Civil Engineering,* **30**(5), pp. 795-806.

Lu, M. 2003. Stability of Unreinforced Masonry Members Under Simultaneous Vertical & Out-of-Plane Lateral Loads. Ph.D., University of Minnesota, United States, Minnesota.

MacGregor, J. (1976). "Safety & Limit States Design for Reinforced Concrete." *Canadian Journal of Civil Engineering,* 3(4), 484-513.

MacGregor, J.G., Oelhafen, U.H. & Hage, S.E., 1975. A Re-Examination of the EI Value for Slender Columns, Special Publication, 50, pp.1-40.

Madsen, H. O., Krenk, S., & Lind, N. C. (1986). *Methods of structural safety.* Prentice-Hall Englewood Cliffs, NJ.

Martini, K. 1997. Finite Element Studies in the Out-of-Plane Failure of Unreinforced Masonry . *In* Proc., 7th Int. Conf. on Computing in Civil & Building Engineering, Vol. 1, pp. 179-184.

Maksoud, A. & Drysdale, R., 1993. Rational Moment Magnification Factor for Slender Unreinforced Masonry Walls, *Proceedings of the 6th North American Masonry Conference, Philadelphia, Pa* 1993, pp. 6-9.

McNary, W.S. & Abrams, D.P. 1985. Mechanics of masonry in compression, *Journal of Structural Engineering*, **111**: 857-870.

Moosavi, H., & Korany, Y. (2014). "Assessment of the Structural Reliability of Loadbearing Concrete Masonry Designed to the Canadian Standard S304. 1." *Canadian Journal of Civil Engineering,* 41(12), 1046-1053.

Moosavi, H. (2016). Structural Reliability of Flexural Load-Bearing Concrete Masonry Walls. University of Alberta.

Naraine, K. & Sinha, S. 1989. Behaviour of Brick Masonry Under Cyclic Compressive Loading, Journal of Structural Engineering, **115**: 1432-1445.

NBCC. (2015). "National building code of Canada."

Nowak, A.S. 2000. Reliability of Structures. McGraw-Hill, Boston, US.

Nowak, A.S. & Lind, N.C. 1979. Practical Code Calibration Procedures, *Canadian Journal of Civil Engineering*, **6**: 112-119.

Nowak, A. S., & Szerszen, M. M. (2003). "Calibration of Design Code for Buildings (ACI 318): Part 1, Statistical Models for Resistance." *ACI Structural Journal.,* 100(3).

Nowak, A.S., Szerszen, M.M., Szeliga, E.K., Szwed, A., & Podhorecki, P.J. 2005. Reliability-Based Calibration for Structural Concrete. UNLCE 05-03, Department of Civil Engineering, University of Nebraska, Lincoln, USA.

Nowak, A., Szerszen, M., Szeliga, E., Szwed, A., & Podhorecki, P. (2008). "Reliability-Based Calibration for Structural Concrete, Report No."

Olatunji, T.M., Warwaruk, J. & Longworth, J., 1986. Behaviour & Strength of Masonry Wall/Slab Joints. Department of Civil Engineering, University of Alberta.

Paloheimo, E. 1975. A Generalization of the Weighted Fractiles Method. CEB-CECM-CIB-FIP-IABSE Joint Committee on Structural Safety, Weisbaden, West Germany.

Payne, D., Brooks, D., & Sved, G. 1990. Analysis & Design of Slender Brick Walls, Masonry International, **4**: 55-65.

Popehn, J.R.B. 2007. Mechanics & Behaviour of Slender, Post-Tensioned Masonry Walls to Transverse Loading. ProQuest.

Priestley, M. & Elder, D. 1983. Stress-Strain Curves for Unconfined & Confined Concrete Masonry. *In* ACI Journal Proceedings, Vol. 80.

Rackwitz, R., & Fiessler, B. (1978). "Structural Reliability Under Combined Random Load Sequences." *Comput. Struct.,* 9(5), 489-494.

Romano, F., Ganduscio, S., & Zingone, G. 1993. Cracked Nonlinear Masonry Stability Under Vertical & Lateral Loads, *Journal of Structural Engineering*, **119**: 69-87.

Rots, J. 1991. Numerical Simulation of Cracking in Structural Masonry, Heron, **36**: 49-63.

Sahlin, S. 1971. Structural Masonry. Prentice-Hall Englewood Cliffs, NJ.

Sasanian, N., 2009. Out-of-Plane Flexural Performance of GFRP-Reinforced Concrete Masonry Walls.

Schueremans, L. & Van Gemert, D., 1998. Reliability Analysis in Structural Masonry Engineering. In Proc. of IABSE Colloquium" Saving Buildings in Central & Eastern Europe, Berlin (Germany).

Schultz, A. & Mueffelman, J. 2003. Elastic Stability of URM Walls Under Transverse Loading, TMS J, August, : 9-18.

Stewart, M.G. & Lawrence, S. 2002. Structural Reliability of Masonry Walls in Flexure, Masonry International, **15**: 48-52.

Stewart, M.G. & Lawrence, S.J. 2006. Reliability-Based Code Calibration of Structural Masonry in Compression Designed to Australian Standards. 259.06.06, University of Newcastle, Australia.

Suwalski, P.D. & Drysdale, R.G. 1986. Influence of Slenderness on the Capacity of Concrete Block Walls. *In* Proceedings of the 4th Canadian Masonry Symposium, Fredericton, NB, Vol. 1, pp. 122-135.

Tesfaye, E. & Broome, T.H. 1977. Effect of Weight on Stability of Masonry Walls, Journal of the Structural Division-ASCE, **103**: 961-970.

Turkstra, C.J. 1983. A Second Moment Safety Analysis of Masonry. In the 4th International Conference on Applications of Statistics & Probability in Soil & Structural Engineering, Italy, Vol. 1, pp. 475-490.

Turkstra, C. J. 1984. A Safety Index Analysis for Masonry Design. In Proceedings of the 4th ASCE Specialty Conference on Probabilistic Mechanics & Structural Reliability, Berkeley, USA, pp. 77-81.

Turkstra, C.J. 1989. Limit States Design in Masonry. In 5th International Conference on Structural Safety & Reliability, San Francisco, USA, pp. 2043-2050.

Turkstra, C. & Daly, M.J. 1978. Two Moment Structural Safety Analysis, *Canadian Journal of Civil Engineering*, 5: 414-426.

Turkstra, C. & Ojinaga, J. 1980. Towards a Canadian Limit States Masonry Design Code. In Proceedings of the 2nd Canadian Masonry Symposium, Carleton University, Ottawa, Ontario, Canada, pp. 133-141.

Turkstra, C., Ojinaga, J., & Shyu, C. 1982. Safety Index Analysis for a Limit States Code. In Proceedings of the 2nd Northern American Masonry Conference, University of Maryland, Maryland, pp. 22.1-22.14.

Turkstra, C., Ojinaga, J., & Shyu, C. 1982. Safety Index Analysis of Brick Masonry. In the International Conference on Masonry Structures, Rome, Italy, pp. 1-9.

Turkstra, C., Ojinaga, J., & Shyu, C. 1983. Development of A Limit States Masonry Code. In Proceedings of the 3rd Canadian Masonry Symposium. Edmonton, Alberta, June, pp. 2.1-2.13.

Vassilev, T., Jager, W., & Pflucke, T. 2002. Nonlinear Transfer Matrix Model for the Assessment of Masonry Buckling Behaviour. *In* Proceedings of the British Masonry Society, pp. 512-517.

Yokel, F.Y. & Dikkers, R.D. 1971. Strength of Load Bearing Masonry Walls, *Journal of the Structural Division*, **97**: 1593-1609.

Yokel, F.Y., Mathey, R.G., Dikkers, R.D., & Estados Unidos. 1971. Strength of Masonry Walls Under Compressive & Transverse Loads. Department of Commerce. National Bureau of Standards. US National Bureau of Standards; for sale by the Supt. of Docs., US Govt. Print. Off.

Zorapapel, G.T. 1991. Reliability of Concrete Masonry Wall Structures. Ph.D., University of California, Los Angeles.

Appendices

APPENDIX A

MATHEMATICA® CODES

Steel Stress-Strain Behaviour

```
(* STEEL STRESS-STRAIN FUNCTION *)
es = 2 × 10^5; (* STEEL MODULUS OF ELASTICITY ASSUMED DETERMINISTIC *)
(* fy IS STEEL YIELD STRESS & єє IS A THE STRAIN AT WHICH STRESS IS NEEDED *)
tied = "False";

(* UNTIED *)
If [tied == "False",
  σs[єє_, fy_] := If[єє < 0, 0, If[єє < fy/es, es єє, fy]]];

(* TIED *)
If [tied == "True",
  σs[єє_, fy_] := If[єє < -fy/es, -fy, If[єє < fy/es, es єє, fy]]];
```

Masonry Stress-Strain Behaviour

```
(* MASONRY STRESS-STRAIN FUNCTION *)

(* THIS MODEL IS BASED ON Priestly and Elder (1983) MODEL EXCEPT THAT
  MAXIMUM STRESS HAPPENS AT EPSILON =
 0.0020 INSTEAD OF 0.0015. THIS IS BECAUSE RECENT STUDIES SHOW THAT
  0.002 IS MORE APPROPRIATE (Drysdale book),
    NOTE: THIS MODEL HAS BEEN CHECKED FOR COMPRESSION STRAIN LESS
  THAN 0.003. FOR LARGER COMPRESSION STRAINS, IT HAS TO BE VERIFIED *)

σm[є_, fm_] := If[є > 65/100/(1000 fm) (* BASED ON TABLE 5 IN S304,
  0.65 MPa FOR GROUTED HOLLOW BLOCK AND BRICK & 0.40 MPa FOR CONCRETE
   BRICK AND BLOCK, 1000fm = SLOPE OF THE GRAPH AT ORIGIN*), 0,
  If[є > 0, 1000 fm є,
    If[є > -2 10^-3, -fm (2 (-є)/(2 × 10^-3) - ((-є)/(2 × 10^-3))^2),
      Min[-fm (1 - 0.5/((3 + 29/100 fm)/(145 fm - 1000) - 2/1000) (Abs[є] - 2 × 10^-3)), -0.2 fm]]]]
```

P-M Interaction Diagram According to CSA-S304

```
(* CONSTRUCT P-M DIAGRAM ACCORDING S304-2004 *)
(* THIS IS FOR FULLY-GROUTED WALLS *)

S304[fm_, fy_, d_, t_, e_] :=
  Module[{ϕm, ϕs, ae, ag, ey, β1, prmax, cb, a, cm, tr, prb, mrb, eb, pr, mr, list, c0,
    c, a1, listp, pmS304, pS304, mS304, thrust, sub, guessP, eu, order, guessP2},
   list = {};
   ϕm = 0.60; ϕs = 0.85; eu = 0.003;
   (*  4.3.2.1 Masonry
    The resistance factor to be used in calculating
    the ultimate limit states for compression,tension,shear,and
    bearing in masonry shall be taken as φm=0.60.
       4.3.2.2 Reinforcement
    The resistance factors to be used in calculating the
      ultimate limit states for force in steel reinforcement shall
    be taken as φs=0.85 for reinforcing bars and wire and φp=
      0.90 for prestressing steel. *)
   ae = b t;
   ag = b t;
   If[fm ≤ 20, β1 = 0.8]; (* ACCORDING TO S304 *)
   If[fm > 20, β1 = 0.8 - 0.1 ((fm - 20)/10)]; (* ACCORDING TO S304 *)
   (* CHECK ρmin AND ρmax *)
   If[Or[ρ > 0.02, ρ < 0.0013], Print["REINFORCEMENT AREA IS NOT OK"]];

   (* AXIAL LOAD ONLY *)
   If[tied == "False", prmax = (0.8 ϕm 0.85 fm ae)/1000];
   If[tied == "True", prmax = (0.8 (ϕm 0.85 fm (ae - ρ ag) + ϕs fy ρ ag))/1000];

   (* BALANCED CASE *)
   cb = eu/(fy/es + eu) d; (* BALANCED NEUTRAL AXIS *)
   a = β1 cb; (* RECTANGULAR BLOCK HEIGHT *)
   cm = ϕm 0.85 fm b a; (* COMPRESSION FROM MASONRY *)
   tr = ϕs ρ ag fy; (* TENSION FROM REBAR *)
   prb = cm - tr; (* NET FORCE IN COMPRESSION IN BALANCED CASE *)
   mrb = cm (t/2 - a/2) + tr (d - t/2); (* BALANCED MOMENT *)
   eb = mrb/prb; (* BALANCED ECCENTRICITY *)

   (* BENDING ALONE *)
```

```
a = a1 /. Solve[{ϕm 0.85 fm b a1 == ϕs σs[(d - a1/β1)/(a1/β1) εu, fy] ρ ag, a1 > 0}, a1][[1]];

If[εu (d - a/β1)/(a/β1) > fy/es, yield = "Steel Yields in pure bending",
 Print["Steel does not yield in pure bending"]];
cm = ϕm 0.85 fm b a;
tr = ϕs σs[(d - a/β1)/(a/β1) εu, fy] ρ ag;
mr = cm (t/2 - a/2) + tr (d - t/2);
AppendTo[list, {mr/10^6, 0}];
c0 = a/β1;

(* OTHER POINTS *)
c = c0 + 1;

While[c < t, {a = β1 c,
  cm = ϕm 0.85 fm b a,
  tr = ϕs σs[(d - a/β1)/(a/β1) εu, fy] ρ ag,
  pr = cm - tr,
  mr = cm (t/2 - a/2) + tr (d - t/2),

  AppendTo[list, {mr/10^6, Min[pr/1000, prmax + c/10 000 (* adding c is
      just for avoiding duplicates in the interpolation *)]}],
  c = c + 1}];
(* Last Point *)
c = t;
a = β1 c;
cm = ϕm 0.85 fm b a;
tr = ϕs σs[(d - a/β1)/(a/β1) εu, fy] ρ ag;
pr = cm - tr;
mr = cm (t/2 - a/2) + tr (d - t/2);
```

```
AppendTo[list, {mr/10^6, Min[pr/1000, prmax + c/10000
    (* adding c is just for avoiding duplicates in the interpolation *)]}];


AppendTo[list, {0, prmax + (c + 1)/10000}];
listp = Table[{list[[i, 2]], list[[i, 1]]}, {i, Length[list]}];
pmS304 = Interpolation[listp, InterpolationOrder → 1];

guessP = 10^-3;
order = 10^IntegerPart[Log[10, list[[-1, 2]]]];
(*Off[InterpolatingFunction::dmval];*)
Do[{While[
    And[guessP < list[[-1, 2]], pmS304[guessP]/guessP > e/1000], guessP = guessP + order],
   guessP = guessP - order,
   order = order/10}, {5}];
sub = FindRoot[pmS304[guessP2]/guessP2 == e/1000, {guessP2, guessP}];
mS304 = pmS304[guessP2 /. sub];
pS304 = guessP2 /. sub;
{list, {{mrb/10^6, prb/10^3}}, {{mS304, pS304}}}

];
```

P-M Interaction Diagram based on Selected Behavioural Model

```
(* CONSTRUCT P-M DIAGRAM BASED ON PARABOLIC MATERIAL BEHAVIOR *)

realPM[fm_, fy_, d_, t_, e_] :=
  Module[{interaction, list, sub, ae, ag, c0, c01, c02, eui, cm, tr, mr,
    c, yield, pr, listp, mReal, pReal, thrust, maxp, finalInteraction,
    finalList, guessP, cStep, order, z, cb, mrb, prb},
   interaction = {};
   list = {};
   (*eui=0.003;*)
   ae = b t;
   ag = b t;
   maxp = 0;
   interaction = (*Parallel*)
    Table[list = {};
     (* BENDING ALONE *)
     c01 = 0.01;
     order = 10;
     Do[{While[-b NIntegrate[σm[(-eui)/c01 x, fm], {x, 0, c01}] <
         σs[(d - c01)/c01 eui, fy] ρ ag, {c01 = c01 + order}],
       c01 = c01 - order,
       order = order/10}, {3}];
     sub = FindRoot[-b Integrate[σm[(-eui)/c02 x, fm], {x, 0, c02}] ==
        σs[(d - c02)/c02 eui, fy] ρ ag, {c02, c01}];
     c0 = c02 /. sub;

     If[eui (d - c0)/c0 > fy/es,
      {(*Print["Steel Yields in pure bending"], *)
       mr = -b NIntegrate[((t/2 - c0 + x) σm[(-eui)/c0 x, fm], {x, 0, c0}] + tr (d - t/2)},
      {yield = "Steel does not yield in pure bending", Print[yield],
       mr = -b NIntegrate[((t/2 - c0 + x) σm[(-eui)/c0 x, fm], {x, 0, c0}] + tr (d - t/2)}];
     AppendTo[list, {mr/10^6, 0}];

     (* BALANCED POINT *)
     cb = eui/(eui + fy/es) d;
```

```
  cm = b NIntegrate[σm[-εui x/cb, fm], {x, Max[0, cb - t], cb}];
  tr = σs[(d - cb)/cb εui, fy] ρ ag;
  mrb = -b NIntegrate[
      (t/2 - cb + x) * σm[-εui x/cb, fm], {x, Max[0, cb - t], cb}] + tr (d - t/2);
  prb = -(cm + tr);

  (* OTHER POINTS *)
  If[c0 < 0, Print["Error c is negative"]];
  cStep = 1;
  c = c0 + cStep;
  While[Or[mr > 10000, Length[list] < 10],
   {cm = b NIntegrate[σm[-εui x/c, fm], {x, Max[0, c - t], c}],
    tr = σs[(d - c)/c εui, fy] ρ ag,
    mr = -b NIntegrate[
        (t/2 - c + x) * σm[-εui x/c, fm], {x, Max[0, c - t], c}] + tr (d - t/2),
    pr = -(cm + tr),

    AppendTo[list, {mr/10^6, pr/1000 (*Min[pr,prmax]*)}],
    cStep = Min[1/Abs[list[[-1, 1]] - list[[-2, 1]]],
      20/Abs[list[[-1, 2]] - list[[-2, 2]]]] cStep,
    c = c + cStep}];
  listp = Table[{list[[i, 2]], list[[i, 1]]}, {i, Length[list]}];
  AppendTo[listp, {listp[[-1, 1]] + 10^-3, 0}];
  maxp = Max[maxp, listp[[-1, 1]]];
  Interpolation[listp, InterpolationOrder → 1]
  , {εui, 0.003, 0.003, 0.0002}];
(*finalList=Table[{p,Max[Table[interaction[[i]][p],{i,Length[interaction]}]]},
   {p,Join[Table[z,{z,0,maxp,10}],{maxp}]}];*)
finalInteraction = interaction[[1]](*Interpolation[
 finalList,InterpolationOrder→1]*);
guessP = 10^-3;
order = 10^IntegerPart[Log[10,maxp]];
Off[InterpolatingFunction::dmval];
Do[{While[
```

```
    And[guessP < maxp, finalInteraction[guessP]/guessP > e/1000], guessP = guessP + order],
   guessP = guessP - order,
   order = order/10}, {3}];
sub = FindRoot[finalInteraction[guessP2]/guessP2 == e/1000, {guessP2, guessP}];

mReal = finalInteraction[guessP2 /. sub];
pReal = guessP2 /. sub;
{list, {{mrb/10^6, prb/10^3}}, {{mReal, pReal}}}
];
```

Code for Reliability Analysis for Dead plus Live Load Combination

```
LaunchKernels[];

(* INITIAL VALUES *)
fmi = 0; (* MASONRY STRENGTH *)
fyi = 0; (* STEEL YIELD STRENGTH *)
di = 0; (* REBAR LOCATION *)
(*ti=0;*) (* WALL (UNIT) THICKNESS *)
(*ρi=0; WE TOOK IT DETERMINISTIC *) (* REINFORCEMENT RATIO AS/BT *)
mdi = 0; (* BENDING MOMENT FROM DEAD LOAD *)
mli = 0; (* BENDING MOMENT FROM LIVE LOAD *)
pdi = 0; (* AXIAL FORCE FROM DEAD LOAD *)
pli = 0; (* AXIAL FORCE FROM LIVE LOAD *)
eli = 0; (* TRANSFORMATION TO LOAD EFFECT *)
wi = 0; (* WORKMANSHIP FACTOR *)
α = 5.00; (* LIVE MOMENT TO DEAD MOMENT RATIO *)
β = 5.00; (* LIVE FORCE TO DEAD FORCE RATIO *)
ρrate = 0.87; (* EFFECT OF RATE OF LOADING *)

rho = {{1,0,0,0,0,0,0,0,0},
       {0,1,0,0,0,0,0,0,0},
       {0,0,1,0,0,0,0,0,0},
       {0,0,0,1,0,1,0,0,0},
       {0,0,0,0,1,0,1,0,0},
       {0,0,0,1,0,1,0,0,0},
       {0,0,0,0,1,0,1,0,0},
       {0,0,0,0,0,0,0,1,0},
       {0,0,0,0,0,0,0,0,1}};

(* NOMINAL VALUES *)
b = 1000; (* WALL BREADTH *)
εu = 0.003; (* MAXIMUM USABLE STRAIN FOR MASONRY *)
es = 2 × 10^5; (* ASSUMED DETERMINISTIC *)
tied = "False";
dif = 10^-3; (* FINITE DIFFERENCE STEP *)
fmList = {5, (*,10,*)20};
fyList = {400};
tList = {190(*,240*)(*,290*)};
ti = tList[[1]];
ρList = {(*0.00,*)0.0013, 0.0025(*,0.005,0.01*)};
(* ALMOST DETERMINISTIC *)
(*wn=0.1 ;*) (* WORKMANSHIP 1.0, 0.80, 0.70 *)
nominalValues = {};
Do[AppendTo[nominalValues, {fmList[[i]], fyList[[j]], tList[[k]], ρList[[l]]}],
  {i, Length[fmList]}, {j, Length[fyList]}, {k, Length[tList]}, {l, Length[ρList]}];

(* $$$$$$$$$$$$$$$$$$$$$$$$$$$$$$$$$$$$$$$$$$$$$$$$$$$$$$$$$$$$$$$$$$$$$$$$$$ *)
```

```
(* STEEL STRESS-STRAIN FUNCTION *)

(* UNTIED *)
If[tied == "False",
  σs[εε_, fy_] := If[εε < 0, 0, If[εε < fy/es, es εε, fy]]];

(* TIED *)
If[tied == "True",
  σs[εε_, fy_] := If[εε < -fy/es, -fy, If[εε < fy/es, es εε, fy]]];

(* $$$$$$$$$$$$$$$$$$$$$$$$$$$$$$$$$$$$$$$$$$$$$$$$$$$$$$$$$$$$$$$$$$$$$$$ *)
(* $$$$$$$$$$$$$$$$$$$$$$$$$$$$$$$$$$$$$$$$$$$$$$$$$$$$$$$$$$$$$$$$$$$$$$$ *)
(* MASONRY STRESS-STRAIN FUNCTION *)

(* THIS MODEL IS BASED ON Priestly and Elder
   (1983) MODEL EXCEPT THAT MAXIMUM STRESS HAPPENS AT EPSILON =
 0.0020 INSTEAD OF 0.0015. THIS IS BECAUSE RECENT STUDIES
  SHOW THAT 0.002 IS MORE APPROPRIATE (Drysdale book),
    NOTE: THIS MODEL HAS BEEN CHECKED FOR COMPRESSION STRAIN LESS THAN
  0.003. FOR LARGER COMPRESSION STRAINS, IT HAS TO BE VERIFIED *)

σm[ε_, fm_] := If[ε > 65/100/(1000 fm) (* BASED ON TABLE 5 IN S304,
    0.65 MPa FOR GROUTED HOLLOW BLOCK AND BRICK & 0.40 MPa FOR CONCRETE
     BRICK AND BLOCK, 1000fm = SLOPE OF THE GRAPH AT ORIGIN*), 0,
   If[ε > 0, 1000 fm ε,
     If[ε > -2 10^-3, -fm (2 -ε/(2 × 10^-3) - (-ε/(2 × 10^-3))^2),
       Min[-fm (1 - 0.5/(3 + 19/100 fm/(145 fm - 1000) - 2/1000) (Abs[ε] - 2 × 10^-3)), -0.2 fm]]]];
(* $$$$$$$$$$$$$$$$$$$$$$$$$$$$$$$$$$$$$$$$$$$$$$$$$$$$$$$$$$$$$$$$$$$$$$$ *)

(* $$$$$$$$$$$$$$$$$$$$$$$$$$$$$$$$$$$$$$$$$$$$$$$$$$$$$$$$$$$$$$$$$$$$$$$ *)
(* CONSTRUCT P-M DIAGRAM ACCORDING S304-2004 *)
(* THIS IS FOR FULLY-GROUTED WALLS *)

S304[fm_, fy_, d_, t_, e_] :=
  Module[{ϕm, ϕs, ae, ag, εy, β1, prmax, cb, a, cm, tr, prb, mrb, eb, pr, mr, list, c0,
    c, a1, listp, pmS304, pS304, mS304, thrust, sub, guessP, εu, order, guessP2},
   list = {};
   ϕm = 0.60; ϕs = 0.85; εu = 0.003;
   (*  4.3.2.1 Masonry
```

```
The resistance factor to be used in calculating
 the ultimate limit states for compression,tension,shear,and
 bearing in masonry shall be taken as φm=0.60.
    4.3.2.2 Reinforcement
 The resistance factors to be used in calculating the
   ultimate limit states for force in steel reinforcement shall
 be taken as φs=0.85 for reinforcing bars and wire and φp=
   0.90 for prestressing steel. *)
ae = b t;
ag = b t;
If[fm ≤ 20, β1 = 0.8]; (* ACCORDING TO S304 *)
If[fm > 20, β1 = 0.8 - 0.1 ((fm - 20)/10)]; (* ACCORDING TO S304 *)
(* CHECK ρmin AND ρmax *)
If[Or[ρ > 0.02, ρ < 0.0013], Print["REINFORCEMENT AREA IS NOT OK"]];

(* AXIAL LOAD ONLY *)
If[tied == "False", prmax = (0.8 φm 0.85 fm ae)/1000];
If[tied == "True", prmax = (0.8 (φm 0.85 fm (ae - ρ ag) + φs fy ρ ag))/1000];

(* BALANCED CASE *)
cb = (εu/(fy/es + εu)) d; (* BALANCED NEUTRAL AXIS *)
a = β1 cb; (* RECTANGULAR BLOCK HEIGHT *)
cm = φm 0.85 fm b a; (* COMPRESSION FROM MASONRY *)
tr = φs ρ ag fy; (* TENSION FROM REBAR *)
prb = cm - tr; (* NET FORCE IN COMPRESSION IN BALANCED CASE *)
mrb = cm (t/2 - a/2) + tr (d - t/2); (* BALANCED MOMENT *)
eb = mrb/prb; (* BALANCED ECCENTRICITY *)

(* BENDING ALONE *)
a = a1 /. Solve[{φm 0.85 fm b a1 == φs σs[(d - a1/β1)/(a1/β1) εu, fy] ρ ag, a1 > 0}, a1][[1]];

If[εu ((d - a/β1)/(a/β1)) > fy/es, yield = "Steel Yields in pure bending"(*,
 Print["Steel does not yield in pure bending"]*)];
cm = φm 0.85 fm b a;
tr = φs σs[(d - a/β1)/(a/β1) εu, fy] ρ ag;
```

```
mr = cm (t/2 - a/2) + tr (d - t/2);
AppendTo[list, {mr/10^6, 0}];
c0 = a/β1;

(* OTHER POINTS *)
c = c0 + 1;

While[c < t, {a = β1 c,
  cm = ϕm 0.85 fm b a,
  tr = ϕs σs[(d - a/β1)/(a/β1) εu, fy] ρ ag,
  pr = cm - tr,
  mr = cm (t/2 - a/2) + tr (d - t/2),
  AppendTo[list, {mr/10^6, Min[pr/1000, prmax + c/10 000 (* adding c is
      just for avoiding duplicates in the interpolation *)]}],
  c = c + 1}];
(* Last Point *)
c = t;
a = β1 c;
cm = ϕm 0.85 fm b a;
tr = ϕs σs[(d - a/β1)/(a/β1) εu, fy] ρ ag;
pr = cm - tr;
mr = cm (t/2 - a/2) + tr (d - t/2);

AppendTo[list, {mr/10^6, Min[pr/1000, prmax + c/10 000
   (* adding c is just for avoiding duplicates in the interpolation *)]}];


AppendTo[list, {0, prmax + (c + 1)/10 000}];
listp = Table[{list[[i, 2]], list[[i, 1]]}, {i, Length[list]}];
pmS304 = Interpolation[listp, InterpolationOrder → 2];

guessP = 10^-3;
```

```
    order = 10^IntegerPart[Log[10, list[[-1, 2]]]];
    (*Off[InterpolatingFunction::dmval];*)
    Do[{While[
        And[guessP < list[[-1, 2]], pmS304[guessP]/guessP > e/1000], guessP = guessP + order],
       guessP = guessP - order,
       order = order/10}, {5}];
    sub = FindRoot[pmS304[guessP2]/guessP2 == e/1000, {guessP2, guessP}];
    mS304 = pmS304[guessP2 /. sub];
    pS304 = guessP2 /. sub;
    (*{list, {{mrb/10^6, prb/10^3}}, {*){mS304, pS304}(*}}*)

   ];
(* $$$$$$$$$$$$$$$$$$$$$$$$$$$$$$$$$$$$$$$$$$$$$$$$$$$$$$$$$$$$$$$$$$$$ *)


(* $$$$$$$$$$$$$$$$$$$$$$$$$$$$$$$$$$$$$$$$$$$$$$$$$$$$$$$$$$$$$$$$$$$$ *)
(* CONSTRUCT P-M DIAGRAM BASED ON PARABOLIC MATERIAL BEHAVIOR *)

realPM[fm_, fy_, d_, t_, e_] :=
  Module[{interaction, list, sub, ae, ag, c0, c01, c02, eui, cm, tr, mr,
    c, yield, pr, listp, mReal, pReal, thrust, maxp, finalInteraction,
    finalList, guessP, cStep, order, z, cb, mrb, prb},
   interaction = {};
   list = {};
   (*eui=0.003;*)
   ae = b t;
   ag = b t;
   maxp = 0;
   interaction = (*Parallel*)
    Table[list = {};
     (* BENDING ALONE *)
     c01 = 0.01;
     order = 10;
     Do[{While[-b NIntegrate[σm[-eui/c01 x, fm], {x, 0, c01}] <
          σs[(d - c01)/c01 eui, fy] ρ ag, {c01 = c01 + order}],
       c01 = c01 - order,
       order = order/10}, {3}];
     sub = FindRoot[-b Integrate[σm[-eui/c02 x, fm], {x, 0, c02}] ==
```

```
    σs[(d - c02)/c02 εui, fy] ρ ag, {c02, c01}];
c0 = c02 /. sub;

If[εui (d - c0)/c0 > fy/es,
 {(*Print["Steel Yields in pure bending"], *)
  mr = -b NIntegrate[((t/2) - c0 + x) σm[(-εui)/c0 x, fm], {x, 0, c0}] + tr (d - t/2)},
 {yield = "Steel does not yield in pure bending", (*Print[yield],*)
  mr = -b NIntegrate[((t/2) - c0 + x) σm[(-εui)/c0 x, fm], {x, 0, c0}] + tr (d - t/2)}];
AppendTo[list, {mr/10^6, 0}];

(* BALANCED POINT *)
cb = εui/(εui + fy/es) d;
cm = b NIntegrate[σm[-(εui x)/cb, fm], {x, Max[0, cb - t], cb}];
tr = σs[(d - cb)/cb εui, fy] ρ ag;
mrb = -b NIntegrate[
    ((t/2) - cb + x) * σm[-(εui x)/cb, fm], {x, Max[0, cb - t], cb}] + tr (d - t/2);
prb = -(cm + tr);

(* OTHER POINTS *)
If[c0 < 0, Print["Error c is negative"]];
cStep = 1;
c = c0 + cStep;
While[Or[mr > 500 000, Length[list] < 10],
 {cm = b NIntegrate[σm[-(εui x)/c, fm], {x, Max[0, c - t], c}],
  tr = σs[(d - c)/c εui, fy] ρ ag,
  mr = -b NIntegrate[
      ((t/2) - c + x) * σm[-(εui x)/c, fm], {x, Max[0, c - t], c}] + tr (d - t/2),
  pr = -(cm + tr),

  AppendTo[list, {mr/10^6, pr/1000 (*Min[pr,prmax]*)}],
```

```
      cStep = Min[1/Abs[list[[-1, 1]] - list[[-2, 1]]],
          20/Abs[list[[-1, 2]] - list[[-2, 2]]]] cStep,
        c = c + cStep}];
    listp = Table[{list[[i, 2]], list[[i, 1]]}, {i, Length[list]}];
    AppendTo[listp, {listp[[-1, 1]] + 10^-3, 0}];
    maxp = Max[maxp, listp[[-1, 1]]];
    Interpolation[listp, InterpolationOrder → 2]
    , {εui, 0.003, 0.003, 0.0002}];
  (*finalList=Table[{p,Max[Table[interaction[[i]][p],{i,Length[interaction]}]]},
     {p,Join[Table[z,{z,0,maxp,10}],{maxp}]}];*)
  finalInteraction = interaction[[1]](*Interpolation[
   finalList,InterpolationOrder→1]*);
  guessP = 10^-3;
  order = 10^IntegerPart[Log[10, maxp]];
  Off[InterpolatingFunction::dmval];
  Do[{While[
     And[guessP < maxp, finalInteraction[guessP]/guessP > e/1000], guessP = guessP + order],
    guessP = guessP - order,
    order = order/10}, {3}];
  sub = FindRoot[finalInteraction[guessP2]/guessP2 == e/1000, {guessP2, guessP}];

  mReal = finalInteraction[guessP2 /. sub];
  pReal = guessP2 /. sub;
  Print[listp];
  (*{list,{{mrb/10^6, prb/10^3}},{*){mReal, pReal}(*)}*)
 ];
(* $$$$$$$$$$$$$$$$$$$$$$$$$$$$$$$$$$$$$$$$$$$$$$$$$$$$$$$$$$$$$$$$$$$ *)

(* $$$$$$$$$$$$$$$$$$$$$$$$$$$$$$$$$$$$$$$$$$$$$$$$$$$$$$$$$$$$$$$$$$$ *)
logNormalEquivalent[μ_, σ_, xi_] := Module[{F, f, α, β, σe, μe},
  α = Log[μ^2/Sqrt[μ^2 + σ^2]]; β = Sqrt[Log[1 + σ^2/μ^2]];
  F = CDF[LogNormalDistribution[α, β], xi];
  f = PDF[LogNormalDistribution[α, β], xi];
  σe = 1/f PDF[NormalDistribution[0, 1], InverseCDF[NormalDistribution[0, 1], F]];
  μe = xi - σe InverseCDF[NormalDistribution[0, 1], F]; {μe, σe}];
```

```
(* $$$$$$$$$$$$$$$$$$$$$$$$$$$$$$$$$$$$$$$$$$$$$$$$$$$$$$$$$$$$$$$$$$$$$$$ *)

(* $$$$$$$$$$$$$$$$$$$$$$$$$$$$$$$$$$$$$$$$$$$$$$$$$$$$$$$$$$$$$$$$$$$$$$$ *)
gumbelMinEquivalent[μ_, σ_, xi_] := Module[{F, f, α, β, σe, μe},
   α = (π μ - Sqrt[6] EulerGamma σ)/π; β = Sqrt[6] σ/π;
   F = CDF[ExtremeValueDistribution[α, β], xi];
   f = PDF[ExtremeValueDistribution[α, β], xi];
   σe = 1/f PDF[NormalDistribution[0, 1], InverseCDF[NormalDistribution[0, 1], F]];
   μe = xi - σe InverseCDF[NormalDistribution[0, 1], F]; {μe, σe}];
(* $$$$$$$$$$$$$$$$$$$$$$$$$$$$$$$$$$$$$$$$$$$$$$$$$$$$$$$$$$$$$$$$$$$$$$$ *)

(* $$$$$$$$$$$$$$$$$$$$$$$$$$$$$$$$$$$$$$$$$$$$$$$$$$$$$$$$$$$$$$$$$$$$$$$ *)
gFunction[fm_, fy_, d_, t_, md_, ml_, pd_, pl_, el_, w_] :=
  Norm[realPM[w ρrate fm, fy, d, t, 1000 (md + el ml)/(pd + el pl)]] - Sqrt[(md + el ml)^2 + (pd + el pl)^2];
(* $$$$$$$$$$$$$$$$$$$$$$$$$$$$$$$$$$$$$$$$$$$$$$$$$$$$$$$$$$$$$$$$$$$$$$$ *)


Do[
 {{fmn, fyn, tn, ρ} = nominalValues[[nomVal]];
  dn = tn/2; (* ASSUMPTION: REBAR IS AT THE CENTER *)
  Do[{(*e=100;*) (* NOMINAL ECCENTRICITY *)
    {mn, pn} = S304[fmn, fyn, dn, tn, e];
    (* NOMINAL AXIAL FORCE AND BENDING MOMENT *)

    (*α=0.25;*) (* LIVE MOMENT TO DEAD MOMENT RATIO *)
    mdn = mn/(1.50 α + 1.25); (* NOMINAL BENDING MOMENT FROM DEAD LOAD *)
    mln = α mn/(1.50 α + 1.25); (* NOMINAL BENDING MOMENT FROM LIVE LOAD *)

    (*β=0.25;*) (* LIVE FORCE TO DEAD FORCE RATIO *)
    pdn = pn/(1.50 β + 1.25); (* NOMINAL AXIAL FORCE FROM DEAD LOAD *)
    pln = β pn/(1.50 β + 1.25); (* NOMINAL AXIAL FORCE FROM LIVE LOAD *)

    PutAppend[{StringJoin[
       "core#=", ToString[$ProcessorCount]]}
     , StringJoin[ToString[nomVal], ".txt"]];

    PutAppend[{StringJoin[
```

```
    "fmn=", ToString[nominalValues[[nomVal, 1]]],
    ",fyn=", ToString[nominalValues[[nomVal, 2]]],
    ",tn=", ToString[nominalValues[[nomVal, 3]]],
    ",rho=", ToString[nominalValues[[nomVal, 4]]],
    ",mdn=", ToString[mdn],
    ",mln=", ToString[mln],
    ",pdn=", ToString[pdn],
    ",pln=", ToString[pln],
    ",eccentricity=", ToString[e]]}, StringJoin[ToString[nomVal], ".txt"]];

PutAppend[" ******************************************** ",
 StringJoin[ToString[nomVal], ".txt"]];
fmDist = ExtremeValueDistribution[1.4250694009233944` ,
  0.32073254381908767` ];
μfm = Mean[fmDist] fmn; vfm = StandardDeviation[fmDist] / Mean[fmDist]; σfm = vfm μfm;
(* DIST. Gumbel according to distribution fit to our prism database *)
μfy = 1.14 fyn; vfy = 0.07; σfy = vfy μfy;
(* DIST. LOGNORMAL, ELLINGWOOD ET AL (1980) *)
μd = 1.00 dn; vd = 4 / dn; σd = vd μd;  (* DIST. NORMAL, ELLINGWOOD ET AL (1980) *)
(*μt=1.00tn;vt=0.002;σt=vt μt; *)(* DIST. NORMAL, OUR PAPER *)
μmd = 1.05 mdn; vmd = 0.100;  σmd = vmd μmd;  (* DIST. NORMAL, BARTLETT(2003) *)
μml = 0.90 mln; vml = 0.170;  σml = vml μml;  (* DIST. GUMBEL, BARTLETT(2003) *)
μpd = 1.05 pdn; vpd = 0.100;  σpd = vpd μpd;  (* DIST. NORMAL, BARTLETT(2003) *)
μpl = 0.90 pln; vpl = 0.170;  σpl = vpl μpl;  (* DIST. GUMBEL, BARTLETT(2003) *)
μel = 1.000; vel = 0.206;  σel = vel μel;  (* DIST. NORMAL, BARTLETT(2003) *)
μw = 0.85; vw = 0.15;  σw = vw μw ;  (* WORKMANSHIP DIST. NORMAL, Turkstra *)

If[e == 0.02 tn, preStep = {fmn, fyn, dn, tn, mdn, mln, pdn, pln, μel, μw}];

(* TABLE (GRID) OF INITIAL VALUES FOR ITERATION
 IN ORDER TO FIND THE GLOBAL MINIMUM OF RELIABILITY INDEX *)
initialValue = {
  Table[fm0, {fm0, (*0.5*)fmn, (*1.25*)fmn, (1.25 fmn - 0.5 fmn) / 3}],
  Table[fy0, {fy0, (*0.75*)fyn, (*1.25*)fyn, (1.25 fyn - 0.75 fyn) / 2}],
  Table[d0, {d0, dn(*-20*), dn(*-20*), ((dn + 20) - (dn - 20)) / 1}],
  (*Table[t0,{t0,tn-5,tn-5,((tn+5)-(tn-5))/1}],*)
  Table[md0, {md0, (*0.75*)mdn, (*1.25*)mdn, (1.25 mdn - 0.75 mdn) / 1}],
  Table[ml0, {ml0, (*0.75*)mln, (*1.25*)mln, (1.25 mln - 0.75 mln) / 1}],
  Table[pd0, {pd0, (*0.75*)pdn, (*1.25*)pdn, (1.25 pdn - 0.75 pdn) / 1}],
```

```
  Table[pl0, {pl0, (*0.75*)pln, (*1.25*)pln, (1.25 pln - 0.75 pln)/1}],
  Table[el0, {el0, (*0.75*)1, 1(*1.25*), (1.25 - 0.75)/1}],
  Table[w0, {w0, (*0.50*)1, (*1.25*)1, (1.25 - 0.50)/1}]};
(*Dynamic[βi];*)

βii = 10;

Do[
 {fmi = 0 (* MEANS NEW INITIAL VALUES MUST BE TAKEN *),
  βi = {},
  While[Or[Length[βi] < 2, Abs[(Part[βi, -1] - Part[βi, -2])/Part[βi, -2]] > 10^-3],
   {If[And[fmi == 0,
      i ≠ Product[Length[initialValue[[j]]], {j, Length[initialValue]}] + 1], {

      remainder = i,
      counter = Ceiling[remainder /
         Product[Length[initialValue[[j]]], {j, 2, Length[initialValue]}]],
      fmi = initialValue[[1]][[counter]],
      (*Print[remainder],
      Print[counter],
      *)

      remainder = remainder - (counter - 1)
         Product[Length[initialValue[[j]]], {j, 2, Length[initialValue]}],
      counter = Ceiling[remainder / Product[Length[initialValue[[j]]],
          {j, 3, Length[initialValue]}]],
      fyi = initialValue[[2]][[counter]],


      remainder = remainder - (counter - 1)
         Product[Length[initialValue[[j]]], {j, 3, Length[initialValue]}],
      counter = Ceiling[remainder / Product[Length[initialValue[[j]]],
          {j, 4, Length[initialValue]}]],
      di = initialValue[[3]][[counter]],


      (*remainder=remainder-(counter-1)
         Product[Length[initialValue[[j]]],{j,4, Length[initialValue]}],
      counter=Ceiling[remainder/Product[Length[initialValue[[j]]],
          {j,5, Length[initialValue]}]],
      ti=initialValue[[4]][[counter]],*)
```

```
  remainder = remainder - (counter - 1)
     Product[Length[initialValue[[j]]], {j, 4, Length[initialValue]}],
  counter = Ceiling[remainder / Product[Length[initialValue[[j]]],
      {j, 5, Length[initialValue]}]],
  mdi = initialValue[[4]][[counter]],


  remainder = remainder - (counter - 1)
     Product[Length[initialValue[[j]]], {j, 5, Length[initialValue]}],
  counter = Ceiling[remainder / Product[Length[initialValue[[j]]],
      {j, 6, Length[initialValue]}]],
  mli = initialValue[[5]][[counter]],


  remainder = remainder - (counter - 1)
     Product[Length[initialValue[[j]]], {j, 6, Length[initialValue]}],
  counter = Ceiling[remainder / Product[Length[initialValue[[j]]],
      {j, 7, Length[initialValue]}]],
  pdi = initialValue[[6]][[counter]],


  remainder = remainder - (counter - 1)
     Product[Length[initialValue[[j]]], {j, 7, Length[initialValue]}],
  counter = Ceiling[remainder / Product[Length[initialValue[[j]]],
      {j, 8, Length[initialValue]}]],
  pli = initialValue[[7]][[counter]],



  remainder = remainder - (counter - 1)
     Product[Length[initialValue[[j]]], {j, 8, Length[initialValue]}],
  counter = Ceiling[remainder / Product[Length[initialValue[[j]]],
      {j, 9, Length[initialValue]}]],
  eli = initialValue[[8]][[counter]],



  remainder = remainder - (counter - 1)
     Product[Length[initialValue[[j]]], {j, 9, Length[initialValue]}],
  counter = remainder,
  wi = initialValue[[9]][[counter]],
  start = {fmi, fyi, di, ti, mdi, mli, pdi, pli, eli, wi}
 }
];

If[And[fmi == 0,
  i == Product[Length[initialValue[[j]]], {j, Length[initialValue]}] + 1],
 {start = preStep, {fmi, fyi, di, ti, mdi, mli, pdi, pli, eli, wi} = start}
];
```

```
ti = tList[[1]];
{μfme, σfme} = gumbelMinEquivalent[ μfm, σfm, fmi];
{μfye, σfye} = {μfy, σfy}(*logNormalEquivalent[ μfy,σfy,fyi]*);
{μmle, σmle} = gumbelMinEquivalent[ μml, σml, mli];
{μple, σple} = gumbelMinEquivalent[ μpl, σpl, pli];

(* STANDARD FORM *)

z1i = (fmi - μfme)/σfme;
z2i = (fyi - μfye)/σfye;
z3i = (di - μd)/σd;
z4i = (mdi - μmd)/σmd;
z5i = (mli - μmle)/σmle;
z6i = (pdi - μpd)/σpd;
z7i = (pli - μple)/σple;
z8i = (eli - μel)/σel;
z9i = (wi - μw)/σw;


gradianG1 = Parallelize[Apply[gFunction, {
    {fmi + dif/2, fyi, di, ti, mdi, mli, pdi, pli, eli, wi},
    {fmi - dif/2, fyi, di, ti, mdi, mli, pdi, pli, eli, wi},
    {fmi, fyi + dif/2, di, ti, mdi, mli, pdi, pli, eli, wi},
    {fmi, fyi - dif/2, di, ti, mdi, mli, pdi, pli, eli, wi},
    {fmi, fyi, di + dif/2, ti, mdi, mli, pdi, pli, eli, wi},
    {fmi, fyi, di - dif/2, ti, mdi, mli, pdi, pli, eli, wi},
    (*{fmi,fyi,di, ti+dif/2,mdi,mli,pdi,pli,eli,wi},
    {fmi,fyi,di, ti-dif/2,mdi,mli,pdi,pli,eli,wi},*)
    {fmi, fyi, di, ti, mdi + dif/2, mli, pdi, pli, eli, wi},
```

$$\left\{fmi,\ fyi,\ di,\ ti,\ mdi - \frac{dif}{2},\ mli,\ pdi,\ pli,\ eli,\ wi\right\},$$

$$\left\{fmi,\ fyi,\ di,\ ti,\ mdi,\ mli + \frac{dif}{2},\ pdi,\ pli,\ eli,\ wi\right\},$$

$$\left\{fmi,\ fyi,\ di,\ ti,\ mdi,\ mli - \frac{dif}{2},\ pdi,\ pli,\ eli,\ wi\right\},$$

$$\left\{fmi,\ fyi,\ di,\ ti,\ mdi,\ mli,\ pdi + \frac{dif}{2},\ pli,\ eli,\ wi\right\},$$

$$\left\{fmi,\ fyi,\ di,\ ti,\ mdi,\ mli,\ pdi - \frac{dif}{2},\ pli,\ eli,\ wi\right\},$$

$$\left\{fmi,\ fyi,\ di,\ ti,\ mdi,\ mli,\ pdi,\ pli + \frac{dif}{2},\ eli,\ wi\right\},$$

$$\left\{fmi,\ fyi,\ di,\ ti,\ mdi,\ mli,\ pdi,\ pli - \frac{dif}{2},\ eli,\ wi\right\},$$

$$\left\{fmi,\ fyi,\ di,\ ti,\ mdi,\ mli,\ pdi,\ pli,\ eli + \frac{dif}{2},\ wi\right\},$$

$$\left\{fmi,\ fyi,\ di,\ ti,\ mdi,\ mli,\ pdi,\ pli,\ eli - \frac{dif}{2},\ wi\right\},$$

$$\left\{fmi,\ fyi,\ di,\ ti,\ mdi,\ mli,\ pdi,\ pli,\ eli,\ wi + \frac{dif}{2}\right\},$$

$$\left\{fmi,\ fyi,\ di,\ ti,\ mdi,\ mli,\ pdi,\ pli,\ eli,\ wi - \frac{dif}{2}\right\}\},\ \{1\}\Big]\Big];$$

$$gradianG = \Big\{$$

$$\frac{(gradianG1[[1]] - gradianG1[[2]])}{dif},$$

$$\frac{(gradianG1[[3]] - gradianG1[[4]])}{dif},$$

$$\frac{(gradianG1[[5]] - gradianG1[[6]])}{dif},$$

$$\frac{(gradianG1[[7]] - gradianG1[[8]])}{dif},$$

$$\frac{(gradianG1[[9]] - gradianG1[[10]])}{dif},$$

$$\frac{(gradianG1[[11]] - gradianG1[[12]])}{dif},$$

$$\frac{(gradianG1[[13]] - gradianG1[[14]])}{dif},$$

$$\frac{(gradianG1[[15]] - gradianG1[[16]])}{dif},$$

$$\frac{(gradianG1[[17]] - gradianG1[[18]])}{dif}$$

$$\Big\}\{\sigma fme,\ \sigma fye,\ \sigma d,\ \sigma md,\ \sigma mle,\ \sigma pd,\ \sigma ple,\ \sigma el,\ \sigma w\};$$

```
  {z1i, z2i, z3i, z4i, z5i, z6i, z7i, z8i, z9i} = 1/(gradianG.rho.gradianG)
    (gradianG.{z1i, z2i, z3i, z4i, z5i, z6i, z7i, z8i, z9i} - (gFunction[
        fmi, fyi, di, ti, mdi, mli, pdi, pli, eli, wi])) (rho.gradianG);
  AppendTo[βi, Simplify[(-gradianG.{z1i, z2i, z3i, z4i, z5i, z6i,
        z7i, z8i, z9i}) / (√(gradianG.rho.gradianG))]];

  fmi = Chop[σfme z1i + μfme];
  fyi = Chop[σfye z2i + μfye];
  di = Chop[σd z3i + μd];
  mdi = Chop[σmd z4i + μmd];
  mli = Chop[σmle z5i + μmle];
  pdi = Chop[σpd z6i + μpd];
  pli = Chop[σple z7i + μple];
  eli = Chop[σel z8i + μel];
  wi = Chop[σw z9i + μw]}],
βii = Min[βii, Part[βi, -1]],
Print[βii],

PutAppend[StringJoin["initial value #", ToString[i]],
 StringJoin[ToString[nomVal], ".txt"]],
PutAppend[StringJoin["e=", ToString[e]],
 StringJoin[ToString[nomVal], ".txt"]],
PutAppend[StringJoin["beta=", ToString[Part[βi, -1]]],
 StringJoin[ToString[nomVal], ".txt"]],

PutAppend[{StringJoin["Nominal Values:",
   "fmn=", ToString[nominalValues[[nomVal, 1]]],
   ",fyn=", ToString[nominalValues[[nomVal, 2]]],
   ",tn=", ToString[nominalValues[[nomVal, 3]]],
   ",rho=", ToString[nominalValues[[nomVal, 4]]],
   ",mdn=", ToString[mdn],
   ",mln=", ToString[mln],
   ",pdn=", ToString[pdn],
   ",pln=", ToString[pln]]}, StringJoin[ToString[nomVal], ".txt"]],

PutAppend[{StringJoin["Initial Values:",
   "fmi=", ToString[start[[1]]],
   ",fyi=", ToString[start[[2]]],
   ",di=", ToString[start[[3]]],
   ",ti=", ToString[start[[4]]],
   ",mdi=", ToString[start[[5]]],
   ",mli=", ToString[start[[6]]],
   ",pdi=", ToString[start[[7]]],
   ",pli=", ToString[start[[8]]],
```

```
      ",eli=", ToString[start[[9]]]]}, StringJoin[ToString[nomVal], ".txt"]],

  PutAppend[{StringJoin["Design Point:",
      "fmi=", ToString[fmi],
      ",fyi=", ToString[fyi],
      ",di=", ToString[di],
      ",ti=", ToString[ti],
      ",mdi=", ToString[mdi],
      ",mli=", ToString[mli],
      ",pdi=", ToString[pdi],
      ",pli=", ToString[pli],
      ",eli=", ToString[eli],
      ",wi=", ToString[wi]]}, StringJoin[ToString[nomVal], ".txt"]],

  PutAppend["~~~~~~~~~~~~~~~~~~~~~~~~~~~~",
   StringJoin[ToString[nomVal], ".txt"]]},
 {i, Product[Length[initialValue[[j]]], {j, Length[initialValue]}] + 1}];

preStep = {fmi, fyi, di, ti, mdi, mli, pdi, pli, eli, wi};

PutAppend[StringJoin["Nominal Values:",
  "fmn=", ToString[nominalValues[[nomVal, 1]]],
  ",fyn=", ToString[nominalValues[[nomVal, 2]]],
  ",tn=", ToString[nominalValues[[nomVal, 3]]],
  ",rho=", ToString[nominalValues[[nomVal, 4]]],
  ",mdn=", ToString[mdn],
  ",mln=", ToString[mln],
  ",pdn=", ToString[pdn],
  ",pln=", ToString[pln]], StringJoin["RESULT", ".txt"]];

PutAppend[StringJoin["e=", ToString[e]], StringJoin["RESULT", ".txt"]];

PutAppend[StringJoin["beta=", ToString[βii]], StringJoin["RESULT", ".txt"]];

PutAppend[StringJoin["Design Point:",
  "fmi=", ToString[fmi],
  ",fyi=", ToString[fyi],
  ",di=", ToString[di],
  ",ti=", ToString[ti],
  ",mdi=", ToString[mdi],
  ",mli=", ToString[mli],
  ",pdi=", ToString[pdi], remainder = remainder - (counter - 1)
     Product[Length[initialValue[[j]]], {j, 5, Length[initialValue]}],
  counter = Ceiling[remainder / Product[Length[initialValue[[j]]],
      {j, 6, Length[initialValue]}]],
  pli = initialValue[[5]][[counter]],
  ",pli=", ToString[pli],
  ",eli=", ToString[eli],
```

```
      ",wi=", ToString[wi]], StringJoin["RESULT", ".txt"]]
  }, {e, {0.02 tn, 0.05 tn, 0.10 tn, 0.11 tn, 0.15 tn, tn/6, 0.2 tn, 0.22 tn,
     0.25 tn, 0.3 tn, tn/3, 0.4 tn, 0.5 tn, 0.6 tn, 0.7 tn, 0.8 tn, 0.9 tn, 0.95 tn,
     1.0 tn, 1.1 tn, 1.2 tn, 1.3 tn, 1.5 tn, 2.0 tn, 2.5 tn, 3.0 tn}}]},
{nomVal,
 2,
 2}]
```